



RISK OF NATURAL HAZARDS ON TECHNICAL-INDUSTRIAL CULTURAL HERITAGE IN SVALBARD

Probability analysis including considerations for climate change

Lappeenranta–Lahti University of Technology LUT
Master's Programme in Circular Economy, Master's thesis
2023

Anni Vehola

Examiners: Associate Professor, Ville Uusitalo
Post-doctoral researcher, Natasha Järviö

Supervisors: Lena Rubensdotter (UNIS)
Anatoly Sinitsyn (SINTEF)

ABSTRACT

Lappeenranta–Lahti University of Technology LUT
LUT School of Energy Systems
Environmental Technology

Anni Vehola

Risk of natural hazards on technical-industrial cultural heritage in Svalbard: Probability analysis including considerations for climate change

Master's thesis

2023

111 pages, 28 figures, 8 tables and 4 appendices

Examiners: Associate Professor Ville Uusitalo

Post-doctoral researcher Natasha Järviö

Keywords: Natural hazards, Risk assessment, Cultural heritage, Permafrost, Permafrost degradation, ArcGIS Online, Climate change, Arctic

Climate change, particularly through Arctic amplification, poses significant concerns for the preservation of cultural heritage sites in the Arctic region, with Svalbard's cultural heritage objects highly vulnerable to the exacerbating natural hazards like permafrost degradation, landslides, and erosion. This thesis presents a comprehensive assessment of the risks associated with ten specific hazards affecting 260 cable car posts and other cultural heritage objects in the Longyearbyen area and Ny-Ålesund, which house the most valuable heritage collections in Svalbard. The study employs a multidisciplinary approach, combining literature analysis, geographical information analysis, PCCH-Arctic Risk Assessment data, and fieldwork. By incorporating climate change projections, the research evaluates the natural hazards and determines the level of risk faced by cultural heritage in Svalbard. The outcomes of this study include an updated and enhanced Risk Assessment and an interactive ArcGIS Online map that highlights the risks associated with each cultural heritage object and cable car line. The findings indicate that approximately 16% of the studied cultural heritage objects in Longyearbyen are exposed to a high level of total risk, primarily due to permafrost degradation, snow avalanches, and rockfalls. Notably, Line 1b of the cable car system exhibits the highest overall risk. This assessment identifies the most vulnerable cultural heritage objects and cable car lines, thereby providing valuable data for prioritizing safeguarding efforts and protecting Svalbard's heritage in the face of natural hazards and climate change.

TIIVISTELMÄ

Lappeenrannan–Lahden teknillinen yliopisto LUT

LUT Energiajärjestelmät

Ympäristötekniikan koulutusohjelma

Anni Vehola

Luonnonkatastrofien riski teknisteollisiin kulttuuriperintökohteisiin Huippuvuorilla: Todennäköisyysanalyysi huomioiden ilmastomuutoksen vaikutukset

Diplomityö

2023

111 sivua, 28 kuvaa, 8 taulukkoa ja 4 liitettä

Tarkastajat: Apulaisprofessori Ville Uusitalo

Tutkijatohtori Natasha Järviö

Avainsanat: Luonnonkatastrofit, Riskiarviointi, Kulttuuriperintö, Ikirouta, Ikiroudan sulaminen, ArcGIS Online, Ilmastomuutos, Arktiset alueet

Ilmastomuutos aiheuttaa merkittäviä huolenaiheita arktisen alueen, kuten Huippuvuorten kulttuuriperintökohteiden säilyttämiselle. Nämä kulttuuriperintökohteet ovat alttiita ilmastomuutoksen vaikutuksesta voimistuville luonnonkatastrofeille, kuten ikiroudan sulamiselle, maanvyörymille ja eroosiolle. Tämä diplomityö tarkastelee kymmentä luonnonkatastrofia ja niiden aiheuttamaa riskiä yhteensä 260:een köysiratarakennelmaan ja muuhun kulttuuriperintökohteeseen Longyearbyenin alueella ja Ny-Ålesundissa, missä Huippuvuorten arvokkaimmat kulttuuriperintökokoelmat sijaitsevat. Tutkimuksessa käytetään monialaista lähestymistapaa, jossa yhdistetään kirjallisuusanalyysi, geoinformatiivinen analyysi, PCCH-Arctic riskiarvion aineisto ja kenttätyöskentelyn materiaali. Tutkimuksessa määritellään luonnonkatastrofien aiheuttama kulttuuriperintöön kohdistuva kokonaisriski. Tämän tutkimuksen tuloksia ovat päivitetty riskiarvio ja interaktiivinen ArcGIS Online -kartta, joka korostaa kuhunkin kulttuuriperintökohteeseen ja köysiratajärjestelmään liittyvät riskit. Löydökset osoittavat, että noin 16 % Longyearbyenin tutkituista kulttuuriperintökohteista on alttiina korkealle kokonaisriskille, mikä johtuu pääasiassa ikiroudan rappeutumisesta, lumivyöryistä ja kivivyöryistä. Köysiratajärjestelmistä, linjalla 1b on suurin kokonaisriski. Tämä arvio tunnistaa haavoittuvassa asemassa olevat kulttuuriperintökohteet ja köysilinjat, tarjoten arvokasta tietoa turvaavien toimien priorisoimiseksi luonnonuhkien ja ilmastomuutoksen vaikutuksessa.

ACKNOWLEDGEMENTS

To keep it short and sweet: I genuinely appreciate all the people who supported me throughout this journey! Special thanks need to be given to Anatoly, who not only involved me in this project but was always there to offer help and give insightful feedback. And to Lena who taught me a great deal about geology and provided invaluable guidance throughout the process. I will always be grateful for the time spent in Svalbard writing this thesis, and above all, our amazing group of master students, also known as the “masters of disasters”. Their camaraderie, collective knowledge, and everyday distractions, not to mention all those fun scooter trips we did together, have made this experience truly memorable and enjoyable. Now on to the next adventures. Tusen takk!

ABBREVIATIONS

CH – Cultural heritage

PC – Probability class

CC – Consequence class

GIS – Geographic Information System

PCCH-Arctic – Polar Climate and Cultural Heritage - Preservation and Restoration Management

NGI – Norwegian Geotechnical Institute

NGU – Norway's National Geological Survey

NVE – Norwegian Waterways and Energy Directorate

Table of contents

Abstract

Acknowledgements

Abbreviations

1. Introduction	11
1.1. Motivation.....	12
1.2. Previous research	13
1.3. Aim of the study	15
2. Background.....	19
2.1. Study area	19
2.2. Climate and topography	20
2.3. Permafrost.....	22
2.4. Climate change on Svalbard	24
3. Natural hazards on Svalbard.....	27
3.1. Permafrost degradation	27
3.2. Solifluction.....	28
3.3. Landslides	29
3.3.1. Shallow landslide and debris flow	30
3.3.2. Rockfall.....	31
3.4. Snow avalanche	32
3.5. Erosion	34
3.5.1. Coastal erosion.....	35
3.5.1. Surface erosion and gullyng	36
3.6. Riverine flooding	37
3.7. Weathering.....	38
4. Studied cultural heritage objects	40
4.1. Study objects in Longyearbyen.....	40
4.2. Study objects Ny-Ålesund	43
5. Materials and Methods	46

5.1.	Risk assessment by PCCH-Arctic (Version 1)	47
5.1.1.	Qualitative assessment	47
5.1.2.	Quantitative assessment	48
5.2.	Used data	50
5.2.1.	Geographical information analysis	50
5.2.2.	Literature analysis	51
5.2.3.	Fieldwork in Longyearbyen	51
5.2.4.	Fieldwork in Ny-Ålesund	54
5.3.	Assigning Probability Class scores for Version 2	57
5.4.	Visualization with ArcGIS online	61
6.	Results	63
6.1.	Updated Probability Class scores	63
6.2.	Overall Risk	67
6.2.1.	Results from PCCH-Arctic Risk Assessment Excel tool Version 2	67
6.2.2.	ArcGIS Online map	70
6.2.3.	Summary of the results	74
6.3.	Snow depth measurements in Longyearbyen	77
6.4.	Cultural heritage objects in Ny-Ålesund	79
6.4.1.	Probability Class scores	79
6.4.1.	Overall Risk	79
7.	Discussion	84
7.1.	Svalbard's cultural heritage at risk	84
7.2.	Arctic warming and natural hazards	87
7.3.	Safeguarding cultural heritage	91
7.4.	Comparison between Version 1 and Version 2	92
7.5.	Limitations and need for future studies	94
7.5.1.	Limited data in the Arctic	94
7.5.2.	Predictability of natural hazards	95
7.5.3.	Scope and subjectivity of the assessment	97
8.	Conclusions	99
	References	101
	Appendix	1

Appendices

List of Figures

Figure 1. Geographical location of the study areas in the context of Northern Europe and the archipelago of Svalbard.	20
Figure 2. Illustration of permafrost ground thermal regime. Permafrost regime consists of a layer of frozen ground (light blue) surrounded by seasonally frozen and non-frozen ground (grey). The surface layer, known as active layer (light grey), is affected by the seasonal variation in air temperature (represented by the black line, with blue and red indicating seasonal temperature curves). Permafrost may contain clusters of ground ice (white). From Matveev (2019).	23
Figure 3. Map of the studied CH objects in the Longyearbyen area.	42
Figure 4. Map of the studied CH objects in the Ny-Ålesund. The numbering of the objects corresponds to Table 2.	45
Figure 5. Flow chart illustrating the phases of the thesis and the linkage between Material and Methods to other parts.	46
Figure 6. Snow depth measurements taken using two different types of probes: an avalanche probe (pictured in A, B, and C) and a thicker iron active layer probe (visible in B and C). Photos by Peter Hamrock and the author.	53
Figure 7. Approximate measuring points for the Cable car posts. Black rectangle represents the frame of the object. B-points are approximately 1 m away from the object, whereas C-points are approximately 10 m away from the object.	53
Figure 8. Laser level measurements in Ny-Ålesund. Photos by Noemi Pasquini.	54
Figure 9. Settlement at London houses in Ny-Ålesund. Photo by Anatoly Sinitsyn/SINTEF.	55
Figure 10. Differential settlements of Green Harbour House in Ny-Ålesund, June 23, 2023. Photo by Anatoly Sinitsyn/SINTEF.	56
Figure 11. Terrain settlements at Luftskipsmasta, June 26, 2023. Photo by Anatoly Sinitsyn/SINTEF.	56
Figure 12. Post nr. 9 at the Cable car line 5 that has survived a debris flow, September 3, 2021. Photos by Anatoly Sinitsyn/SINTEF.	58
Figure 13. Example of the procedure for collecting background data for the PC analysis.	59

Figure 14. Assignment of PC scores for Cable car line 1b.....	64
Figure 15. The highest ranked CH objects in the Longyearbyen area in terms of aggregated average risk of Heritage Loss (referred as HL in the figure) (PCCH-Arctic Risk Assessment Excel Tool).....	68
Figure 16. Aggregated risk of Heritage Loss (referred as HL in the figure) from natural hazards to the post nr. 6 on Cable car line 1b (PCCH-Arctic Risk Assessment Excel Tool).	69
Figure 17. Aggregated average risk of Heritage Loss (referred as HL in the figure) for Cable car line 1b (PCCH-Arctic Risk Assessment Excel Tool).	70
Figure 18. Zoomed-out overview of the Cable car lines. The darker the colour, the higher the total risk, i.e. red colour indicating higher risk, yellow the least risk.	71
Figure 19. Pop-up window showing more information about each Cable car line.	71
Figure 20. Zoomed-in overview of the Cable car lines. The darker (redder) and the bigger the symbol of the object, the larger the risk.	72
Figure 21. Symbolology of each CH object. Intervals were determined to be <30%, 30-60%, and >60%.	73
Figure 22. Showing the pop-up window for a CH object.	74
Figure 24. Post Nr. 6 at the Cable car line 5. This post is resting on a small bump/hill that is probably created as a result of frost heave, which is stimulated by absence of snow in winter, September 3, 2021. Photo by Anatoly Sinitsyn/SINTEF.	78
Figure 25. Ranking of the CH objects in Ny-Ålesund in terms of the aggregated average risk of Heritage Loss (PCCH-Arctic Risk Assessment Excel Tool).	80
Figure 26. Contribution of different natural hazards to the risk of Heritage Loss for Luftskipsmasten (PCCH-Arctic Risk Assessment Excel Tool).	81
Figure 27. Overview of the CH objects in Ny-Ålesund. Yellow colour of CH objects indicates a total risk of Heritage Loss below 30%. Luftskipsmasten is coloured orange as it has a total risk of Heritage Loss of 36%.	82
Figure 28. Showing the pop-up window for a CH object in Ny-Ålesund.	83

List of Tables

Table 1. Studied CH objects in the Longyearbyen area (Norwegian name in the parentheses). Descriptions from (<i>Hjem - Kulturminnesøk</i> , no date; Knudsen and Tokle Yri, 2010; Reymert, 2016).	40
Table 2. Descriptions of CH objects in Ny-Ålesund (Norwegian name in parentheses if applicable). Descriptions from (Reymert, 2016).	43
Table 3. PC (left) and CC (right) scores (Bekele & Sinitsyn 2023).	48
Table 4. Lower bound and upper bound probability estimates corresponding to the five PCs (Bekele & Sinitsyn 2023).	49
Table 5. Lower bound and upper bound Heritage Loss estimates corresponding to the five CCs (Bekele and Sinitsyn, 2023).	49
Table 6. Observations of potential hazards based on satellite pictures/ literature. Pictures from (<i>TopoSvalbard - Norsk Polarinstitutt</i> , no date).	60
Table 7. Criteria for evaluating the probability of slope hazards.	61
Table 8. Summary table for the total risk posed by the Cable car lines and other CH objects in Longyearbyen. The table includes three risk categories based on the threshold values from the ArcGIS map: total risk below 30%, between 30 and 60% and above 60%. For the Cable car lines the main natural hazards, contributing to the total risk, are also mentioned.	75

1. Introduction

Climate change is having a profound impact on the Arctic region, and the effects are particularly visible in the Arctic due to the phenomenon known as Arctic amplification. The rate of warming in the Arctic is projected to be up to five to seven times faster than in temperate regions (Hanssen-Bauer *et al.*, 2019; Wickström *et al.*, 2020; Isaksen *et al.*, 2022; Rantanen *et al.*, 2022). This accelerated warming has led to various changes in the Arctic environment, including increased rainfall, melting glaciers and sea ice, a shorter cold season, and an increase in extreme weather events such as floods and storms (Førland *et al.*, 2011; Descamps *et al.*, 2017; Isaksen *et al.*, 2022). Additionally, the Arctic is experiencing degradation of permafrost, leading to significant disruptions such as landslides and erosion (Hanssen-Bauer *et al.*, 2019).

These climate-related disruptions pose not only environmental and societal challenges but also endanger the preservation of cultural heritage (CH) sites (Valagussa *et al.*, 2021). CH refers to monuments, groups of buildings, and sites of exceptional universal value from a historical, artistic, scientific, ethnological, or anthropological perspective (UNESCO, 2021). CH sites in the Arctic provide valuable insights into the history of the region and contribute to the cultural identity of local communities (Lombardo, Tanyas and Nicu, 2020). Natural hazards such as permafrost degradation (Humlum *et al.*, 2003; Etzelmüller *et al.*, 2011; Boike *et al.*, 2018; Hanssen-Bauer *et al.*, 2019), coastal erosion (Jaskólski, Pawłowski and Strzelecki, 2018; Nicu *et al.*, 2020, 2021a; Sinitsyn *et al.*, 2020), surface erosion and gullyying (Martin *et al.*, 2002; Fortier, Allard and Shur, 2007; Nicu *et al.*, 2023), riverine flooding (Hanssen-Bauer *et al.*, 2019; Haverkamp *et al.*, 2022; Meyer, 2022), snow avalanches (Eckerstorfer, 2012; Eckerstorfer, Christiansen, Rubensdotter, *et al.*, 2013; Lofthus, 2020; Hancock, 2021), debris flows and shallow landslides (Martin *et al.*, 2002; Highland and Bobrowsky, 2008; Hungr, Leroueil and Picarelli, 2014), solifluction (Matsuoka, 2001; Hall *et al.*, 2002; Prick, 2003; Harris *et al.*, 2007), rockfalls (Highland and Bobrowsky, 2008; Kuhn *et al.*, 2021), and weathering (André, 1997; Van Everdingen, 1998; Hall *et al.*, 2002; Prick, 2003) can cause significant damage to heritage sites. Therefore, it is crucial to evaluate

the potential risks and assess the natural hazards for the management and preservation of these vulnerable CH sites.

Located between 74° and 81° northern latitudes, Svalbard, an archipelago in the Arctic Ocean, is experiencing some of the most rapid temperature increases (Isaksen *et al.*, 2016; Descamps *et al.*, 2017; Rantanen *et al.*, 2022). The region is rich in CH, making it a significant area to study the impacts of natural hazards and climate change on CH objects. Longyearbyen, the administrative centre of Svalbard, holds historical importance due to its coal mining past, and many remnants of this history form a substantial part of Svalbard's CH.

1.1. Motivation

Svalbard has a unique CH resulting from its proximity to the North Pole and its accessibility through the open waters warmed by ocean currents. Since its discovery by Willem Barentsz in 1596, people from various parts of the world have visited and lived in the archipelago on a seasonal basis, engaging in activities such as hunting, trapping, exploration, research, and mineral resource prospecting and extraction (*Svalbard Archipelago - UNESCO World Heritage Centre*, no date).

In the past, Svalbard was primarily known for hunting commodities such as whale blubber, arctic fox pelts, polar bear furs, and other products from whaling and hunting activities (Prestvold, 2015). However, towards the end of the 19th century, minerals were discovered, and coal emerged as the most significant resource of interest (Prestvold, 2015). Advent city was the first mining town on Svalbard, but coal production there lasted only a few years until 1908 (Knudsen and Tokle Yri, 2010). Some buildings and material were moved to Hiorthhamn, where parts of the building masses are still standing (Knudsen and Tokle Yri, 2010). Longyearbyen was established as the first permanent settlement by the American-owned Coal Company in 1906 but was sold to Store Norske coal company ten years later (Knudsen and Tokle Yri, 2010). Ny-Ålesund was founded in 1916 for coal mining purposes,

but the focus shifted to research after 1963 due to a series of major accidents (Reymert, 2016). In 1920, Norway took over the sovereignty, and an international treaty was signed granting all signatory countries the right to carry out economic activities in Svalbard (*The Svalbard Treaty*, 1920).

The rich CH-presence on Svalbard is a reflection of the extensive exploration and exploitation of its natural resources. All evidence of human activity prior to 1946 is automatically considered as CH and protected under the Svalbard Environmental Protection Act (2001). The CH sites on Svalbard cover different historical eras, from whaling industry to extractive industries, research, and expeditions, and World War II, and encompass buildings or ruins, hunting and fishing equipment, graves, crosses, inscriptions, and any movable objects, and are mainly located in coastal areas due to more human activities near the ocean (Knudsen and Tokle Yri, 2010; Holmgaard *et al.*, 2019; Nicu *et al.*, 2021a). The focus of this study is on technical-industrial CH, which includes the material proofs of coal mining activities in the region. Although Svalbard's CH is not currently listed on the UNESCO World Heritage List (*UNESCO World Heritage Centre - World Heritage List*, no date), the protection of CH in Svalbard is emphasized under various international agreements and regulations. Under The Svalbard Treaty (1920), Norway is obligated to protect the archipelago's natural environment, including its wildlife and CH. Svalbard Environmental Protection Act (2001) explicitly prohibits the destruction, damage, or disturbance of CH sites such as historical buildings, mining structures, and cemeteries. Moreover, Svalbard falls under the jurisdiction of the Norwegian Cultural Heritage Act (1978), which safeguards CH sites throughout Norway.

1.2. Previous research

A considerable body of research has been conducted on climate and natural hazards in Svalbard, providing valuable insights into the changing environment and its potential impacts on CH sites. The recent climate report by Hanssen-Bauer *et al.* (2019) reported the long-term impacts of climate change in Svalbard. While the report does not provide a detailed analysis of natural hazards, it acknowledges the likelihood of their interaction with

the changing climate, particularly emphasizing the impact of climate change on permafrost degradation. Isaksen et al. (2016, 2022) have contributed to the understanding of temperature changes in Svalbard, analysing the regional trends and variations. Similarly, (Førland *et al.*, 2011) studied the temperature and precipitation development at Svalbard from 1900 to 2100.

Different hazard mapping studies have been carried out in small select areas of Svalbard to assess the risks of natural hazards such as snow avalanches, landslides, floods, and rock falls. Two studies, one conducted by Multiconsult in 2016 (Multiconsult, 2016) and another by Skred AS in 2022 (Skred AS, 2022), were financed by the Norwegian Waterways and Energy Directorate (NVE). The studies mapped slope hazards in some parts of Longyearbyen and identified areas that are most at risk. Even though, these studies do not provide specific projections for future climate change impacts on slopes, they suggest that climate change may lead to changes in the frequency and intensity of natural hazards in Svalbard and highlight the need for ongoing monitoring and risk assessments.

In the context of CH sites, several studies have focused on developing hazard mapping frameworks to identify and assess risks. Nicu et al. (2021, 2022, 2023) have studied thaw slumps and gully erosion in Svalbard, projecting the potential impacts of these phenomena on CH. They have contributed to understanding the vulnerabilities of CH sites to specific hazards. Additionally, Nicu et al. (2020, 2021b) examined how coastal erosion affects one complex CH site in central Svalbard (Hiorthhamn), highlighting the importance of considering shoreline dynamics in preservation efforts. Beyond Svalbard, broader studies have explored the impacts of climate change on historical sites worldwide. For example, Sesana et al. (2021) conducted a literature review on the impacts of climate change on CH studying different climate stressors and their effects on CH. Specific to arctic regions, Hollesen et al. (2018) examined the impacts of climate change on the archaeological and environmental archives, discussing the damage caused by hazards such as coastal erosion and permafrost thaw. Similarly, Boro and Hermann (2020), have focused on understanding the implications of climate change for historical sites in the northern areas, providing guidance and tools for managing the risks. Barr and Chaplin (2004, 2008, 2011) conducted research on the importance of preserving and managing polar heritage, acknowledging the

challenges and dangers facing polar heritage due to natural processes and changing climate conditions.

The Norwegian Geotechnical Institute (NGI) has been actively involved in researching natural processes in Svalbard and Longyearbyen since 1985. NGI's research primarily centres on understanding the natural processes shaping the landscape and assessing the hazards they pose to human settlements and infrastructure. Areas of focus include permafrost degradation, landslides, rockfalls, avalanches, and glacial melt. The research conducted by NGI contributes to the broader understanding of natural hazards in Svalbard and provides insights into their potential impacts on CH sites.

Various sources provide general information and resources about CH in Norway, including The Norwegian Directorate for Cultural Heritage (Riksantikvaren, no date), and the National Heritage Database (Askeladden) and Cultural Heritage Search (Kulturminnesøk, no date) provided by them. These sources are valuable references for understanding and managing CH in Svalbard. Additionally, the Governor of Svalbard has conducted studies (e.g. Knudsen and Tokle Yri, 2010; Skauen Sandodden, Tokle Yri and Solli, 2013; Reymert, 2016), that explore CH around Svalbard, particularly in the Longyearbyen area and Ny-Ålesund. These reports contribute to the knowledge base of CH in the region and provide insights into its significance and vulnerabilities.

1.3. Aim of the study

The previous efforts of CH preservation in Svalbard have largely focused on individual objects or infrastructures within close proximity to each other, leading to a gap in comprehensive research on the general risks posed by natural hazards to CH objects across larger areas. Despite the high-priority designation of the most valuable CH objects in Svalbard's catalogue of the cultural heritage sites (Skauen Sandodden, 2013), there is a lack of prioritization for their restoration in the management plan (Skauen Sandodden, Tokle Yri and Solli, 2013). Additionally, projections regarding the long-term impacts of climate change on natural hazards and their effects on CH in Svalbard are lacking.

In 2022, the Polar Climate and Cultural Heritage - Preservation and Restoration Management (PCCH-Arctic) project (Sinitsyn *et al.*, 2022), funded by the Research Council of Norway, conducted a pilot study that aimed to address the aforementioned gap with point evaluations of CH objects in Longyearbyen and Ny-Ålesund. The PCCH-Arctic project, running from 2021 to 2024, seeks to develop a knowledge base for the sustainable preservation and future utilization of CH in the Arctic, considering the changing climate and demographic conditions. Collaboration for the project involves SINTEF, the University of Oslo (UiO), the Norwegian Meteorological Institute (MET), the University Centre in Svalbard (UNIS), and user partners including the Municipality of Longyearbyen (Longyearbyen Lokalstyre), Store Norske Spitsbergen Kulkompani (SNSK), Kings Bay AS, and Svalbard Museum. This thesis builds upon the pilot study conducted by the PCCH-Arctic project, expanding both the scientific and process aspects of the evaluation, while also acting as a detailed quality control of the primary estimations. Furthermore, an emphasis is put on structuring the datasets in GIS environment and developing an interactive communication tool based on the expanded evaluations from this project.

Both the pilot study (referred to as Version 1) and the expanded assessment (referred to as Version 2) assesses the risks of natural hazards in total on 260 CH objects including Cable car posts (taubanebukker) in Longyearbyen and other CH objects in Hiorthhamn and Ny-Ålesund. These locations contain the largest collection of CH objects in Svalbard, with Longyearbyen hosting around 212 Cable car posts and several other structures, and Ny-Ålesund housing 29 protected buildings of the highest historical value. These CH objects are among the most visible traces of the mining activities, and clearly show the strong impact of the mining activities left in the town and the immediate surrounding area. This study provides an expanded scope and detail to the primary assessment by PCCH-Arctic for a comprehensive understanding of the vulnerabilities and potential risks faced by the CH in Svalbard. To achieve the aim of the study, the following research hypotheses (RH) are developed, and research questions (RQ) are addressed:

RH1: Natural hazards pose a significant risk to Svalbard's CH.

RH2: The projected climate warming amplifies the frequency and probability of most natural hazards affecting CH in Svalbard.

RQ1: Which of the studied CH objects in Longyearbyen and Ny-Ålesund are most at risk to natural hazards?

RQ2: What natural hazards are affecting the studied CH objects in Longyearbyen and Ny-Ålesund and how are the hazards distributed relatively among them?

RQ3: How is climate change assumed to affect the occurrence of natural hazards in Svalbard?

The study employs a multidisciplinary approach that integrates literature analysis, geographical information analysis, data from PCCH-Arctic Risk Assessment, and fieldwork. This approach provides both qualitative and quantitative inputs to develop Version 2 of the PCCH-Arctic Risk Assessment Version 1 (Bekele and Sinitsyn, 2023). Probabilities of natural hazards will be re-evaluated and inputted into PCCH-Arctic Risk Assessment Excel Tool, from where the updated risk assessment results will be transferred to GIS for visualization using ArcGIS online. The assessment will be extended to incorporate the impact of climate change, considering a 50-year assessment period. The natural hazards considered in the study include permafrost degradation, solifluction, debris flow, shallow landslides, rockfalls, snow avalanches, coastal erosion, riverine flooding, surface erosion and gully, and weathering, as these are recognized as significant hazards in Svalbard. Some data collected during field activities during the thesis writing process, will be utilized in the broader PCCH-Arctic project, although not directly incorporated into this specific study.

The updated risk assessment and the created interactive ArcGIS visualization map allow for a comprehensive understanding of the potential risks that natural hazards pose to individual CH objects as well as summarized risks for connected groups of CH objects (Cable car lines) in the region. This knowledge can then be used to develop effective management strategies to mitigate the risks and ensure the preservation of these sites for future

generations. By identifying the specific areas at risk, targeted interventions can be facilitated and resources for risk management prioritized, which is particularly important in remote and hard-to-access areas like Svalbard, where resources are limited. Moreover, the knowledge and approach derived from this study have broader applicability beyond Svalbard, in places where natural hazards pose threats to CH objects, and new tools for evaluation and communication of hazard and risks are needed or can be helpful/important.

The thesis is structured as follows: Chapter 2 introduces the study area and its climate setting, establishing the contextual background for the research. Chapter 3 delves into the natural hazards prevalent in the study area, providing a comprehensive overview of the potential risks faced by CH. In Chapter 4, the studied CH objects are explored in detail. Chapter 5 outlines the materials and methods employed in the study. The obtained results are presented in Chapter 6, followed by a discussion in Chapter 7. Finally, Chapter 8 summarizes the key findings and presents concluding remarks.

2. Background

The distinct geographical and climatic setting of Svalbard, characterized by polar conditions and prevailing permafrost have a profound impact on the region's landscape and infrastructure. Consequently, this chapter aims to provide an understanding of the geographical, climatic and environmental context of the study area, needed for comprehending the study's findings on CH objects. It covers the location, climate and topographic setting of the study area, along with an examination of the characteristics of permafrost and the existing and projected impacts of climate change on Svalbard.

2.1. Study area

Svalbard is an Arctic Archipelago, located between 74° and 81° degrees north, about midway between Norway and North Pole. The study area is located on Spitsbergen, the largest island within the Svalbard archipelago. Spitsbergen can be characterized as a landscape with mountains, valleys, and a long coastline. The coastal areas comprise rugged cliffs and rocky beaches, while the inland areas are dominated by glaciers and barren tundra landscapes. The study contains CH objects in the vicinity of Longyearbyen, Hiorthhamn, and Ny-Ålesund (Figure 1). Longyearbyen, the primary settlement and administrative centre of Svalbard, serves as a hub for CH sites. It is home to approximately 2,500 residents, making it the most populous area on Svalbard (*Population of Svalbard*, 2023). The CH objects around Longyearbyen are located in diverse, ranging settings from relatively flat terrain to steep slopes. Hiorthhamn, located on the opposite side of the Adventfjorden, lies approximately three kilometres away from Longyearbyen. The CH sites in Hiorthhamn are situated in a relatively flat and open area near the shoreline. This settlement rests at the base of the Hiorthfjellet mountain, which reaches a height of 926 meters (*TopoSvalbard - Norsk Polarinstitutt*, no date). Ny-Ålesund stands approximately 100 kilometres northwest of Longyearbyen. It holds the title of being the northernmost permanent year-round settlement on Earth. Ny-Ålesund hosts 16 research stations and accommodates a year-around population of around 35 individuals alongside up to 180 researchers during summer

(Dallmann, 2015). The CH objects in Ny-Ålesund are located on a flat and open ground, primarily within the town area.

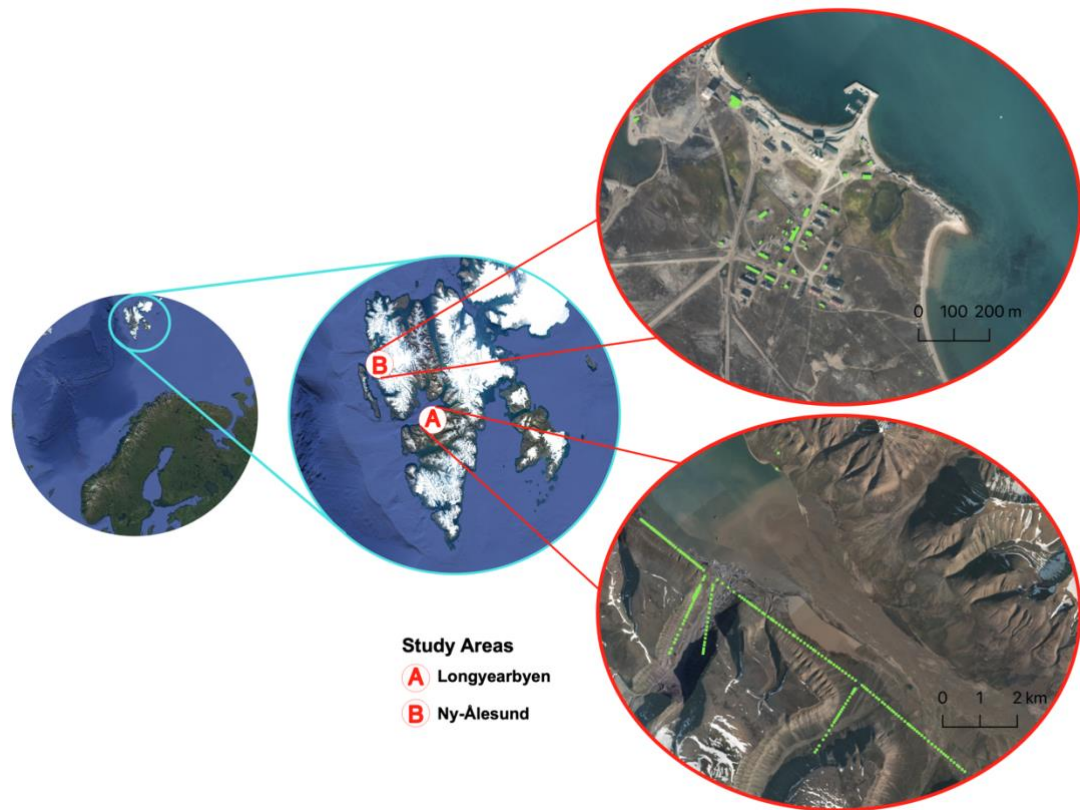


Figure 1. Geographical location of the study areas in the context of Northern Europe and the archipelago of Svalbard.

2.2. Climate and topography

The topography and geomorphology of Svalbard is very diverse, influenced by many geological eras seen in the bedrock types and tectonic variability. Parts of the islands are dominated by horizontally laminated sedimentary rocks, while other parts have tectonically deformed and metamorphosed sequences forming near-vertical structures in the bedrock strata, which creates a more sharply alpine topography. The area around Longyearbyen features plateau mountains and U-shaped valleys with steep to moderately steep slopes. These large-scale landforms are developed into semi-horizontal sedimentary bedrock

formations dominated by coal-bearing sequences, horizontally layered shales, sandstones and siltstones (Dallmann, 2015). In contrast more northerly positioned town of Ny-Ålesund is situated on a low-lying flat raised-beach with only thin cover of weathering materials and beach/marine deposits and little geomorphology (Miccadei, Piacentini and Berti, 2016).

Svalbard's climate falls under the polar tundra category according to the Koeppen-Geiger climate classification (Eckerstorfer and Christiansen, 2011a). Longyearbyen experiences a mean annual air temperature of -2.3 °C, while Ny-Ålesund records -2.5 °C (MET Norway, 2023). In terms of precipitation, Longyearbyen receives an average of 221mm annually, whereas Ny-Ålesund receives over half more, with 544 mm (10-year averages from 2013-2022) (MET Norway, 2023). When comparing the temperatures and precipitation levels to other areas located at the same latitudes, the climate in Svalbard is considerably more temperate (Hanssen-Bauer *et al.*, 2019; Pedersen *et al.*, 2022).

Svalbard's general climate is affected by various atmospheric and oceanic factors such as ocean currents, thermal air masses, and sea ice coverage (Hanssen-Bauer *et al.*, 2019; Wickström *et al.*, 2020). The warm water from the West Spitsbergen current flows along the west coast of Svalbard, while the east coast is influenced by cold polar water (Eckerstorfer and Christiansen, 2011a). Consequently, the west coast experiences less sea ice compared to the east coast (Søreide *et al.*, 2020; Isaksen *et al.*, 2022). This circulation pattern impacts the transfer of heat from the ocean to the lowermost atmosphere, leading to reduced moisture levels and air temperatures in the west coast (Wickström *et al.*, 2020; Isaksen *et al.*, 2022).

Airflows over Svalbard are mainly influenced by two pressure systems: the low-pressure system close to Iceland, and the high-pressure system over Greenland (Hanssen-Bauer *et al.*, 2019). The North Atlantic Cyclone track brings moist air with mild temperatures, leading to warmer conditions, while the alternation between cold anticyclonic air from the east and northeast and moist cyclonic air masses causes cold, clear weather and significant temperature fluctuations during winter (Hanssen-Bauer *et al.*, 2019). Additionally, weather events such as the Siberian high, a cold anticyclonic over eastern Siberia, contribute to winter temperature and precipitation patterns. When cold air spreads over Europe, the flow of air

over the Nordic Sea becomes strong and southerly, causing warm air to move towards Svalbard and resulting in heavy precipitation (Humlum *et al.*, 2003; Eckerstorfer and Christiansen, 2011a).

The wind patterns on Svalbard are greatly affected by the topography and pressure systems. The majority of winds flow through fjords and valleys, with a prevailing direction from the southeast (Eckerstorfer and Christiansen, 2011a). During winter storms the direction often shifts to the west or southwest. The channelling effect through valleys results in higher average wind speeds compared to plateaus, with the highest speeds occurring from November to February (Christiansen, Humlum and Eckerstorfer, 2013). Svalbard's snow climate classified as a "High Arctic maritime snow climate" (Eckerstorfer and Christiansen, 2011a), is highly influenced by wind patterns, leading to high wind speeds, snow drifting, and variations in snow coverage, ranging from snow-free patches to areas with several meters of snow. Throughout most of the winter, the snowpack remains cold but the maritime influence in the region leads to occasional warm spells and rain-on-snow events, resulting in significant melting (Eckerstorfer and Christiansen, 2011a). The snowpack in Svalbard persists for 8 to 10 months (Eckerstorfer, 2012).

2.3. Permafrost

In Svalbard, 60% of the archipelago is covered by glaciers, while the remaining area is permafrost (Humlum *et al.*, 2003). Permafrost refers to ground that remains at or below 0 °C for a minimum of two years and is widespread in high latitude or high elevation regions globally (Van Everdingen, 1998; Boike *et al.*, 2018; Biskaborn *et al.*, 2019; Matveev, 2019). Its spatial distribution and depth are influenced by regional and global climate factors as well as local conditions such as slope angle and aspect, surface water, vegetation, and snow cover (Etzelmüller *et al.*, 2011). These factors also determine the degree to which air temperatures influence the ground temperature conditions, i.e., the thermal regimes. Permafrost temperatures are higher near the coastline due to the ocean's heat source, while thick snow cover reduces permafrost depth (Humlum *et al.*, 2003; Christiansen *et al.*, 2020). Generally,

total permafrost depth increases with higher latitudes, and on Svalbard ranges from 100 m near the coastlines to around 400 m in higher areas (Dallmann, 2015).

Permafrost consists of three main layers: the active layer, the perennially frozen permafrost layer, and the unfrozen bedrock or soils beneath the permafrost (Boike *et al.*, 2018) (Figure 2). The active layer is the uppermost layer of the permafrost, which thaws in the summertime and freezes in the wintertime (Matveev, 2019). It plays a crucial role in permafrost systems as it effectively buffers permafrost from warm summer air temperatures. Changes in ground surface conditions or summer climate patterns can affect the depth of the active layer. On Svalbard, the active layer has a thickness ranging from 0.8 m to 2.5 m (Kuhn *et al.*, 2021).

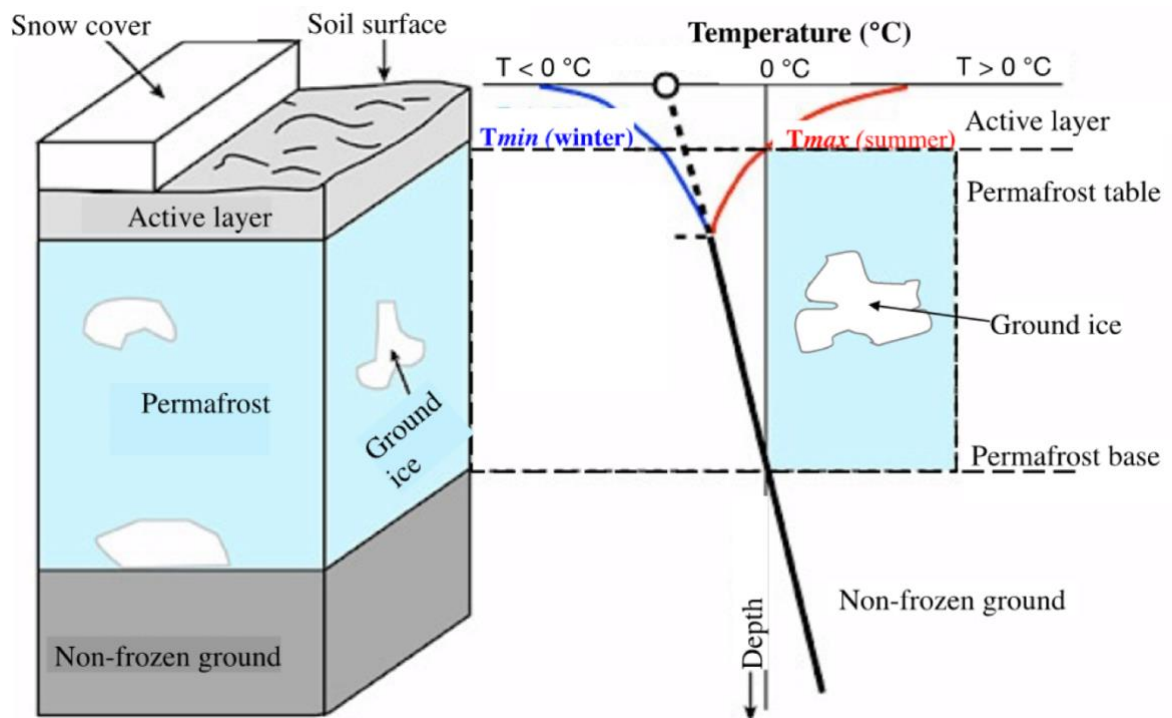


Figure 2. Illustration of permafrost ground thermal regime. Permafrost regime consists of a layer of frozen ground (light blue) surrounded by seasonally frozen and non-frozen ground (grey). The surface layer, known as active layer (light grey), is affected by the seasonal variation in air temperature (represented by the black line, with blue and red indicating seasonal temperature curves). Permafrost may contain clusters of ground ice (white). From Matveev (2019).

Ground ice, which refers to ice between solid particles in frozen soil both in the active layer and the perennially frozen soil, is a crucial part of the permafrost system on Svalbard. It serves two important functions. Firstly, ground ice can cause significant pressure changes and material redistribution, resulting in ground movement and shape changes, a process known as frost heaving (Van Everdingen, 1998). Secondly, it alters the physical properties of the ground, changing how the ground interacts with its surroundings and responds to external forces (Christiansen *et al.*, 2020). The permafrost in Svalbard's sedimentary lowlands is typically ice-rich, implying that a greater amount of energy is required to thaw the ice within the permafrost layer (Dallmann, 2015). However, when the ice melts, it can lead to ground settlement and changes in the landscape.

Snow serves as an effective thermal insulator, reducing the heat flow from the ground, ice on bodies of water, or man-made structures when they are covered by snow (Uwera, 2019). The insulating effect of snow on ground temperature arises from its composition of frozen water and air, which results in a low thermal conductivity. The insulation capacity of snow remains relatively constant above a snow depth of 25 cm (Burke *et al.*, 2020). In winter, the cooling of the ground coupled with the presence of a snow cover hinders the heat exchange between the ground and the atmosphere, resulting in a reduced ability for heat escape from permafrost soils (Instanes, 2016). As a consequence, increased snow cover can lead to thicker active layer in the subsequent summer and elevated temperatures of permafrost at deeper depths (Instanes, 2016).

2.4. Climate change on Svalbard

Climate change has led to significant changes in temperature patterns and precipitation levels. Between 2001 and 2015 the average annual temperature for Longyearbyen/Svalbard Airport increased by 2.5 °C, while in Ny-Ålesund, it increased by 1.8 °C compared to the period from 1971 to 2000 (Isaksen *et al.*, 2016). Average temperatures have increased in all seasons, but the greatest increases have occurred in winter and spring (Førland *et al.*, 2011; Isaksen *et al.*, 2016; Hanssen-Bauer *et al.*, 2019). Over the years, there has been a notable

shift in the frequency of days with specific temperature ranges. Comparing the period from 1961 to 1990, with the period from 1991 to 2018, there has been an increase of 25 days in the number of annual days with temperatures exceeding 0 °C and an increase of 22 days with temperatures exceeding 5 °C (Nordli *et al.*, 2020). Conversely, the number of days with temperatures colder than -10 °C and -20 °C has decreased by 42 days and 27 days, respectively (Nordli *et al.*, 2020). These warming trends have led a decrease in sea ice extent in the whole Barents Sea since the 1980s, with winter sea ice concentration dropping from 40-50 % to 15-25 % during the period from 2011-2020 (Isaksen *et al.*, 2022). These changes align with projections that indicate further temperature increases and rapid climate shifts in Svalbard (Førland *et al.*, 2011; Nordli *et al.*, 2014; Gjelten *et al.*, 2016; Descamps *et al.*, 2017; Hanssen-Bauer *et al.*, 2019; Isaksen *et al.*, 2022). Climate models suggest that by 2071-2100, Svalbard could experience warming of around 3 °C, 6 °C, and 10 °C for the RCP2.6, RCP4.5 and RCP8.5 scenarios respectively, compared to the period from 1971-2000 (Hanssen-Bauer *et al.*, 2019). RCPs are the representative concentration pathways defined by IPCC (IPCC, 2021) where RCP2.6 is the best scenario, RCP4.5 the medium scenario and RCP8.5. the worst-case scenario.

Precipitation data from Longyearbyen/Svalbard airport, collected since the 1910s, reveals a consistent increase in annual precipitation at rate of 3% to 4% per decade (Førland *et al.*, 2020). Solid precipitation has shown a decrease of 11 to 32 % over the past 50 years at all studied stations (Bjørnøya, Hopen, Svalbard Airport, and Ny-Ålesund), whilst the amount of liquid precipitation has increased by 3-46% during the same time period (Førland *et al.*, 2020). Winter events resulting in rain-on-snow will have a significant impact on local conditions and infrastructure (Wickström *et al.*, 2020). This trend is expected to continue, accompanied by the likelihood of more extreme weather events such as heavy rain (Hanssen-Bauer *et al.*, 2019; Pedersen *et al.*, 2022). For example, Førland *et al.* (2011), project a potential 12% increase in annual precipitation since 1981 in the Longyearbyen area by the year 2100. However, it should be noted that obtaining accurate precipitation measurements is challenging due to the harsh weather conditions in the Arctic (Førland *et al.* 2011).

The shifting climate patterns will have significant impacts on the permafrost of Svalbard. These impacts will be explored in greater detail in the upcoming chapter, which focuses on natural hazards in Svalbard, introducing permafrost degradation in Chapter 3.1.

3. Natural hazards on Svalbard

Natural hazards are events and processes that occur in nature without human interference. They can involve for instance, movement of material or erosion or gravitation, and can become disastrous when causing significant harm to people, natural systems and infrastructure. This chapter introduces the most common natural hazards in Svalbard and their relation to physical setting such as slope, geology and waterways.

3.1. Permafrost degradation

Permafrost degradation consists of thickening of the active layer during summer, warming of permafrost at depth, and development of residual thaw zones (taliks) (Esch and Osterkamp, 1990). Permafrost limits groundwater flow and stabilizes frozen, loose sediments (Frederick *et al.*, 2016). As the thaw depth surpasses the depth of seasonal freezing, taliks (unfrozen patches of ground) will start to form (Esch and Osterkamp, 1990). Increasing temperatures and water presence can also lead to the development of thermokarst, which includes landform changes such as surface depressions and uneven terrain or the formation of lakes, ponds and wetlands (Uwera, 2019). The ongoing thawing at the permafrost table will lead to continuous settlement caused by the melting of ice within ice-rich permafrost. Therefore, permafrost thawing, and degradation can have wide-ranging effects on processes that shape both physical and human environment.

Climate change exacerbates the degradation of permafrost. Temperature projections suggest a continued rise in the number of warm days (plus degree days) and decrease in the number of frost days resulting in longer thaw season and increased active layer depths and higher permafrost temperatures (Biskaborn *et al.*, 2019; Hanssen-Bauer *et al.*, 2019). Particular vulnerable are low-lying and well-drained areas where taliks may form (Etzelmüller *et al.*, 2011; Hanssen-Bauer *et al.*, 2019). According to Etzelmüller *et al.* (2011) substantial degradation is not likely to occur before around 2060 in regions that are undisturbed by human activity. Zheng *et al.* (2019) modelled the effects of river flow on permafrost and

found out that advancing spring flood season will warm permafrost more than extended warm season.

Calculations by Enevoldsen (2022) suggest that the active layer could increase up to two meters by 2050 in Svalbard, leading to elevated ground temperatures and decreased strength of the frozen soil. Permafrost in Svalbard has already experienced annual warming of 0.06 to 0.15 °C since 2009 at 10m depth (Hanssen-Bauer *et al.*, 2019). Thawing permafrost releases GHG emissions, creating a feedback loop that amplifies climate change (Biskaborn *et al.*, 2019). Furthermore, degrading permafrost conditions reduce slope stability (Uwera, 2019), through ground shear strength, loss of ice/rock interlocking, an increase in hydraulic permeability, and ice segregation (Saemundsson, Morino and Conway, 2021). These factors contribute to the potential of more frequent and larger slope failures in the future.

3.2. Solifluction

Solifluction is a slow downslope soil movement process, also referred to as gelifluction in permafrost regions (Van Everdingen, 1998), that is caused by the freeze-thaw cycles, in areas where higher vegetation is sparse or lacking (Highland and Bobrowsky, 2008; Hanssen-Bauer *et al.*, 2019; Saemundsson, Morino and Conway, 2021). It is the primary form of slow mass moving in Svalbard, influenced by seasonal frost heave, thaw consolidation and rainfall in the summer (Harris *et al.*, 2011). The solifluction surface soil is often patterned on the surface due to differential soil heaving, and often forms trails downslope (Highland and Bobrowsky, 2008), including sheets, lobes, stripes, steps, creeps (Akerman, 2005). The downslope displacement of soil is typically no more than 1 meter per year (Matsuoka, 2001; Saemundsson, Morino and Conway, 2021), however, solifluction lobes and sheets may move faster (Matsuoka, 2001). Also, steep debris slopes are very susceptible for solifluction (De Haas *et al.*, 2015). In the Norwegian sediment classification system (Norwegian SOSI-standard for quaternary geological maps), two types of solifluction sediments are identified: stone-rich solifluction material and fine-grained organic-rich solifluction soil (Rubensdotter, 2022).

While solifluction is a natural process, climate change may influence solifluction activity by controlling the thermal and moisture regimes near the ground surface (Matsuoka, 2001). One of the main ways in which climate change may impact solifluction is through changes in ground freezing conditions. Long-term warming can alter the ground freezing condition, which can affect solifluction in several ways. A warm summer in the colder regions can lead to partial thawing of ice-rich permafrost, resulting in temporary increase in the depth and speed of soil movement (Matsuoka, 2001; Hanssen-Bauer *et al.*, 2019). In addition, changes in the vegetation cover due to climate change, could also impact solifluction as vegetation helps to stabilize the soil and reduce the impact of freeze-thaw cycles, thus decreasing solifluction movement (Matsuoka, 2001). Changes in precipitation patterns may also impact solifluction with greater rainfall in autumn or meltwater from late laying snow, possibly enhancing solifluction. In sum, solifluction is relevant as hazard primarily through slow destabilization and deformation of structures built on and in the active layer zone. This is relevant primarily for the valley bottoms in the Longyearbyen area.

3.3. Landslides

Landslides can be categorized based on the materials involved and types of movement. Materials could be divided into; rocks and boulders, clay, mud, silt, sand, gravel, peat, and ice, whereas movement ranges between falls, slides, flows, topples, spreads, and slow slope deformations, as classified by Hungr, Leroueil and Picarelli (2014) for temperate regions. Common to all types of landslides is the term “failure” that initiates the process of movement. The combined effect of climatic factors such as changing precipitation patterns, increasing permafrost degradation and active layer thickness are likely to result in higher number of different slope failures in the future (Hanssen-Bauer *et al.*, 2019; Kuhn *et al.*, 2021). Some common landslides in Svalbard include debris flows, shallow landslides, and rock falls, which will be further explained below.

3.3.1. Shallow landslide and debris flow

Shallow landslides are rapid movements of unsaturated material and organic debris downslope, occurring when a shallow flow of loose material slides on a flat surface parallel to the ground (Hungr, Leroueil and Picarelli, 2014). These types of landslides usually occur at steep gradients and often deposit material at changes in slope along the transport path (Martin *et al.*, 2002). Shallow landslides consist of debris slides and debris avalanches, which differ based on their degree of saturation and cohesion (Hungr, Leroueil and Picarelli, 2014). Shallow landslides can initiate debris flows. These types of landslides can be triggered by extreme meteorological factors, such as intensity of rainfall during summer months, average yearly summer air temperatures, and thawing degree days (Martin *et al.*, 2002; Hungr, Leroueil and Picarelli, 2014).

Debris flows are a fluid continuation of shallow landslides or other increased water triggered surface erosion of sediment in for example small creek or steep channels (Hungr, Leroueil and Picarelli, 2014). They are characterized by rapid turbulent downhill movement of sediment in tracks (Highland and Bobrowsky, 2008; Hungr, Leroueil and Picarelli, 2014). The introduction of water from sources such as rainfall or snowmelt can trigger debris flows, which often occur repeatedly in the same location, following previous paths of destruction (Andre, 1990). Debris flows typically exhibit distinct characteristics, prominently featuring levees that run parallel to the central track and terminal depositional lobe or lobes (Andre, 1990; Saemundsson, Morino and Conway, 2021). As material moves downhill it often erode the underlying slope material and add it to the flow (Highland and Bobrowsky, 2008).

Sedimentary sandstones, siltstones, and shales found around the Longyearbyen area have yielded a wide range of sediments through weathering and abrasion processes (e.g. glacial erosion or erosion by snow avalanches), including many fine-grain sediments that are ideal for the formation of debris flows, in combination with the steep hillslopes and the presence of permafrost (De Haas *et al.*, 2015). Debris flows occurring in Svalbard are primarily associated with steep gradients exceeding 30-35° (Andre, 1990). Debris flows can be extremely fast-moving and destructive, with velocities that can reach up to 80 km/h in

valleys below steep cliffs (Dallmann, 2015). The speed of the flow is influenced by the steepness of the slope and the degree of water saturation in the mass, with steeper slope and higher water saturation leading to faster flow velocities (Dallmann, 2015). Debris flows are most commonly associated with the melting season, but they can occur at any time when the temperature is above 0 °C (Dallmann, 2015). Andre (1990) noted that the debris flows on Svalbard tend to be relatively small in size. This is attributed to the limited depth of the active-layer, which constrains the volume of available debris, thereby restricting the overall volume of debris flows.

Permafrost is a significant internal factor in the occurrence and triggering of debris flows and shallow landslides on Svalbard. This is because permafrost acts as a barrier to water percolation, which can lead to accumulation of excess water in the soil and very high pore-water pressures in the sediment just above the freezing-horizon (Andre, 1990). Therefore, active layer melting in the summertime combined with heavy rainfall, leads to excess water, that cannot be absorbed into the lower ground (Andre, 1990; Hanssen-Bauer *et al.*, 2019; Nicu, Lombardo and Rubensdotter, 2021). The high water-content above the permafrost surface leads to locally high pore-water pressure which can trigger failures of the surface sediment. The high inter-sediment water content also reduces friction between particles which may accelerate shallow failures (called active-layer detachments) into debris flows, if occurring on steep enough slopes (Nicu, Lombardo and Rubensdotter, 2021). The initial failure opens up new frozen ground to further thaw, release of ground-ice and potential failure, leading over time to the developments of larger depressions (called retrogressive thaw slides) (Nicu *et al.*, 2022). Shallow landslides are relevant on most of Longyearbyen slopes, while debris flows are relevant primarily for the steeper slopes (>20 degrees).

3.3.2. Rockfall

Rockfalls are caused when single rocks detach from cliffs and fall abruptly downward, impact the slope below and often continue some distance through rolling or bouncing on the slope (Highland and Bobrowsky, 2008). Impact with ground or obstacles can break the rocks into smaller pieces. Larger rocks tend to travel further due to greater weight and velocity.

Rockfalls usually occur on steep or vertical slopes (Highland and Bobrowsky, 2008). Smaller rockfalls could be activated by freeze-thaw events of permafrost but larger rockfalls usually arise from long-term geological processes (Hanssen-Bauer *et al.*, 2019). Around Longyearbyen area, the sedimentary sandstones, siltstones, and shales have weak to moderate rock mass strength, resulting in high rates of rock wall weathering and rockfalls (De Haas *et al.*, 2015). This is especially true for steep northwest facing slopes where cornice fall avalanches cause intensive erosion (Siewert *et al.*, 2012; Eckerstorfer, Christiansen, Vogel, *et al.*, 2013).

Projected increasing precipitation and warming permafrost are likely to weaken the rock mass through expanding joints and melting ice, thus leading to higher number of rock slope failures (Kuhn *et al.*, 2021). Melting decreases rock mass' shear strength but also increases the water level, which advances permafrost degradation through heat input (Kuhn *et al.*, 2021). Permafrost degradation on the other hand could affect the triggering of larger rockslides (Kuhn *et al.*, 2021). Rockfalls are relevant primarily for the steep slopes, with near-vertical cliff faces, in the Longyearbyen area.

3.4. Snow avalanche

Snow avalanches are a sudden release of snowpack and are a common type of slope process in cold climates, particularly in steep terrains with high snowfall (Hancock, 2021). The occurrence of avalanches is determined by a complex interplay between terrain, weather, and snowpack conditions. Terrain characteristics define the areas where avalanches are likely to occur, while weather conditions, such as snowfall and wind, affect the current state of the snowpack (Hancock, 2021). The characteristics of the snowpack, including its metamorphic processes, also play a significant role in determining the type of avalanches that can occur. Snow metamorphism can cause the snow layer to become either stronger, with snow crystals easily attaching to each other, or weaker, with bonds between snow crystals being difficult to form (Hancock, 2021). Warm air masses or large temperature fluctuations are the most common triggers of avalanches on Svalbard (Eckerstorfer and Christiansen, 2011). These conditions can cause changes in the snowpack's stability, making

it more prone to failure. Snow avalanches can occur in both as dry and wet forms. Avalanche activity in Longyearbyen has been found to greatly increase towards the end of the season, most releases occurring in April and May (Eckerstorfer and Christiansen, 2011).

Slab avalanches are generally the most common type of avalanche on Svalbard (Engeset *et al.*, 2020), however, according to Eckerstorfer and Christiansen (2011b) cornice fall avalanches are more common around the Longyearbyen area due to suitable topography of plateau mountains and rather constant wind causing snow drift to the plateau edges. Slab avalanches typically occur on slopes steeper than 30° , most often releasing on gradients between 35 and 40° (Eckerstorfer, 2012; Harvey *et al.*, 2018). They usually result from a collapse in weak layer, that causes the above slab layer to move downhill (Eckerstorfer, 2012). These types of avalanches are in general the largest (Eckerstorfer and Christiansen, 2011a) and the most detrimental to both human lives and infrastructure globally (Harvey *et al.*, 2018). This can also be seen from two recent large-scale avalanches in Longyearbyen in 2013 and 2015, where houses were destroyed and two people died in the latter occurrence (Engeset *et al.*, 2020). Slab avalanches occur often after a winter storm, where precipitation and strong wind leads to snowdrifts and slab development (Eckerstorfer and Christiansen, 2011a).

Cornices often build up on the lee sides of slopes as a result of snowdrift coming from the large mountain plateaus. The prevailing South-East wind direction in the snow season causes cornices to be most frequent on West and North-West oriented slopes (Eckerstorfer and Christiansen, 2011a), as documented in multiple studies around Longyearbyen (Eckerstorfer, 2012; Vogel, Eckerstorfer and Christiansen, 2012). If the built-up snow collapses, it creates a cornice fall avalanche. As a secondary product, cornice fall avalanches can create loose snow avalanches or slab avalanches (Eckerstorfer and Christiansen, 2011b). Cornice fall avalanches tend to occur more often towards the end of the winter season when the weather is getting warmer (Eckerstorfer and Christiansen, 2011b).

Other types of avalanches are loose snow avalanches and slush avalanches. Loose snow avalanches start from a point of cohesionless snow, often dispersing into triangle formation

(*Glossary – EAWS, 2023*). They are commonly smaller than slab avalanches often occurring from May onwards (Eckerstorfer and Christiansen, 2011a). In slush avalanches the snowpack has a high water concentration and they are released due to heavy melting or rain (*Glossary – EAWS, 2023*). They can transfer high amounts of land with them and thus they are regarded very dangerous for humans and infrastructure. Slush avalanches can occur on slopes with considerably less inclination (*Glossary – EAWS, 2023*).

Extreme events such as heavy rainfall and snowfall and strong winds are likely to increase in the future (Hanssen-Bauer *et al.*, 2019). However, understanding their specific influence on the snow avalanche regime in Svalbard is a more complex matter. Hanssen-Bauer *et al.* (2019) project that, wet snow avalanches and slush avalanches are likely to become more frequent in the future due to warmer winters and increased rain. Wet snow avalanches can occur during any time of the year, with rain on snow events. On the other hand, towards the end of the century, dry snow avalanches are projected to decrease due to warming temperatures and shortening snow season (Hanssen-Bauer *et al.*, 2019). Regarding cornice fall avalanches, Eckerstorfer and Christiansen (2011b) anticipate the frequency to remain the same since this type of avalanche is significantly influenced by the local terrain. Snow avalanches are relevant primarily for the steep slopes in the Longyearbyen area but may influence areas below the release areas onto relatively low slope angles.

3.5. Erosion

Erosion in general refers to the process by which soil, rock, and other materials are gradually worn away and transported by forces such as water, wind, and ice (Zachar, 1982). This transport of materials by external agents distinguishes erosion from weathering which involves no movement. Two types of erosion are explored: coastal erosion and surface erosion and gullyng.

3.5.1. Coastal erosion

Coastal erosion refers to breaking down of materials as a result of both thermal and mechanical factors (Nielsen *et al.*, 2022). It involves a movement of sediments along the coast due to the action of waves, currents, and other natural forces (Sinitsyn *et al.*, 2020). The thawing of permafrost and melting of ground ice cause soil destabilization and collapse, while ocean waves physically erode the coast (Guégan, 2015; Jaskólski, Pawłowski and Strzelecki, 2018; Nielsen *et al.*, 2022). The loss of sea ice increases the reach of ocean waves and the duration of open water, making the coast more vulnerable to erosion (Guégan, 2015; Jaskólski, Pawłowski and Strzelecki, 2018; Nielsen *et al.*, 2022). Shoreline lengths have decreased in Svalbard (Nicu *et al.*, 2020, 2021b) and elsewhere in the Arctic (Frederick *et al.*, 2016; Guégan and Christiansen, 2016), and as a result of climate change and the resulting warmer air and permafrost temperatures and lessened sea ice, erosion rates are expected to continue rising in the future (Nielsen *et al.*, 2022). Erosion rates in the Arctic have been found to be the same or even surpass those of temperate regions due to thawing permafrost and extreme weather (Lantuit *et al.*, 2011; Frederick *et al.*, 2016). The combining effect of seasonal frost, sea ice cover and permafrost results in very high rates of coastal erosion in some Arctic regions (Sinitsyn *et al.*, 2020).

As temperatures rise, the melting sea ice provides less protection against larger waves (Frederick *et al.*, 2016) and the delayed freeze-up of sea ice means that coastal areas are exposed to storms during a longer period, which further exacerbates the problem of erosion (Nielsen *et al.*, 2022). Guégan (2015) studied the rates and mechanisms of coastal erosion and found that coastal erosion rates in Svalbard and Greenland are among the highest in the world. Aligning with these findings, Nicu *et al.* (2020) suggest the coastal erosion rates in Hiorthhamn to be on average 1.5-2 m per year, posing a significant risk for CH in the region. Aga *et al.* (2023) reports increasing retreat rates of rock cliffs at the shoreline near Ny-Ålesund, especially for the southwest facing coastline. Besides the direct impacts of climate change on coastal erosion, Jaskólski, Pawłowski and Strzelecki (2018) found out that human activities such as land-use change, and urbanization are exacerbating the impacts of climate change on the coastal zone. Coastal erosion is relevant for the CH objects in Longyearbyen area and Ny-Ålesund located near the shoreline.

3.5.1. Surface erosion and gullying

Soil erosion can take various forms depending on factors such as the region, soil type and properties, precipitation regime, slope characteristics, and land use and management. It can be classified according to multiple factors, for instance based on the erosive agent, such as precipitation or wind, or form of erosion such as surface or underground (Zachar, 1982). The common types of soil erosion can be considered to be sheet, rill, and gully erosion (Nicu *et al.*, 2022). Sheet erosion tends to concentrate on minor incisions and can evolve into rills, which may further develop into gullies as they widen and incise into the soil (Zachar, 1982). Since soil erosion is largely a result of water movement, erosion rates can considerably increase during large flood events caused by extreme rainfall (Wu *et al.*, 2018; Hanssen-Bauer *et al.*, 2019). In the Arctic regions, the limited vegetation along with permafrost affect the erosion processes. The freeze-thaw cycle has a significant impact on soil erosion, with snowmelt being identified as more erosive factor compared to rainfall (Wu *et al.*, 2018). Permafrost serves as a mitigating factor for erosion, however, as the temperature of the active layer increases, a greater amount of sediment becomes available for transportation (Etzel Müller and Frauenfelder, 2009). Consequently, the anticipated rise in the occurrence of debris slides and flows will contribute to erosion and the supply of sediment to rivers (Etzel Müller and Frauenfelder, 2009).

Gullying is a type of erosion that occurs when there is a water flow into ice wedges that causes tunnelling and sinkholes in the channels (Fortier, Allard and Shur, 2007). In cold climates, where gullies are called thermo-erosion gullies due to their interaction with permafrost, gullies form when heat transfer from small water tracks increases the depth of the active layer and thaws the underlying, ice-rich ground (Veillette, Fortier and Godin, 2015; Nicu *et al.*, 2022). This can cause oversaturated soils and, if the surface soils are extracted by small gullying, a gradual expansion in the gully network (Fortier, Allard and Shur, 2007). The process may start small but once a depression is formed, slumping and mechanical erosion can accelerate it, leading to soil subsidence, channel incision, and continued erosion (Nicu *et al.*, 2022). The erosion gullies grow both uphill and by deepening

and widening the initial incision (Nicu *et al.*, 2022). Fluvial surface erosion and gullying are relevant primarily for the lowermost slopes and valley bottoms in the Longyearbyen area.

3.6. Riverine flooding

Floods occur when the water flow surpasses the capacity of the riverbanks, resulting in overflow and consequent flooding in nearby low-lying areas (*Riverine Flooding / National Risk Index*, no date). Flooding in the Arctic is primarily a result of the melting snow and the degradation of permafrost, which leads to an increase in water flow in rivers and streams (Haverkamp *et al.*, 2022). Thus, triggering factors for floods are mainly related to meteorological conditions of precipitation and warming weather. Increased melting of glaciers and snow will increase flooding (Hanssen-Bauer *et al.*, 2019; Meyer, 2022). Snowmelt floods will decrease in areas where snow season is getting shorter, yet rain floods will increase and further melt the glaciers and snow (Hanssen-Bauer *et al.*, 2019).

While fluvial flows appear to have only a minor geomorphic effect on steep slopes, small, incised channels on debris slopes continuously convey small amounts of discharge from snowmelt in spring and summer. These channels may be fed by snow patches that persist until late summer in protected depressions, resulting in formation of streams. Fluvial flow originating from higher sections of slopes can saturate the remaining snow with an excess of water, potentially triggering slush avalanches. Fluvial flows hold considerable role in shaping the landscape on fans with large catchments, and in valley bottoms, where there is a potential for the accumulation of substantial amounts of water. (De Haas *et al.*, 2015.)

Dalheim Ottem (2022) and Pallesen (2022) studied the fluvial and sedimentary systems in Longyearbyen and found out that climate change is causing changes in the hydrological regime of the region, including changes in water discharge, sediment transport, and water temperature. These changes could also have an impact on the CH objects within proximity to rivers and fluvial tracks. River flooding is relevant primarily for the near-flat valley bottoms in the Longyearbyen area.

3.7. Weathering

Weathering is a process where soils, rocks, minerals or other materials break down locally as a result of physical, chemical and biological processes (*Weathering*, no date). It is considered in cold climate, weathering is largely mechanical in nature, with low temperatures driving the processes related to frost action and limiting chemical weathering (Hall *et al.*, 2002). Mechanical weathering can occur for example due to the freezing and thawing of water within rock or mineral particles (Van Everdingen, 1998; Matsuoka and Murton, 2008). Water penetrates rock pores, then expands as a result of freezing, and creates stress inside the rock (Prick 2002). In cold conditions, mechanical weathering can be a very efficient process for breaking-up soil and rock (Van Everdingen, 1998; Hall *et al.*, 2002). Freeze-thaw weathering leads to the deterioration of rocks, sediments, and soils. This process promotes mechanical fragmentation of rocks, resulting in loose material that is readily available for transport (Saemundsson, Morino and Conway, 2021). The projected increase in fast fluctuations in temperatures, could further intensify this weathering processes.

Chemical weathering includes solution and oxidation, while biological and biochemical weathering involves rock-colonizing organisms such as lichens (Hall *et al.*, 2002). These processes can occur singly or in combination and may generate microcracks that favor fine-debris production. Whilst chemical weathering is fastest in warm, dry climate, it has been considered to occur also in cold climate to some degree (Hall *et al.*, 2002; Prick, 2003).

There are not many studies done regarding the weathering rate of rocks in the Arctic. André (1997) found that post-glacial rock wall retreat has been generally slow in the Arctic, with Holocene cliff recession largely influenced by chemical and biological weathering agents. Local bedrock conditions favouring frost shattering were found to be the main reason for high retreat rates observed in some Arctic locations. However, the studied sites in the central and western Spitsbergen have different metamorphological conditions than areas around Longyearbyen. In the study by André (1997), Ny-Ålesund is relatively close to the other study area in Kongsfjorden, where frost shattering was expected to be the dominant

type. However, there are no large rock walls around the CH objects in Ny-Ålesund where this could occur and destroy the objects. Weathering is relevant primarily for the CH objects located in direct proximity to rock cliffs both in Longyearbyen area and Ny-Ålesund.

4. Studied cultural heritage objects

This chapter introduces the studied CH objects first in the Longyearbyen area (including Hiorthhamn) and then in Ny-Ålesund. There are in total 260 studied objects in this thesis. A description and a map for CH objects both in the Longyearbyen area and Ny-Ålesund are shown.

4.1. Study objects in Longyearbyen

The selection of CH objects examined in this thesis is based on the PCCH-Arctic project. They selected the CH objects based on the prioritization of the project's user partners and criteria defined in PCCH-Arctic Report 1 (Sinitsyn *et al.*, 2022). A list of the studied CH objects, along with their descriptions and information on the absence, collapse, or damage of Cable car posts (which were also included in the study), can be found in Table 1. To visualize the locations of the studied Cable car lines and other CH objects, refer to Figure 3.

Table 1. Studied CH objects in the Longyearbyen area (Norwegian name in the parentheses). Descriptions from (*Hjem - Kulturminnesøk*, no date; Knudsen and Tokle Yri, 2010; Reymert, 2016).

Name of the object	Number of objects studied	Description
Cable car lines		
Cable car line 1a (Taubanelinje 1a)	11 foundations	Cable car line leading to mine 1a. Built in 1907/08. The line was 1.2 km long. Only some foundations remain.
Cable car line 1b (Taubanelinje 1b)	24 posts and 1 tensioning station	Cable car line leading to mine 1b. Built in 1939. The line was 2.4 km long. Two objects have collapsed, one is absent, and one has been crashed by a snow avalanche.
Cable car line 2a (Taubanelinje 2a)	5 foundations	Cable car line leading to mine 2a. Started operating in 1921. The line was 1.5km long.

		All the posts were later removed, only some foundations remain.
Cable car line 2b (Taubanelinje 2b)	18 posts and 1 angle station	Cable car line to mine 2b. Started operating in 1937. The line was 2 km long. Three objects are completely gone, two have been crashed by a snow avalanche, one has collapsed, and one has only foundations left.
Cable car line 3 (Taubanelinje 3)	41 posts and 1 tensioning station	Cable car line leading to mine 3. Was built in 1937. One object has only foundations left.
Cable car lines 5 (Taubanelinje 5)	22 posts, 1 tensioning station	Cable care line leading to mine 5. Four objects have only foundations left, and one is absent.
Cable car line 6 (Taubanelinje 6)	40 posts, 1 tensioning station	Cable car line leading to mine 6.
Cable car line 5-6 (combined line for both mines 5 and 6) (Taubanelinje 5-6)	45 posts, 2 tensioning stations	Combined Cable car line leading to both mines 5 and 6. Three objects have collapsed, and two have been likely crashed by a snow avalanche and are missing the upper structure.
Mines		
Mine 1a (Gruve 1a)	1	First mine to be opened in Longyearbyen. Mining started in 1906 but the actual coal production started in 1908-1909. Fatal explosion occurred in 1920, destroying the main facilities and causing the close down of the mine.
Mine 2b (Gruve 2b)	1	The mine was constructed in 1937. It suffered from multiple fires and an explosion throughout its operation and was attacked by the Germans during World War II. The mine was excavated in 1968.
Mine 5 (Gruve 5)	1	The first mine to be opened outside of Longyeardalen, located about 8km from Longyearbyen. Excavation started in 1957 and ended in 1971.
Mine 6 (Gruve 6)	5 buildings/ entrances	Located about 10km from Longyearbyen. Coal production started in 1969 and the mine was closed in 1981.
Buildings/other		
Titan crane (Titankrana)	1	An old cargo crane put into use in 1953. Was used to load coal into ships.
Old Cable car center (Taubanesentralen)	1	The cable car center that stands there today was built in 1957 over the old cable car center. There were cable cars from mines 1, 2 and 5 into the center and then coal was transported to the recovery plant with Cable car line 3. Last cable cars stopped operating in 1987.
Angle station in Endalen (Vinkelstasjon ved Endalen)	1	An angle station to connect Cable car lines 5-6, 5, and 6.

Coal cable car station in Hiorthhamn (Taubanestasjonen i Hiorthhamn)	1	A large wooden loading facility for coal. Coal from the mine up in the mountain side was stored here before it was shipped out to Adventfjorden. The station was built in 1938-40.
Residential barrack in Hiorthhamn (Boligbrakke G i Hiorthhamn)	1	Old housing barrack in Hiorthhamn.
Studied objects in total	226	

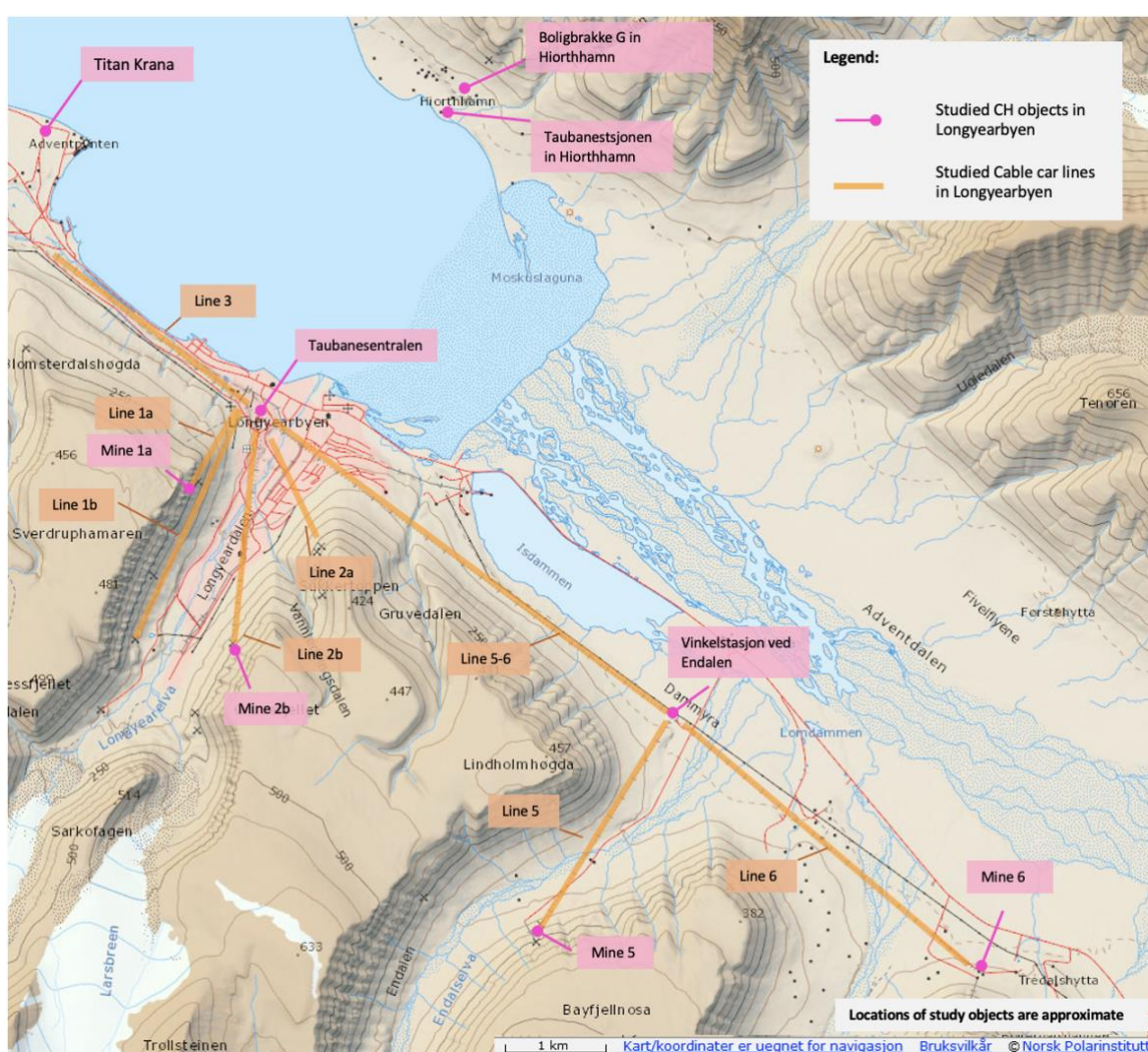


Figure 3. Map of the studied CH objects in the Longyearbyen area.

In the Longyearbyen area, the CH objects mainly consists of Cable car posts or their foundations. Additionally, a few mine entrances, structures and buildings were studied. In Hiorthhamn, the studied CH objects comprise an old house and a coal transportation facility.

In total there were 226 CH objects studied in the Longyearbyen area. The cableway posts from Mines 1A,1B, 2A, 2B and 3 are automatically protected in accordance with the Svalbard Environment Act, while the Cable car posts from Mines 5 and 6 are protected by decision under the same legislation (Flyen and Mattsson, 2013).

4.2. Study objects Ny-Ålesund

In contrast to Longyearbyen, the CH objects in Ny-Ålesund primarily consist of old houses and facilities. Table 2 provides a list of the studied objects, along with their descriptions. The numbering of the objects in the table corresponds to the numbering of the objects on the map depicted in Figure 4. In total, there were 34 studied objects in Ny-Ålesund.

Table 2. Descriptions of CH objects in Ny-Ålesund (Norwegian name in parentheses if applicable). Descriptions from (Reymert, 2016).

	Name of the object	Description
1.	The Airship mast (Luftskipsmasta)	An airship mast built in 1926 during Roald Amundsen's North Pole expedition with the airship Norge.
2.	Green harbour house (Green Harbour-Huset)	The oldest house in Ny-Ålesund. Built in 1909 or 1912 by the Green Harbor Coal Co formerly to the mining area and later moved to Ny-Ålesund.
3.–6.	London houses (London husene) <ul style="list-style-type: none"> • London 1 • London 2 • London 3 • London 4 	Believed to have been built in 1912 in New London on the Blomstrand peninsula. Moved to Ny-Ålesund in 1949-1950 and improved into family homes.
7.	School (Skolen)	A school built in 1917.
8.	Telegraph station (Telegrafan)	Built in 1918 both for the operation of the mine and connection with the mainland. Was moved to its current location after World War II.
19.	Meseet	Shop that was set up in 1920. Nowadays a museum and an information center.
10.	Museumshytta/hytte lysegrønn	An eight-man barrack built in 1918. Served as a family home until 1963 and is now a museum.
11.	Veteranhytta/hytaa lyseblå	A six-man barrack built in 1918. Later converted into a house.
12.	Sysselbu	A six-man barrack built in 1918. Later converted into a house.
13.	Museum	A six-man barrack built in 1918. Later renovated to become a museum.
14.	Amundsenvillaen	Was originally built to accommodate the mining company's director and board members when they would come to visit.

		Later named as Amundsenvillaen according to a polar explorer Roald Amudsen who lived there for few weeks in 1925 and 1926.
15.	The North pole hotel (Nordpolhotellet)	The biggest housing building in Ny-Ålesund, a 76-man barrack built in 1919 for the miners. Later transformed into a hotel.
16.	Yellow house (Gult hus)	Foreman's mess built in 1919.
17.	White house (Hvitt hus)	Residence for the operations manager, built in 1919.
18.	Blue house (Blått hus)	Office building, built in 1919.
19.	Mellageret	Built in 1919, now the town's gathering place.
20.	Post office (Posthuset)	Built as a library and has also served as a school. Built in 1920.
21.	The iron warehouse (Jernlageret)	The iron warehouse built in 1927.
22.	Sætra	Operated as the mine day facility, was moved to the town, and converted into a family home in the 1950s.
23.	Båtnaust (22)	Boathouse built during the first operating period (1916-1941).
24.	Båtnaust (23)	Boathouse built before 1921.
25.	Båtnaust (24)	Boathouse in Thiisbukta, used to be a barge to bring coal from the shore to the ships. Built during the first operating period (1916-1941).
26.	Trønderheimen	Workers' barracks that were placed on the vacant site of the hospital. Built in 1945.
27.	Mexico	Worker's barracks with twin rooms and common rooms. Name is believed to originate from the fact that lively social gatherings took place in there.
28.	The hospital/ Scooter garage (Sykehuset/Skutergerasjen)	Served as a hospital from 1945 until the mining operations ceased in 1963. Nowadays a scooter garage and a warehouse.
29.	The community house (Samfunsshuset)	Large community hall for weekly gatherings, bringing everyone in town together. Built in 1945.
30.	Saga	Built during the second working period (1945-1963).
31.	Old power station (Gamle kraftstasjonen)	Old power station built in 1949.
32.	Dog yard (Hundegården)	Dog yard built in 1949.
33.	Dokkehus	Built in 1953.
34.	Transformatorhus	Built in 1956.

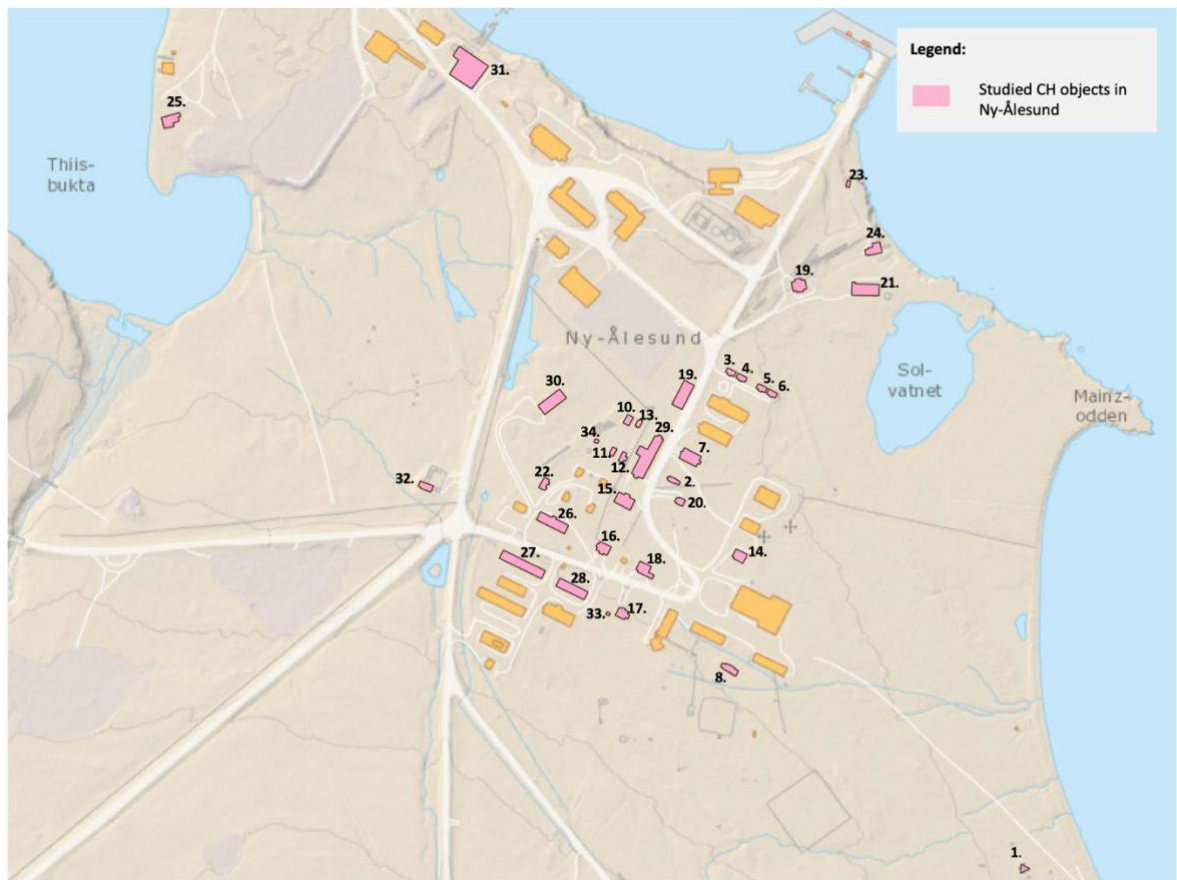


Figure 4. Map of the studied CH objects in the Ny-Ålesund. The numbering of the objects corresponds to Table 2.

5. Materials and Methods

The methodology employed by PCCH-Arctic to create their Risk Assessment Version 1, along with the corresponding Excel tool, serves as the theory basis for the updated assessment conducted in this thesis. Chapter 5.1 provides an explanation of this methodology. This methodology is further developed with data from literature, geographical information and fieldwork, introduced in Chapter 5.2 to assess new probabilities, and hence to create an expanded and more nuanced risk assessment Version 2 for the ten studied natural hazards on CH objects, a process explained in Chapter 5.3. Based on the results of the new risk assessment, an interactive ArcGIS map is created, to showcase the risks associated with CH objects and Cable car lines. The creation of this map is described in greater detail in Chapter 5.4. The linkages between the methodology and utilized materials with the other phases of the study are summarized in Figure 5.

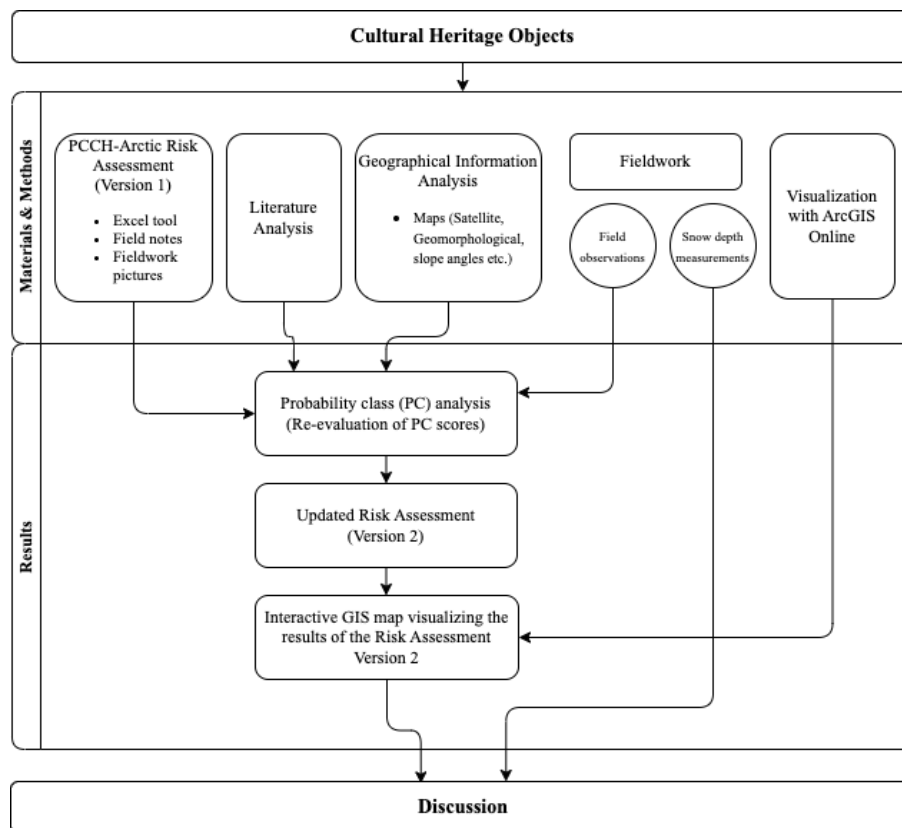


Figure 5. Flow chart illustrating the phases of the thesis and the linkage between Material and Methods to other parts.

5.1. Risk assessment by PCCH-Arctic (Version 1)

Risk consists of the combination of probability and consequence, where both elements have to be considered to accurately assess risk (Paolini *et al.*, 2012). It shall be noted that risk always refers to the future, i.e., to an event that has not materialized yet. Due to a wide range of risks that CH is facing, assessing potential risks is crucial for dealing with the unwanted impacts on the objects. Risk assessment consists of risk identification, analysis, evaluation, and it is part of larger risk management process, that additionally consists of establishment of the context before assessing the risks and after, treatment of the risks (Paolini *et al.*, 2012). PCCH-Arctic Arctic (Bekele and Sinitsyn, 2023) conducted the risk assessment based on the Norwegian standard NS 5815:2006 (Risikovurdering av Anleggsarbeid – *eng. Risk Assessment of Construction Work*), which provides guidelines and requirements specifically for conducting risk assessments in construction projects. This standard aligns with the principles and concepts outlined in the international standard ISO 31000:2009 (Risk management – Principles and guidelines). The following subchapters 5.1.1. and 5.1.2. shortly explain the qualitative and quantitative risk assessments carried through by PCCH Arctic (for details see Bekele and Sinitsyn, 2023), that will be the basis for the new risk assessment Version 2 executed in this thesis.

5.1.1. Qualitative assessment

The risks posed by various natural hazards on each CH object were categorized into risk classes. The classes for the probability of a natural or human-caused hazard and its impact on a CH object were rated on a scale of 1 to 5, with 1 being the lowest class (highly unlikely hazard event/ minimal impact) and 5 being the highest class (highly probable hazard event/ significant impact). These probability classes (PC) and consequence classes (CC) and their descriptions are based on the NS 5815:2006 standard and are presented in Table 3.

Table 3. PC (left) and CC (right) scores (Bekele & Sinitsyn 2023).

Probability Class (PC)	Description	Consequence Class (CC)	Description
1	Very unlikely	1	Negligible
2	Unlikely	2	Minor
3	Possible	3	Moderate
4	Likely	4	Significant
5	Very likely	5	Severe

During the risk identification stage, each CH object was assigned a PC and CC score for each natural hazard. PC scores were determined considering the geographical location of the CH object and the natural hazards in that area. PCCH-Arctic utilized past studies, hazard maps, and field work in the area to assess the probability of natural hazards occurring at each location. In cases where this data was not available, PC scores were assigned based on reasonable estimates (educated guesses) made by Bekele and Sinitsyn (2023), taken into consideration the specific location of each object.

The CCs were assigned based on type of hazard, the object's location, and its current condition. The object's current condition was particularly significant for evaluating the consequences of permafrost degradation. It was assumed that a CH object in good physical condition would be better able to withstand permafrost degradation, resulting in lower impact compared to CH objects in poor physical condition. The evaluation of impacts from other hazards was determined through engineering judgement by Bekele and Sinitsyn (2023).

5.1.2. Quantitative assessment

The quantitative risk analysis was carried out to numerically determine risk a CH object is exposed to, unlike the qualitative risk analysis which provides a general description of the level of risk. To calculate the risk, PCCH-Arctic assigned numerical estimates to the earlier defined probability and consequence classes, referred to as the lower bound and upper bound thresholds. For the probabilities, the lower bound represents the minimum likelihood of a hazard happening, while the upper bound represents the maximum likelihood (Table 4).

Table 4. Lower bound and upper bound probability estimates corresponding to the five PCs (Bekele & Sinitsyn 2023).

Probability Class	Description	Lower Bound Probability	Upper Bound Probability
1	Very unlikely	0.1 %	1.0 %
2	Unlikely	1.0 %	5.0 %
3	Possible	5.0 %	10.0 %
4	Likely	10.0 %	20.0 %
5	Very likely	20.0 %	50.0 %

To quantify the consequences of a natural hazards on a CH site, PCCH-Arctic employed a concept of Heritage Loss based on (Giuliani *et al.*, 2021). Heritage Loss represents a numerical estimation of the potential physical damage that may be inflicted on a CH object due to natural or human-made hazards. For example, a complete destruction of a CH object by a snow avalanche would result in a Heritage Loss of 100%. Similar to the numerical scores of PCs, Heritage Loss is measured in percentage, and lower bounds and upper bounds are defined for each of the five CCs to represent the minimum and maximum expected Heritage Loss (Table 5).

Table 5. Lower bound and upper bound Heritage Loss estimates corresponding to the five CCs (Bekele and Sinitsyn, 2023).

Consequence Class	Description	Lower Bound Heritage Loss	Upper Bound Heritage Loss
1	Negligible	0.0 %	5.0 %
2	Minor	5.0 %	10.0 %
3	Moderate	10.0 %	30.0 %
4	Significant	30.0 %	50.0 %
5	Severe	50.0 %	100.0 %

The probability and Heritage Loss estimates for the quantitative risk assessment were automatically derived from the corresponding PC and CC scores in the qualitative assessment, and the total risk faced by a CH object was defined as the Risk of Heritage Loss. Risk of Heritage Loss is the product of the probability of the hazard and the corresponding consequence of the hazard, i.e. the Heritage Loss estimate, as follows:

*Risk of Heritage Loss = Probability of Hazard * Heritage Loss (i.e. consequence of hazard)*

The outcome is presented as a range, with lower bounds and upper bounds indicating the minimum and maximum estimated risk of Heritage Loss for each CH object.

5.2. Used data

Here the different types of data used, to conduct the updated version of the Risk Assessment, are described. The data sources include geographical information analysis, literature data, and fieldwork data.

5.2.1. Geographical information analysis

This thesis relies on geographical information provided by various institutions and organizations to assess the probabilities of natural hazards for CH objects in Svalbard. The Norwegian Polar Institute's 1:100 000 map series data of Svalbard (Melvær, 2014a) was particularly helpful, as it offers detailed information on the archipelago's topography and geography, serving as the basis for the analysis and as the base map for all other maps.

Riksantikvaren (*Home - Riksantikvaren*, no date), the Norwegian Directorate for Cultural Heritage, has also shared crucial information on CH objects in Svalbard, including their coordinates and some descriptions. Additionally, recent years have seen the production of several geomorphological maps for the Longyearbyen area. These maps, such as Todalen (Rubensdotter *et al.*, 2015), Longyeardalen (Rubensdotter, 2022), Endalen (Geldard, 2019), Hiorthhamn (Preliminary Dynacoast map; Svalcoast, no date), and the coastal area from Longyearbyen towards the airport (Preliminary Dynacoast map; Svalcoast, no date), utilize a Svalbard-specific version of the Norwegian SOSI-standard (Systematic Organisation of Spatial Information standard), providing information on surficial geomorphology, primary surface sediments, slope processes, and potential natural hazards.

Norway's national geological survey (NGU) has also conducted a preliminary susceptibility assessment for debris flows around the Longyearbyen area (Rubensdotter, unpublished), and NVE financed a risk assessment, mapping slope hazards (Skred AS, 2022). Moreover, a digitally constructed hill shade map based on elevation data with 5 m resolution from 2009 supplied by the Norwegian Polar Institute (Melvær, 2014b) was used. All these different map data were imported into GIS as shapefiles or tiff files to study the probabilities of different hazards.

5.2.2. Literature analysis

To conduct a comprehensive risk assessment of natural hazards affecting CH objects in Svalbard, a literature review using a broad range of keywords related to natural hazards, climate change, cultural heritage, and Svalbard, was conducted. These keywords included terms such as "natural hazards," "landslides," "snow avalanches," "erosion," "weathering," "climate change," "Arctic," "Svalbard," "cultural heritage in Svalbard," "impacts of natural hazards on cultural heritage," and "climate change impacts on natural hazards" etcetera. Various databases, including Scopus and Google Scholar, and library search engine were used to identify relevant studies. This review aimed to identify potential natural hazards that may impact CH objects, their probability of occurrence, and the factors that contribute to their occurrence. Through this approach, the importance of considering current and future climate conditions in Svalbard was recognized. Climate projections were used to understand the impact of changes in temperature, precipitation, and permafrost conditions on natural hazards and CH objects.

5.2.3. Fieldwork in Longyearbyen

To gain a better understanding of the current state of the CH objects, fieldwork was conducted in the Longyearbyen area as well as in Ny-Ålesund. While some snow depth data had been collected for the PCCH-Arctic project in previous years, new measurements were taken to observe any changes in the conditions. This data will be further used as part of the

PCCH-Arctic project. In addition to snow depth measurements, additional field visits to some of the Cable car lines were made to better understand the probability of different natural hazards on CH objects, as part of the risk assessment.

The fieldwork for measuring the snow depths was carried out during the period of April 25 to May 3, 2023, when the snow accumulation was expected to be at its peak. However, it is worth noting that there was a warmer period in the week preceding the fieldwork, during which temperatures briefly rose above 0 °C and there were some rain events. This should be taken into account while interpreting the results. To measure the snow depth, both an active layer probe and an avalanche probe (Figure 6) were used. First, the active layer probe was used to reach the ground, and then the avalanche probe was used to measure the snow depth. For the Cable car posts, seven measurements were taken, one from the middle and two from each side, approximately 1m and 10m away, as illustrated in Figure 7. For the other CH objects, multiple measurements were taken around each object.

The objects inspected during the fieldwork were the case study objects identified by the PCCH-Arctic project (Appendix 1). Furthermore, Cable car line 6 was studied in detail by taking measurements from every 5th Cable car post, and additional measurements were also taken from Cable car line 5-6. The snow depth data collected will be used to identify any patterns or trends in snow accumulation and snow depth. Snow thickness can be linked to permafrost degradation for the cases where there are ground depressions around the CH objects, as they can accumulate water and thaw the permafrost even more. Snow depth measurements can be found from Appendix 2.

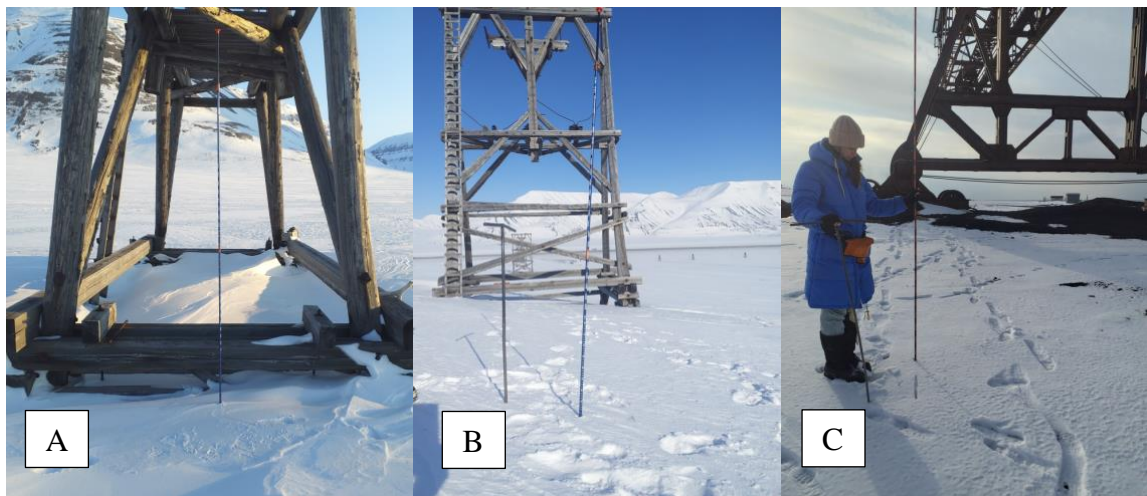


Figure 6. Snow depth measurements taken using two different types of probes: an avalanche probe (pictured in A, B, and C) and a thicker iron active layer probe (visible in B and C). Photos by Peter Hamrock and the author.

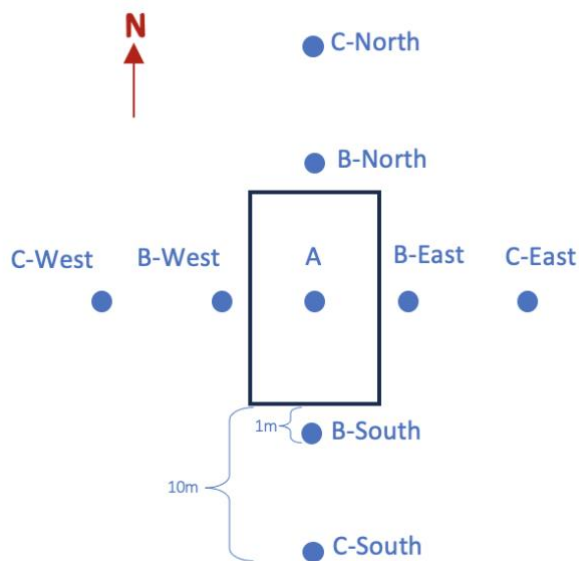


Figure 7. Approximate measuring points for the Cable car posts. Black rectangle represents the frame of the object. B-points are approximately 1 m away from the object, whereas C-points are approximately 10 m away from the object.

To further clarify potential hazards for Cable car lines 3 and 5-6, some additional field observations were conducted. These visits were particularly useful in gaining a better understanding of the solifluction scores and the likelihood of a rockfall for both lines. For

line 3, the field observations also helped to better understand the risk of weathering. Visiting the sites, helped in getting better understanding of the position of CH objects in relation to potential hazards, providing important additional insights for evaluating the PC scores for natural hazards. These field visits were conducted on May 30 for line 3 and on July 4, 2023, for line 5-6.

5.2.4. Fieldwork in Ny-Ålesund

Fieldwork was conducted in Ny-Ålesund from June 22 to June 26, 2023, to measure the foundations of selected CH objects, including Green Harbor House, London Houses, Post House, and the Airship Mast, using a laser level (Figure 8). The primary goal was to assess the settlement of these objects on permafrost, and the levelling data collected during this fieldwork established the first ever baseline measurements for these objects.



Figure 8. Laser level measurements in Ny-Ålesund. Photos by Noemi Pasquini.

While the data cannot yet be utilized to explain the year-to-year settlement patterns of the objects on permafrost, it does reveal differences in the foundations from one corner to another within the same building, forming the basis for evaluating the geotechnical performance of the foundations. For instance, in the case of London House 1, which underwent renovation and levelling in 2010, the northwest corner is 12 cm lower than the northeast corner (Figure 9). According to general guidelines regarding structures on

permafrost, over 10 cm settlement in the foundation after 30 years of load application is regarded as a foundation failure (Instanes, 2017). Hence, the 12 cm level difference observed for London House 1 over a mere 13-year period is clearly unacceptable. Additionally, settlements of foundations have the potential to cause ruptures in the connected piping system, impacting both drinking water and sewage. A rupture of a drinking water pipe can contribute to permafrost degradation due to water flow, leading to further settlement in the foundations, while a rupture of a sewerage pipe can pose significant health risks.



Figure 9. Settlement at London houses in Ny-Ålesund. Photo by Anatoly Sinitsyn/SINTEF.

Visual observations of Green Harbour House revealed that there were both settlement within the building and settlement in the surrounding terrain (Figure 10). Settlements within the house can be attributed to two factors: rot decay of timber in the foundation, particularly the frame positioned directly on the ground. Surrounding terrain is settled because of permafrost degradation, which is likely influenced by uneven snow accumulation around the house.



Figure 10. Differential settlements of Green Harbour House in Ny-Ålesund, June 23, 2023. Photo by Anatoly Sinitsyn/SINTEF.

Observations and measurements at Luftskipsmasta (Figure 11) revealed terrain settlements around of 20 cm. It, however, does not seem that the active layer has reached the bottom of the foundation. Reported depth of active layer thickness in the area (Byelva) increased from 180 cm to 200 cm during the last decade (Hanssen-Bauer et al., 2019), which creates significant concern on the stability of Luftskipsmasta in the nearest future.



Figure 11. Terrain settlements at Luftskipsmasta, June 26, 2023. Photo by Anatoly Sinitsyn/SINTEF.

Measurements and visual observations of differential settlements of buildings and structures (London Houses, the Green Harbour House, and Luftskipsmasta) and terrain around them provided additional confidence in assigning the risk of permafrost degradation and the consequence classes.

5.3. Assigning Probability Class scores for Version 2

Version 1 risk assessment carried out by PCCH-Arctic for the studied CH objects was reviewed and version 2 of the assessment was produced by looking further into geomorphological maps and other material, combined with field observations. In general, for the new Version 2, the PC scores were re-evaluated, but CC scores were taken as they were from the old assessment, exceptions explained below.

To update the PC scores, some changes and clarifications were first made. The division of the hazard category *landslides/debris flows* was separated into two distinguish categories *Shallow landslide* and *Debris flow*. This allowed for a more nuanced analysis, as the probabilities of these two hazards varied significantly from place to place as well as their triggering mechanisms in time and space throughout the year. Debris flows are mostly triggered by rain episodes on steep slopes, while shallow landslides are more dependent on ground-ice conditions, occurring also on much lower slope angles. Even though in general no CC scores were evaluated in this version, due to the division of the category into two, new CC scores had to be assigned. The existing scores for *landslides/debris flows* were used for shallow landslides, while for debris flows, CC scores were set to be one unit less than the shallow landslide scores for each object. This decision was based on the observation that while a nearby landslide has typically resulted in a complete destruction of an object, there have been several cases where an object has survived a debris flow (Figure 12). In addition, the category *Gully erosion* was extended to incorporate additional elements of water-driven surface erosion and the category name was changed to *Surface erosion and gullying*. Gully erosion was not found to be typical around the studied objects but could still not be ruled out as in general the sedimentology in Svalbard is suitable for gullying.



Figure 12. Post nr. 9 at the Cable car line 5 that has survived a debris flow, September 3, 2021. Photos by Anatoly Sinitsyn/SINTEF.

The process of assigning the probabilities consisted of the following steps:

1. Looking at the angle of slope for each object. This included looking at the slope at the object, about 2.5 below and 2.5m above the object.
2. Looking at the geomorphology around the object to find out the prevailing sediments around the object. This type of map was not available for all of the study areas.
3. Assessing new scores based on the available data and writing a short explanation for each assigned value.

The following material was used in the evaluation:

- Orthophoto and topographic maps
- Satellite images
- Geomorphology maps
- Fieldwork notes/pictures for Version 1
- Literature
- Slope elevation information
- Field observations
- Field measurements for the specific case study objects.

This process is mainly applicable for CH objects in the Longyearbyen area, as for Ny-Ålesund only a very limited material was available, and judgements were mainly based on


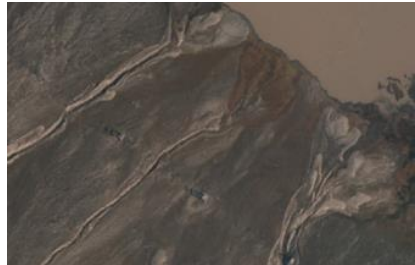
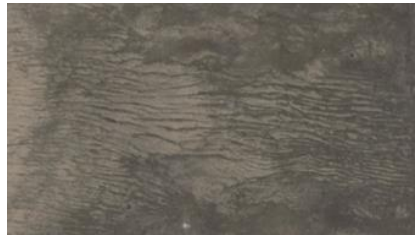
satellite images from TopoSvalbard, supported by field observations. Figure 13 displays the analysis and the data that was obtained for each CH object before assessing the new PC scores of the hazards for the studied CH objects around Longyearbyen.

Taubanelinje 1b		Slope angle (°)			Surface sediments		
CH object	Riksantikvaren ID	In the middle of the object	~2,5m below	~2,5m above	SOSI- standard code	Classification	Based on
Bukk Nr. 1	158657-1	21.9	23.3	16.7	121	Mining dumb	(Rubensdotter 2022)
Bukk Nr. 2	158657-2	18.7	19.1	18.7	307	Rockfall debosit	(Rubensdotter 2022)
Bukk Nr. 3	158657-3	21.1	21.6	23.7	309	Snow avalanche deposit	(Rubensdotter 2022)
Bukk Nr. 4	158657-4	24.7	31.1	26.6	309	Snow avalanche deposit	(Rubensdotter 2022)
Bukk Nr. 5	158657-5	25.9	28.3	25.1	309	Snow avalanche deposit	(Rubensdotter 2022)
Bukk Nr. 6	158657-6	25.2	25.8	26.3	317	Snow avalanche and rockfall deposit	(Rubensdotter 2022)

Figure 13. Example of the procedure for collecting background data for the PC analysis.

One of the major sources of data for evaluating the PC scores was the satellite images and aerial photographs. As most of the hazards leave some marks in the nature, there are some distinguished patterns that can be used to study old occurrences of hazards. Older events can be used as an indicator for suitable area for the hazard at question. Table 6 shows how the common slope hazards were identified from aerial photographs and satellite images, examined together with slope and sediment information.

Table 6. Observations of potential hazards based on satellite pictures/ literature. Pictures from (*TopoSvalbard - Norsk Polarinstitutt*, no date).

Classification	Description	Slope information	Example of recent activity
Snow avalanche	The snow avalanche deposit displays a darker outer rim and a lighter-colored center. The grains within the deposit are uniform in composition and have angular shapes, often with knocked edges, resulting in a precarious stacking arrangement. Deposits left by slush avalanches exhibit braided-like morphologies. (Rubensdotter et al., 2015; Geldard, 2019; Rubensdotter, 2022.)	Depends on the avalanche type but slab avalanches most commonly triggered on slopes 30-45° (Eckerstorfer, 2012).	
Debris flow	A track with levees on both sides can be observed, characterized by the presence of coarse-grained debris, forming on a slope where loose material is available. Within the same catchment, multiple debris flows can occur, resulting in the formation of a debris flow fan. At the end of the deposit, lobes can be seen where the debris flows come to a stop, and it is not uncommon to find plugs within the tracks caused by subsequent events. (Rubensdotter et al., 2015; Geldard, 2019; Rubensdotter, 2022.)	Most commonly triggered on slopes above 30° (Andre, 1990). Fine-grain materials like till, fluvial and periglacial sediments.	
Solifluction	Solifluction is the slow downslope movement of unconsolidated soils within the active layer, which is influenced by freeze-thaw processes. The movement of soil leads to the formation of distinct lobes or extensive sheets of solifluction deposits. (Rubensdotter et al., 2015; Geldard, 2019; Rubensdotter, 2022.)	Predominantly on low gradient slopes.	
Rockfall	Rockfall deposit is observed beneath a rockfall source area, characterized by a steep surface profile and limited horizontal movement. The deposit consists of angular grains that correspond to the geological composition of the surrounding valley slopes. Notably, the surface texture and color display a gradual vertical transition across the deposit. The grains closer to the rockfall source exhibit lighter shades, while those further downslope appear darker. (Rubensdotter et al., 2015; Geldard, 2019; Rubensdotter, 2022.)	Most commonly on steep slopes.	Single bigger rocks

For the slope hazards, slope angle, sediments, and signs of recent activity were the main factors indicating probability. The criteria used for evaluating the probabilities for slope hazards are shown in Table 7. For riverine flooding, coastal erosion, gullying, and weathering close proximity to the initiating source was used as the main indicator. Permafrost degradation was judged based on field work pictures/notes as well as sediment and ground ice conditions. Warming up of the climate was accounted for by considering a 50-year time period when evaluating the probabilities. It shall be noted that for *rockfall*, the hazard was identified if a rock could roll downslope and hit an object, while back dripping rockfall below the object was considered as part of *weathering*.

Table 7. Criteria for evaluating the probability of slope hazards.

Classification	Criteria
1 - Very unlikely	Wrong sedimentology for the process, wrong interval of angle of slope for the processes or irrelevant process setting
2 - Unlikely	Wrong surface sedimentology for the process, relevant interval of angle of slope for the processes, possibly right sedimentology in close proximity laterally or vertically
3 - Possible	Right sedimentology for the process, right angle of slope for the processes, not needed proximity to older event of the same process
4 - Likely	Right sedimentology for the process, right angle of slope for the processes, needs to be in relevant proximity to older event of the same process
5 - Very unlikely	Right sedimentology for the process, right angle of slope for the processes, needs to be in close relevant proximity to recent event of the same process

5.4. Visualization with ArcGIS online

After the new PC scores were assigned for each CH object, ArcGIS Online was used to visualise the results of the Risk Assessment of natural hazards. ArcGIS Online is a web-based Geographic Information System (GIS) platform that allows for the creation and sharing of interactive maps and applications. This platform was selected for its openness and accessibility, enabling the production of user-friendly and widely available results.

First, the required data from the PCCH-Arctic Risk Assessment Excel tool were prepared for import. A spreadsheet was created to collect all the required information, including the object name, ID number in the Askeladden database of Norwegian Directorate of cultural heritage (Riksantikvaren), coordinates, description, year of construction (if available), the sum of average risk of Heritage Loss for each CH object, and the share of each individual natural hazard towards that total risk score. This data was then imported as csv files to create shapefiles that could be modified in ArcGIS online.

Next, the data was analysed and visualized with ArcGIS Online's mapping and visualization tools. The data was visualized using various techniques, including styling based on both colour and size, to clearly show which CH objects are at the most risk from natural hazards. Pop-up windows were further used to display additional information and data related to each CH object. The pop-up windows include a pie chart that shows the normalized distribution of different hazards for each object, showing the comprehensive view of the most likely hazards.

In addition to the single studied CH objects, the studied Cable car lines (eight in total) were also visualized using color-coded polygon lines to show the overall risk level of the lines with respect to the other Cable car lines. Each Cable car line was assigned a summary pop-up window that contains information about the main hazards for that specific line.

6. Results

This section provides an analysis of the updated PC scores and the overall risk of natural hazards on CH objects in Svalbard. This chapter is divided into several subheadings, including updated PC scores and overall risk of natural hazards that showcases results from the PCCH-Arctic Risk Assessment Excel tool, results from the ArcGIS online map tool, and a summary of the results from Longyearbyen. Additionally, the chapter also includes results from the snow depth measurements. Finally, the results of the risk assessment for Ny-Ålesund are presented.

6.1. Updated Probability Class scores

As an example, Figure 14 visualizes the assignment of PC scores for some of the CH objects on Cable car line 1b. With detailed analysis for each CH object, PC scores were assigned. Conditional formatting helped to colour code scores that differed from Version 1 analysis. Explanation/comment was added for each new value. Once the probabilities of hazards for all CH objects were examined, the scores, together with explanations, were moved into the PCCH-Arctic Risk Assessment Excel tool, to create Version 2 of the assessment.

Tauban		VER 1 Probability class (PC) rates										VER 2 PC rates																			
CH object		P	SC	E	S	RC	S	G	RC	SE + d	W	P	Explanation P	S	Explained	D	Explanation	S	Explained	R	Explained	S	Explained	C	Explained	H	Explained	SE & W	Explained	W	Explained
Bukk Nr. 1		5	5		5	5	5	1	1	1	1	5	Reconstituted land, warming effect on the permafrost. Water pooling possible because object on flat area but slope above.	4	Lot of signs of SOL within close proximity (uneven patterns)	5	DF within near proximity to the object, very likely to reach the object in the future	2	No SL visible, a lot of disturbed soil around so hard to classify. Could occur	5	Many source areas, big boulders near the object	4	On the edge of an avalanche zone, within proximity to recent events	1	Not relevant, not within proximity to the coastline	1	No signs of rivers/streams within proximity	1	No signs within proximity	1	No signs of weathering of cliffs within proximity
Bukk Nr. 2		5	5		5	5	5	1	1	1	1	5	Water pooling possible because object on flat area but slope above.	4	Lot of signs of SOL within close proximity (uneven patterns)	5	DF within near proximity to the object, very likely to reach the object in the future	2	No SL visible, a lot of disturbed soil around so hard to classify. Could occur	5	In the rock fall deposit, big boulders near the object, many source areas	3	No recent signs, on the edge of potential runoff zone	1	Not relevant, not within proximity to the coastline	1	No signs of rivers/streams within proximity	1	No signs within proximity	1	No signs of weathering of cliffs within proximity
Bukk Nr. 3		2	1		5	5	5	1	1	1	1	2	Entirely based on ver 1 classification	1	Not many signs, coarse sediments and snow avalanches	3	No signs within close proximity, snow avalanche deposit	1	Some signs of active layer detachment further down but not likely to impact the object.	5	Many source areas	3	No signs within close proximity, potential snow avalanche deposit	1	Not relevant, not within proximity to the coastline	1	No signs of rivers/streams within proximity	1	No signs within proximity	1	No signs of weathering of cliffs within proximity
Bukk Nr. 4		2	1		5	5	5	1	1	1	1	2	Entirely based on ver 1 classification	1	Not many signs, coarse sediments and snow avalanches	4	Debris flows within close proximity, but in avalanche deposit so likely to go on the side of the object	1	Some signs of active layer detachment further down but not likely to impact the object.	5	Many source areas	5	In a SA deposit. Recent activity visible	1	Not relevant, not within proximity to the coastline	1	No signs of rivers/streams within proximity	1	No signs within proximity	1	No signs of weathering of cliffs within proximity
		2	1		5	5	5	1	1	1	1	2		2	Some signs further down the slope, not likely because of		No signs within close		Some signs of active layer detachment further				In a SA		Not relevant.		No signs of				

Figure 14. Assignment of PC scores for Cable car line 1b.

The assessment of natural hazards impacting the CH objects in Svalbard went through a revision, where the PC scores were revised from Version 1. Even though, most of the scores remained similar in both versions, there were also some differences. Apart from single and smaller one-unit changes in PC scoring, the main differences between versions arose from the following assumptions/changes in each natural hazard category.

Permafrost degradation: The PC rating from previous evaluations was mainly followed, except in areas with “sensitive sediments”, the rating was increased based on geomorphology maps. "Sensitive sediments" were characterized to include the following: high ground ice content and surface water content, fine-grained sediments, and alluvial deposits. In addition, objects on a relatively flat surface were considered more susceptible for degradation due to the possibility for water pooling. Also, signs of impacts of permafrost degradation on structures, such as cracking of foundations, were used to prescribe areas with higher permafrost degradation.

Solifluction: PC scores were modified (mainly increased) for some CH objects, where sediment material was classified as solifluction in the geomorphology maps (e.g. Rubensdotter et al., 2015; Geldard, 2019; Rubensdotter, 2022). The precise score was set based on the sediment type, observations of solifluction-connected surface patterns, with also an eye on the angle of slope, assuming that higher gradients are associated with increased solifluction rates and therefore, higher risk of impact on the CH. In addition, satellite pictures were used to determine proximity to older events of solifluction, which was used, together with the sediment and slope information, as a support for a higher probability score. Where surface sediments were classified as solifluction material, a PC score of at least 3 (Possible) was automatically given.

Debris flow: Due to the modification of a single category Landslide/debris flow to separate categories, the PC scores for debris flow were changed considerably for some of the CH objects. Also, it was noticed that some fluvial tracks were mistaken for debris flows in Version 1, which also resulted in differences in the revised version.

Shallow landslide: Due to the same reason as above (separation of landslides and debris flows), the PC scores for shallow landslides were different from the original scores. As there were not many signs of existing shallow landslides close to the CH objects, the scoring was mainly based on suitable conditions for future landslides, i.e. at least moderate inclination and sediments susceptible for land sliding (e.g. fine-grained sediments, loose sediments, weathered material).

Rockfall: Rockfall scoring was updated and mainly followed a simplified logic as it is almost impossible to project whether a single boulder will hit a CH object, even if a rockfall were to occur in the area. Since individual rockfall boulders were difficult to identify from aerial imagery, judgments were based mainly on the inclination of the slope, the type of source area and distance to the source area, and the surrounding surface sediments. For example, for Cable car line 1b, the PC scoring was changed approximately in the middle of the line from 4 to 5 (likely to very likely), due to change in the type of source area to more vertical rock wall with boulders that seem more susceptible for falling off.

Snow avalanche: PC scores for snow avalanches were modified to be more case-by-case specific. For example, if a CH object is clearly in an old avalanche fan it was given a higher score than the subsequent object that is only within proximity to old signs of activity. Inclination of the slope, surface sediments (e.g. sediments classified as snow avalanche deposits more susceptible to this type of risk), older events of the hazard, and prevailing wind conditions were the main factors in assigning the PC scores.

Coastal erosion: Only two CH objects in Longyearbyen area are within close proximity to the coastline, Taubanesentralen in Hiorthhamn and Titankrana. The PC scores for these remained the same as in Version 1 assessment. However, the PC score for Boligbrakke G in Hiorthhamn was lowered from 3 to 2 (possible to unlikely), considering the over 300m distance to the coastline and 50-year study time period, aligning with the scoring of other CH objects with similar distance to the coastline.

Riverine flooding: Taken the study period of 50 years and the expected increase in rain due to climate change, a PC score higher than 1 (very unlikely) for riverine flooding was given to CH objects also within close proximity to streams/creeks/old fluvial tracks.

Surface erosion and gullying: In the revised version surface erosion was added into the category, which changed the PC scoring of this hazard for about 30 CH objects based on the fieldnotes for Version 1, and cases similar to those mentioned in the fieldnotes. For these CH objects, PC score was increased from 1 or 2 (very unlikely or unlikely) to 3,4 or 5 (possible, likely, or very likely), depending on the proximity to erosional processes and observed severity of the erosion. Only a few places were found where actual gullies or initiations/susceptible conditions for future initiations are within close proximity to the CH objects. Gullying was considered a potential hazard also if the object is within close proximity to fluvial tracks with a sufficient slope gradient, as this could be considered a favourable initiation point for a gully in the future. It was noticed that in Version 1, PC score

was higher for objects that were close to any ravines/channels, and not specifically gullies. This also explains some of the differences between versions in scoring for this hazard.

Weathering: PC scores for weathering were considered higher than 1 (very unlikely) only for Cable car line 3, where close proximity of some CH objects to large ravines/edges increased the probability for this hazard. Unlike in Version 1, for majority of the posts in line 3, the PC score was increased from 1 (very unlikely) to at least 2 (unlikely), due to the prevailing sediment material that was classified as ‘weathering material’ according to the geomorphology map (Preliminary Dynacoast map; Svalcoast, no date) for all but three first Cable car posts. Weathering was judged based on the distance to a weathering front, relative to the size of the object.

6.2. Overall Risk

This section shows the results for the overall risk of Heritage Loss for the CH objects. First the results from the PCCH-Arctic Risk Assessment Tool are shown, followed by the ArcGIS online visualizations. A summary of the results is showed at the end.

6.2.1. Results from PCCH-Arctic Risk Assessment Excel tool Version 2

Once the PC scores were assigned for each hazard for each object, the total risk could be calculated using the PCCH-Arctic Risk Assessment Excel Tool. Figure 15 illustrates the highest-ranked CH objects in the Longyearbyen area (including absent/destroyed ones), based on the aggregated average risk of Heritage Loss, including all the objects that have risk higher than 60%. The results indicate that objects located within Cable car line 1b exhibit the highest exposure to the combined effects of natural hazards. Following Cable car line 1b in terms of aggregated risk exposure, several posts on Cable car line 2b and entrance to the mine, as well as posts on lines 5-6, 5, and 1a, are identified as significant points of exposure. Post nr. 6 on Cable car line 1b (Taubanelinje 1b, Bukk Nr. 6) exhibits the highest average risk of Heritage Loss when considering the combined effects of hazards. Figure 16 displays

the contributions made by the considered natural hazards to the aggregated risk of Heritage Loss for this Cable car post. The figure reveals that snow avalanches and rockfalls pose the most significant risks to this specific object.

Aggregated Risk for:	Sum of Avg Risk of HL	Rank based on Avg Risk of HL
Taubanelinje 1b, Bukk Nr. 6 (158657-6)	87,64 %	1
Taubanelinje 2b, Bukk Nr. 2 (158986-2)	83,64 %	2
Taubanelinje 1b, Bukk Nr. 7 (158657-7)	82,29 %	3
Taubanelinje 1b, Bukk Nr. 1 (158657-1)	81,59 %	4
Taubanelinje G5-6, Bukk Nr. 33 (87889-42)	80,34 %	5
Taubanelinje G5-6, Bukk Nr. 38 (87889-47)	74,84 %	6
Taubanelinje G5-6, Bukk Nr. 32 (87889-41)	74,34 %	7
Taubanelinje 1b, Bukk Nr. 8 (158657-8)	73,29 %	8
Taubanelinje 2b, Bukk Nr. 3 (158986-3)	71,39 %	9
Taubanelinje 1b, Bukk Nr. 4 (158657-4)	70,42 %	10
Taubanelinje 2b, Bukk Nr. 1 (158986-1)	69,59 %	11
Taubanelinje 1b, Bukk Nr. 12 (158657-12)	69,44 %	12
Taubanelinje 1b, Bukk Nr. 2 (158657-2)	68,34 %	13
Taubanelinje 1b, Bukk Nr. 5 (158657-5)	67,82 %	14
Taubanelinje 1a, Foundation 9 (159054-9)	67,69 %	15
Taubanelinje 1a, Foundation 8 (159054-8)	67,69 %	15
Taubanelinje 1a, Foundation 6 (159054-6)	67,69 %	15
Taubanelinje 1a, Foundation 5 (159054-5)	67,69 %	15
Taubanelinje 1a, Foundation 7 (159054-7)	67,69 %	15
Taubanelinje 1b, Bukk Nr. 18 (158657-18)	67,02 %	16
Gruve2b (136716)	66,62 %	17
Taubanelinje G5-6, Bukk Nr. 9 (87889-17)	65,87 %	18
Taubanelinje G5-6, Bukk Nr. 30 (87889-39)	65,34 %	19
Taubanelinje G5, Bukk Nr. 1 (87889-78)	64,91 %	20
Taubanelinje 1b, Bukk Nr. 10 (158657-10)	64,84 %	21
Taubanelinje 1b, Bukk Nr. 19 (158657-19)	64,79 %	22
Taubanelinje 1b, Bukk Nr. 17 (158657-17)	64,79 %	22
Taubanelinje 1b, Bukk Nr. 20 (158657-20)	62,99 %	23
Taubanelinje G5, Bukk Nr. 10 (87889-69)	62,84 %	24
Taubanelinje 1b, Bukk Nr. 11 (158657-11)	62,09 %	25
Taubanelinje 1a, Foundation 4 (159054-4)	61,44 %	26
Taubanelinje G5, Bukk Nr. 2 (87889-77)	60,80 %	27
Taubanelinje 2b, Bukk Nr. 4 (158986-4)	60,64 %	28
Taubanelinje 1b, Bukk Nr. 13 (158657-13)	60,24 %	29
Taubanelinje 2b, Bukk Nr. 5 (158986-5)	60,09 %	30

Figure 15. The highest ranked CH objects in the Longyearbyen area in terms of aggregated average risk of Heritage Loss (referred as HL in the figure) (PCCH-Arctic Risk Assessment Excel Tool).

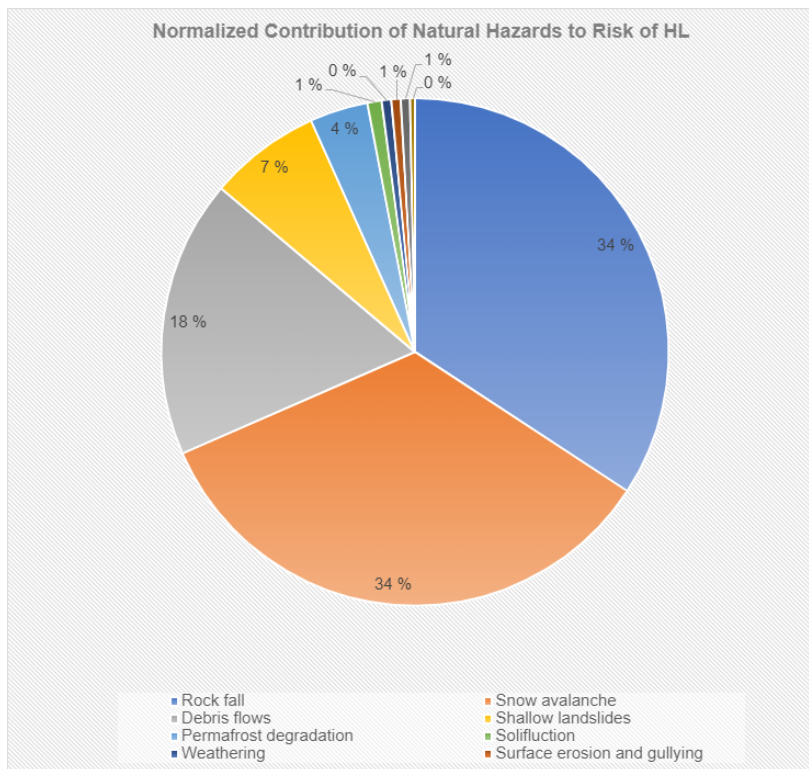


Figure 16. Aggregated risk of Heritage Loss (referred as HL in the figure) from natural hazards to the post nr. 6 on Cable car line 1b (PCCH-Arctic Risk Assessment Excel Tool).

In addition to the analysis of individual CH objects, the study examined the Cable car lines (eight in total) to identify the primary hazards affecting each Cable car line and determine the lines at the highest risk. The findings provide insights into the specific risks associated with each Cable car line. For Cable car lines 1a, 1b, and 2b, snow avalanches were found to contribute the most to the overall risk of Heritage Loss, whereas for Cable car lines 3, 5, 5-6, and 6, permafrost degradation emerged as the most prevalent hazard. In the case of Cable car line 2a, shallow landslides contributed the most to the overall risk of Heritage Loss. As an example, for the most hazardous Cable car line 1b, the contribution of the natural hazards to the total risk of Heritage Loss is shown in Figure 17.

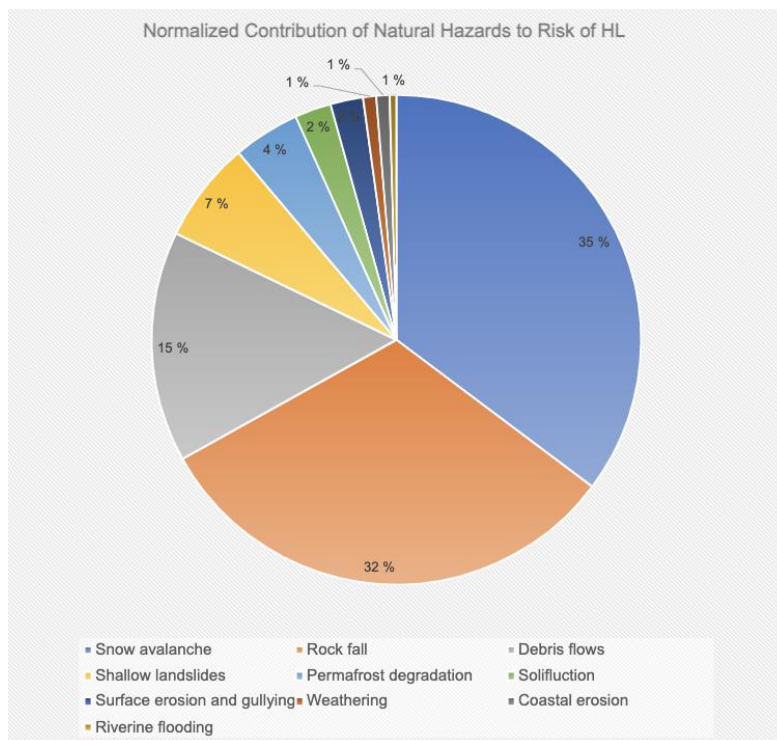


Figure 17. Aggregated average risk of Heritage Loss (referred as HL in the figure) for Cable car line 1b (PCCH-Arctic Risk Assessment Excel Tool).

Examining the contributing natural hazards reveals that snow avalanche and rockfall, followed by debris flow play the main role in the aggregated risk of Heritage Loss for Cable car line 1b. For a more detailed display of the results for each Cable car line, see Appendix 3. For Version 1 results see PCCH-Arctic Report nr. 2 (Bekele and Sinitsyn, 2023). Results of the level of risk for CH objects and Cable car lines are summarized in Chapter 6.2.3.

6.2.2. ArcGIS Online map

The total scores and hazard distribution for each object were visualized in GIS. The map shows detailed hazard evaluation for each studied heritage object near Longyearbyen and Ny-Ålesund. The zoomed-out view shows overall hazard evaluation for each of the 8 Cable car lines in Longyearbyen, with red indicating highest risk and yellow lower risk (Figure 18). Clicking on a Cable car line opens a popup window with information on the Cable car line at question (Figure 19).

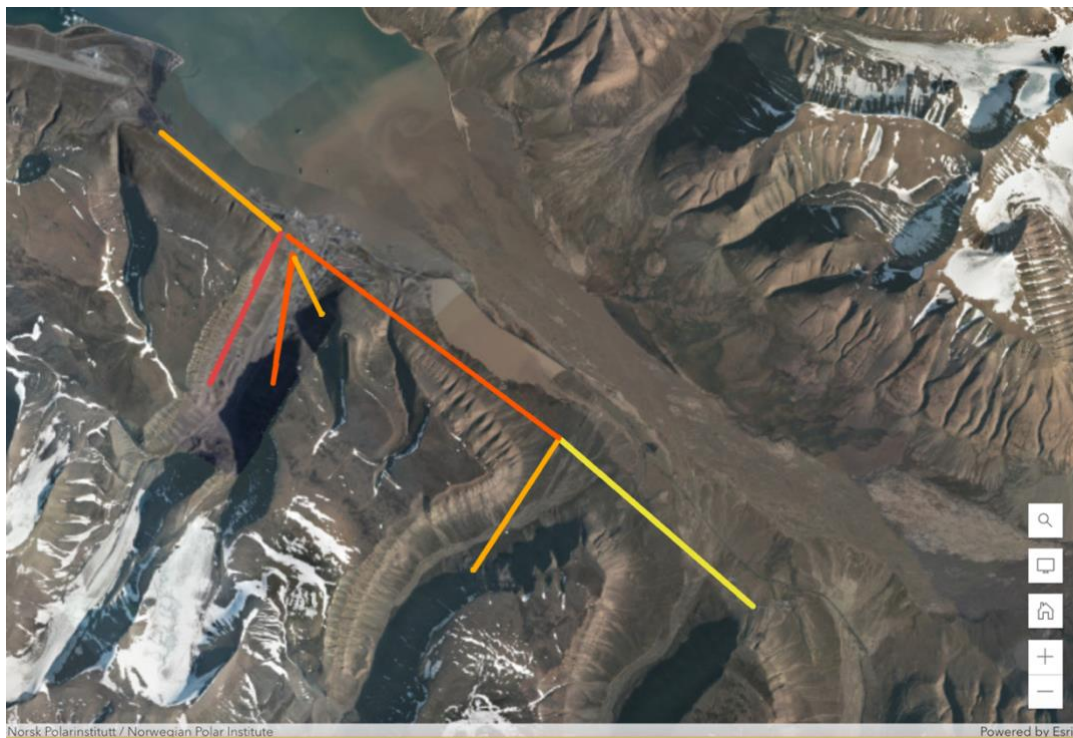


Figure 18. Zoomed-out overview of the Cable car lines. The darker the colour, the higher the total risk, i.e. red colour indicating higher risk, yellow the least risk.



Figure 19. Pop-up window showing more information about each Cable car line.

Zooming in shows individual posts and objects (Figure 20), coloured and sized based on their average Heritage Loss risk (Figure 21). The colour and size coding threshold values were decided based on the mean value (33.4%) of average Heritage Loss risk for all CH objects in Longyearbyen, where the darker (redder) and the bigger the symbol of the object, the larger the risk. The objects having a total average Heritage Loss risk between 30-60 %, were considered to be at moderate risk, and the ones above and below at high and low risk respectively.

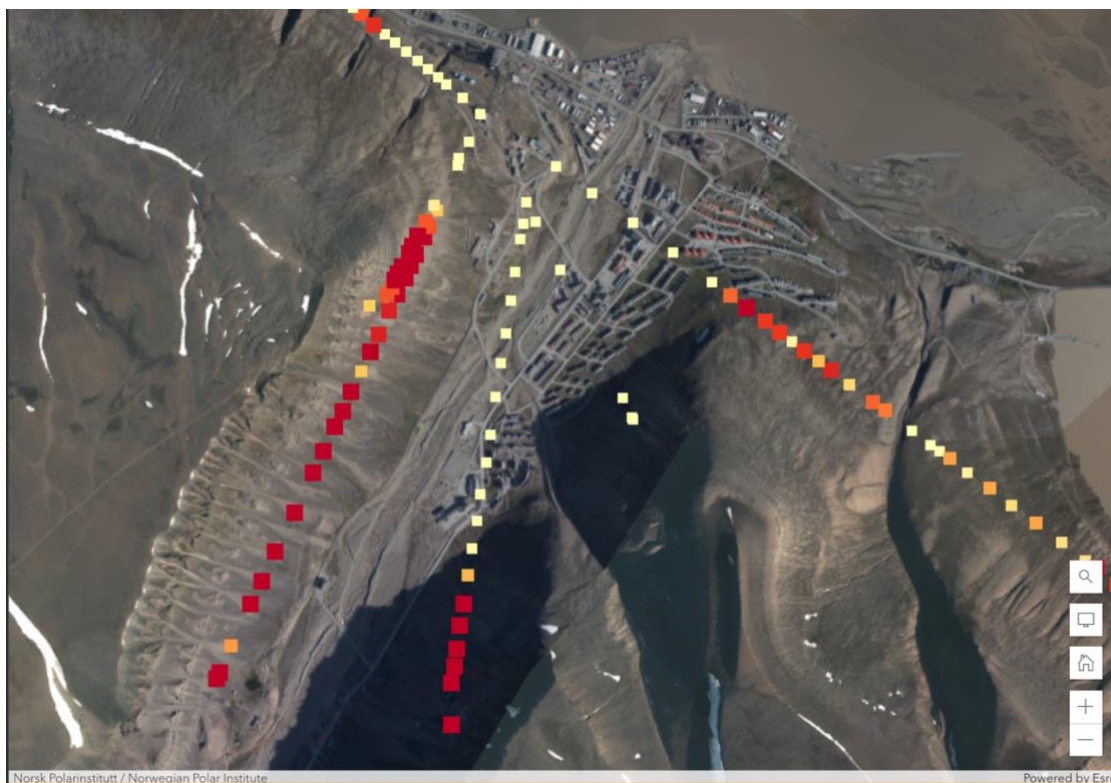


Figure 20. Zoomed-in overview of the Cable car lines. The darker (redder) and the bigger the symbol of the object, the larger the risk.

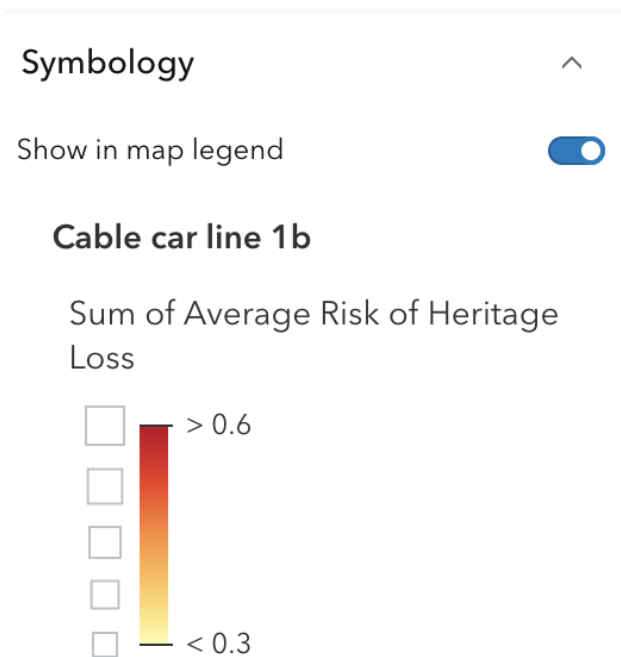


Figure 21. Symbology of each CH object. Intervals were determined to be <30%, 30-60%, and >60%.

A user can click any of the CH objects to open a pop-up window and gain additional information about the object (Figure 22). This pop-up window will show the aggregated average total risk of Heritage Loss for that specific CH object; Rank within the Cable car line (for the CH objects being part of a Cable car line), Askeladden ID for more information; pie chart that shows the distribution of natural hazards, and on the second page a picture of the CH object (if available). In addition, for objects that are destroyed or have been removed, there is a text indicating this below the main information. Hovering over a pie slice gives the percentage and name of the natural hazard at question.

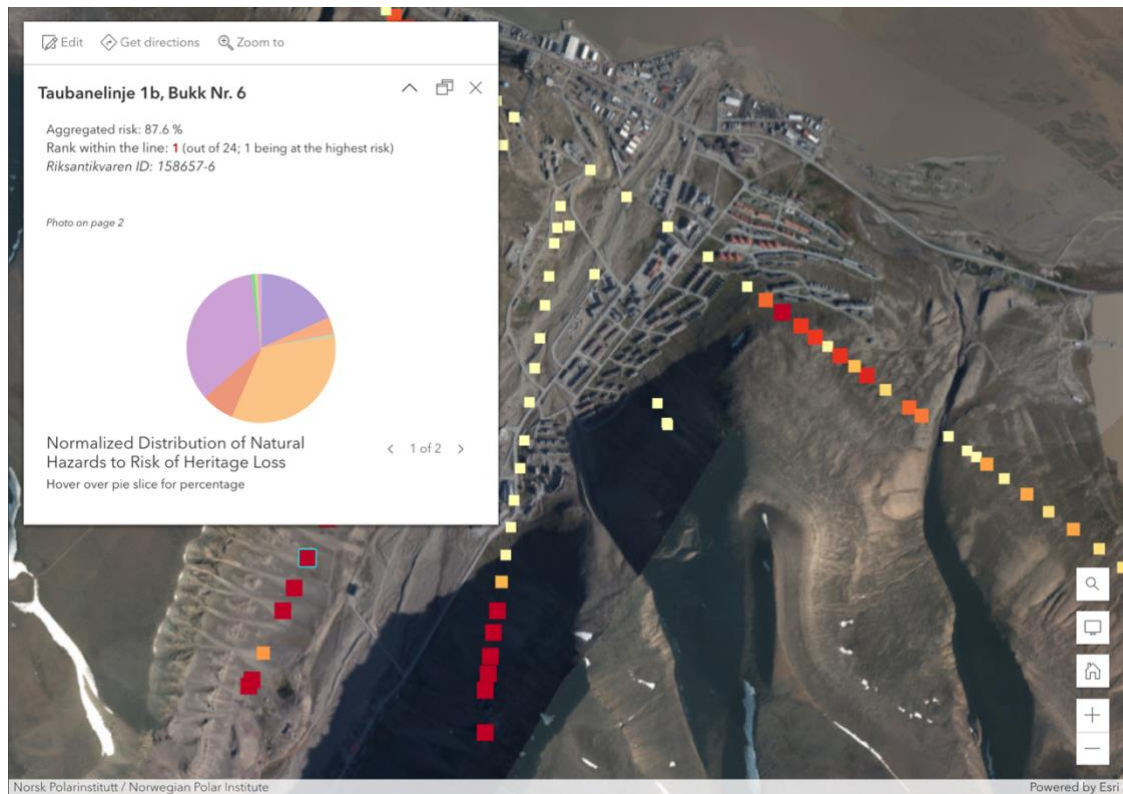


Figure 22. Showing the pop-up window for a CH object.

6.2.3. Summary of the results

Table 8 presents the distribution of CH objects in Longyearbyen based on the three threshold groups used for visualizing results in ArcGIS online. The table also includes information about the main natural hazards associated with each of the eight Cable car lines. The analysis reveals that half of the CH objects in Longyearbyen are posed with relatively low level of total risk of Heritage Loss (below 30%). About one third are exposed to a medium level of risk (total risk between 30 and 60%), while 16% face a high level of total risk of Heritage Loss (above 60%). Regarding all CH objects, the main natural hazards identified are permafrost degradation, snow avalanches and rockfalls. Examining the Cable car lines, it was revealed that permafrost degradation is the biggest contributor to overall risk for 50 % (4/8) of the Cable car lines, whereas snow avalanches are the main hazard for 37.5 % (3/8) of the Cable car lines.

Table 8. Summary table for the total risk posed by the Cable car lines and other CH objects in Longyearbyen. The table includes three risk categories based on the threshold values from the ArcGIS map: total risk below 30%, between 30 and 60% and above 60%. For the Cable car lines the main natural hazards, contributing to the total risk, are also mentioned.

	Sum of average risk of Heritage Loss <30%	Sum of average risk of Heritage Loss 30-60%	Sum of average risk of Heritage Loss >60%	Main natural hazards of the Cable car line
Cable car line 1a (11 CH objects)	1 (9 %*)	4 (36 %)	6 (55 %)	Snow avalanches (42 %**), Debris flows (23 %), Rock falls (17 %)
Cable car line 1b (25 CH objects)	2 (8 %)	7 (28 %)	16 (64 %)	Snow avalanches (35 %), Rock falls (32 %), Debris flows (15 %)
Cable car line 2a (5 CH objects)	5 (100 %)	-	-	Shallow landslides (41 %), Permafrost degradation (15%), Debris flows (9%)
Cable car line 2b (19 CH objects)	12 (63 %)	2 (11 %)	5 (26 %)	Snow avalanches (27 %), Rock falls (26 %), Debris flows (17 %)
Cable car line 3 (42 CH objects)	24 (57 %)	18 (43 %)	-	Permafrost degradation (26 %), Surface erosion & gullyng (20 %), shallow landslides (14 %)
Cable car line 5-6 (47 CH objects)	13 (28 %)	28 (60 %)	6 (13 %)	Permafrost degradation (22 %), shallow landslides (17 %), snow avalanches (17%)
Cable car line 5 (23 CH objects)	9 (39 %)	11 (48 %)	3 (13 %)	Permafrost degradation (26 %), Rockfalls (19 %), debris flows (14 %)
Cable car line 6 (41 CH objects)	40 (98 %)	1 (2 %)	-	Permafrost degradation (32 %), Solifluction (20 %) Surface erosion & gullyng (18 %)
Other objects in Longyearbyen (13 CH objects)	8 (62 %)	4 (31 %)	1 (8%)	-
Total (226 CH objects)	114 (50%)	75 (33%)	37 (16%)	-

*Percentage share of the total number of CH objects on that Cable car line/group.

** Contribution of the hazard to the total risk of Heritage Loss on that line.

Overall, it can be observed that **Cable car line 1b** faces the highest risk of Heritage Loss, with 16 out of the 25 CH objects (64%) exposed to the highest identified level or risk. The primary hazards for Line 1b are snow avalanches, rockfalls and debris flows. Snow avalanches and rockfalls each contribute to approximately one-third of the overall the risk, while debris flows account for 15%. Shallow landslides and permafrost degradation also contribute to the total risk to some degree.

Following Cable car line 1b, **Cable car line 1a** demonstrates the second highest overall risk, with six out of 11 (55%) objects exposed to the highest level of risk. Snow avalanches pose the greatest threat for this line, followed by debris flows and rockfalls.

The majority of the objects on **Cable car line 2b** are exposed to low overall risk. However, the first five CH objects (26%) on the Cable car line, located on a steep slope, are exposed to the highest level of risk. Consequently, the primary contributors to the total risk for this line are snow avalanches, rockfalls and debris flows.

Cable car line 5-6, the longest line consisting of 47 CH objects, has significant proportion of the objects facing medium risk (60%). 6 objects (13%) are exposed to the highest level of risk. Among these objects, snow avalanches are the primary contributor to the total risk for four out of six objects. However, when considering the overall risk of the entire Cable car line, permafrost degradation poses the most substantial risk. Shallow landslides and snow avalanches contribute equally to the overall risk of the line. Given the length and varying terrain of this line, the distribution of natural hazards is relatively mixed, with different hazards posing the main risk for different CH objects.

For Cable car line 5, permafrost degradation, rockfall and debris flow are the main hazards, accounting for around 64% of the total risk. Shallow landslides, snow avalanches and solifluction also pose a risk to some of the CH objects along the line. On this line, three out of 23 objects are exposed to the highest level of total risk.

Moving on to **Cable car line 3**, none of the objects face the highest level of risk, and the majority fall under the lowest level of overall risk. The main hazards for this line include permafrost degradation, surface erosion and gullying, and shallow landslides. Diverging from other Cable car lines, weathering is considered a risk for some of the CH objects on this line, contributing to 10% of the total risk.

Cable car lines 6 and 2b experience relatively low levels of total risk, with no objects along these lines exposed to the highest level of risk. For Cable car line 2a, all objects have the lowest level of total risk, while for Cable car line 6, only one object faces a medium level of risk. The main hazards for Line 2b are shallow landslides, permafrost degradation, and debris flows. As for Line 6, permafrost degradation, solifluction, and surface erosion and gullying are the primary contributors to the overall risk.

Amongst **other CH objects in Longyearbyen** (a total of 13), one object, namely, the Mine entrance for Cable car line 2b, is exposed to the highest level of total risk. Similar to the Cable car posts at high risk on that line, the main hazards for this object are rockfalls, debris flows and snow avalanches.

6.3. Snow depth measurements in Longyearbyen

Snow depth measurements were taken in the Longyearbyen area, and the results showed significant variations in snow depth both within individual measurement points for a given CH object and between different CH objects. No discernible patterns were observed in the data, and many of the measuring points showed no snow at all. The largest measurement of 167 cm was recorded on Cable car line 5-6, however this measuring point was located on a scooter track, which may have affected the accuracy of the measurement. Despite the experienced snowy winter, the snow depth is not shown in all places due to the variable wind that causes snow drift. Depending on the prevailing wind direction and the tunnel effect in the valleys, some Cable car posts have collected snow, whereas some posts are snowless.

Generally, the snow depth measurements at the Cable car posts were deeper than those taken around structures and buildings. These support earlier hypothesis that Cable car posts can trap snow (Sinitsyn *et al.*, 2022).

In general, in Adventdalen (Cable car lines 5-6 and 6), objects are catching more snow which leads to higher snow accumulation around the objects and thus increased permafrost degradation due to the insulating effect of snow. In Endalen (Cable car line 5), on the other hand, snow is not accumulated around the objects and thus the terrain around is not settling in those places. It even seems that terrain has some "uplift" there due to probable frost heave, that may be intensified by absence of insulation from the snow (Figure 23). Snow cover is a major source of water, and thus the correlation between snow depth and melt water around each object is assumed to be highly correlated.



Figure 23. Post Nr. 6 at the Cable car line 5. This post is resting on a small bump/hill that is probably created as a result of frost heave, which is stimulated by absence of snow in winter, September 3, 2021. Photo by Anatoly Sinitsyn/SINTEF.

6.4. Cultural heritage objects in Ny-Ålesund

The results for the CH objects in Ny-Ålesund will be showed here, followed by the same order as for the results for Longyearbyen. First, the evaluation of PC scores is explained, followed by the overall risk of Heritage Loss for the CH objects.

6.4.1. Probability Class scores

Due to limited data for the area of Ny-Ålesund, the PC scores for this region mostly followed the scoring of the Version 1 assessment, with the exception of riverine flooding, coastal erosion and weathering probabilities for a few of the CH objects. The PC score for riverine flooding was increased from very unlikely to unlikely for two CH objects, Hundegården and Telegrafan, located near streams or creeks. This rating considers the slight possibility of the water source having some impact, rather than ruling out the hazard completely. This reasoning was applied to all CH objects located near streams, creeks, or rivers. The PC score for coastal erosion was increased from very unlikely to possible for Gamle kraftstasjonen due to its proximity to the coast. The judgment was mainly made based on satellite images and onsite observations, and even though there are studies observing the accelerating rock cliff retreat rates near the coastline of Ny-Ålesund (Aga *et al.*, 2023), overtime observations would be needed for this specific coastline to see how it has changed. Finally, the PC score for weathering was increased from very unlikely to possible for Båtlaus 22, due to its location beneath a cliff. This judgment was based on satellite images and fieldwork observations.

6.4.1. Overall Risk

A risk ranking for CH objects in Ny-Ålesund was performed with the updated probability scores (Figure 24). Similar to Version 1 Assessment, Air ship mast (Luftskipsmasta) was found to be the object with the highest aggregated risk of Heritage Loss. The aggregated risk for the objects in Ny-Ålesund is significantly lower compared to those observed for objects in Longyearbyen and it shows less variation amongst the different heritage objects.

Aggregated Risk for:	Sum of Avg Risk of HL	Rank based on Avg Risk of HL
Luftskipsmasta	36,04 %	1
Gamle kraftstasjonen	24,63 %	2
Båtnaust (22)	24,63 %	2
Båtnaust (24)	21,65 %	3
Båtnaust (23)	21,65 %	3
Jernlageret	17,06 %	4
Hundegården	17,06 %	4
Museum	15,92 %	5
Mellageret	15,92 %	5
Blått hus	15,92 %	5
Samfunnshuset	15,92 %	5
Mexico	15,92 %	5
Gult hus	15,92 %	5
Saga	15,92 %	5
Transformatorhus	15,92 %	5
Hvitt hus	15,92 %	5
Trønderheimen	15,92 %	5
Telegrafen	11,06 %	6
Veteranhytta/hytta lyseblå	9,92 %	7
Green Harbour-Huset	9,92 %	7
Sysselbu	9,92 %	7
Meseet	9,92 %	7
Dokkehus	9,92 %	7
London 2	9,92 %	7
Skolen	9,92 %	7
London 3	9,92 %	7
London 1	9,92 %	7
Sætra	9,92 %	7
Nordpolhotellet	9,92 %	7
Posthuset	9,92 %	7
London 4	9,92 %	7
London husene	9,92 %	7
Amundsenvillaen	9,92 %	7
Sykehuset/Skutergarasjen	6,92 %	8
Museumshytta/hytte lysegrønn	4,20 %	9

Figure 24. Ranking of the CH objects in Ny-Ålesund in terms of the aggregated average risk of Heritage Loss (PCCH-Arctic Risk Assessment Excel Tool).

The analysis highlights the significance of permafrost degradation as the primary natural hazard contributing to the risk of heritage objects in Ny-Ålesund (Figure 25). For the CH objects located at the coastal area, coastal erosion is considered as the second biggest contributor to the overall risk.

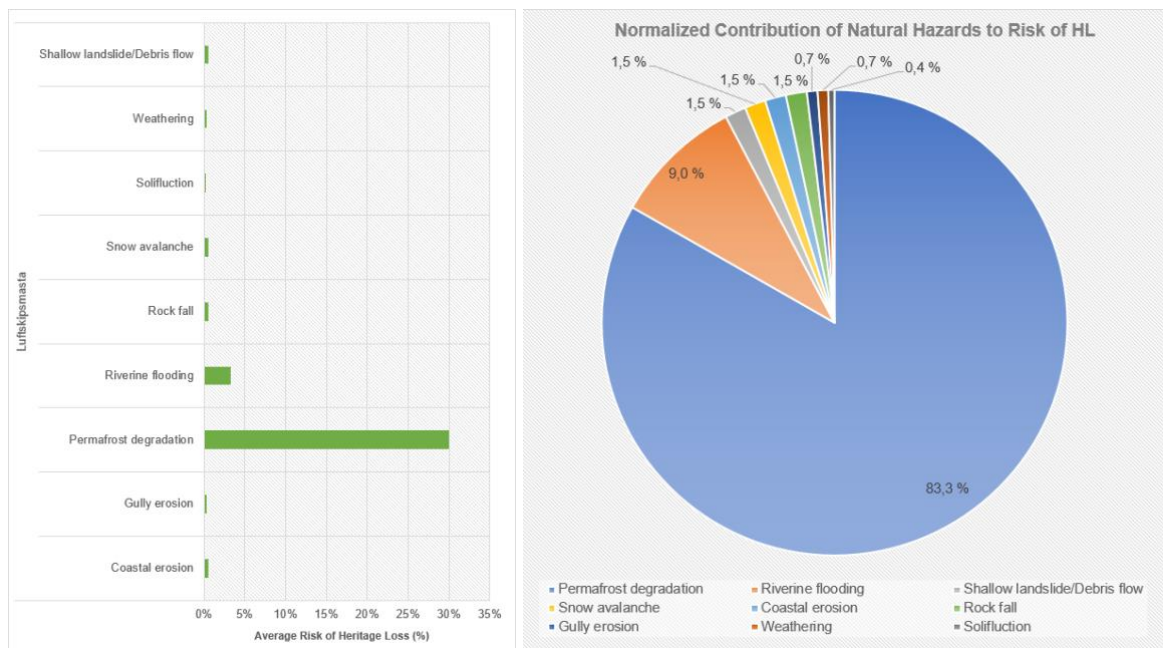


Figure 25. Contribution of different natural hazards to the risk of Heritage Loss for Luftskipsmasten (PCCH-Actic Risk Assessment Excel Tool).

As shown in Figure 25, all except one CH object has a total average risk of over 30%. Therefore, in the GIS map all CH objects in Ny-Ålesund are coloured yellow, except for the Luftskipsmasten that has an overall risk of 36% and is thus orange in colour (Figure 26).



Figure 26. Overview of the CH objects in Ny-Ålesund. Yellow colour of CH objects indicates a total risk of Heritage Loss below 30%. Luftskipsmasta is coloured orange as it has a total risk of Heritage Loss of 36%.

The pop-up windows for CH object in Ny-Ålesund reveal similar information as for the objects around Longyearbyen, but they also have short descriptions of the building purpose of the houses/structures (Figure 27).

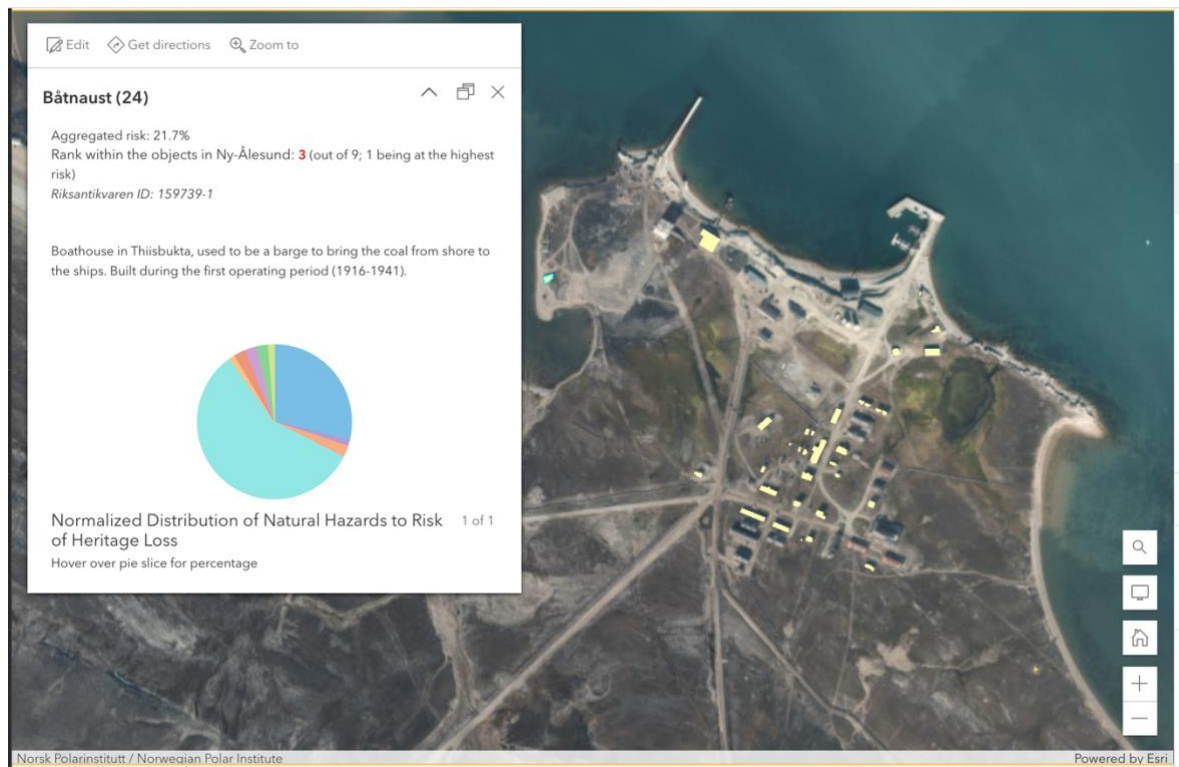


Figure 27. Showing the pop-up window for a CH object in Ny-Ålesund.

7. Discussion

This chapter will discuss the results of the study and answer the studied research questions. The findings of this study support the first research hypothesis, which states that natural hazards pose a significant risk to CH in Svalbard. The second research hypothesis, which states that projected climate warming increases the occurrences and intensifies the probabilities of most natural hazards on CH, was also supported by the findings of this study. The chapter begins by highlighting the variation in exposure to different natural hazards among the studied CH objects. After the implications of Arctic warming on natural hazards are addressed. To safeguard the CH in Svalbard, the chapter explores various factors that should be considered in deciding and prioritizing preservation efforts. Finally, the chapter acknowledges limitations and the need for future studies.

7.1. Svalbard's cultural heritage at risk

The results of this project showed that there is a great variation of exposure to natural hazards within the studied CH objects. Exposure to different hazards is dictated by factors such as topography, geology, climate and hydrology, and thus the geographical differences are large. Generally, objects that are located on a steep slope, were found to have higher overall risk score. From the Cable car lines, 1b is clearly the most at risk to natural hazards, followed logically by 1a that is located right above the Cable car line 1b. However, Cable car line 1b consists of foundations only, which are more resistant to natural hazards than standing Cable car posts. PCCH-Arctic took this into consideration when assigning the CC scores for Cable car line 1a and 2a, and thus the lower overall risk scores for Cable car line 1a are justified compared to Cable car line 1b. These Cable car lines' position on a steep slope, makes them especially vulnerable to avalanches and rockfalls, which out of all the studied hazards are one of the most destructive ones. Consequently, the sediments for many of the Cable car posts on 1b are classified as rockfall deposit or snow avalanche deposit (Rubensdotter, 2022).

In Svalbard, the prevailing wind direction is usually from South-East (Eckerstorfer and Christiansen, 2011). The CH objects located on steep slopes, have different types of avalanche risks depending on their orientation and exposure to the wind. Taken this wind direction, Cable car line 1b is under common wind conditions on the windward side of the slope. Windward side could be less prone to snow avalanches as wind helps to stabilize snowpack. However, as climate models suggest that as the Arctic continues to warm, there could be changes in atmospheric circulation patterns that could alter wind patterns and speeds in Svalbard and other Arctic regions (Cisek, Makuch and Petelski, 2017; Pilguy *et al.*, 2019). The anticipated changes in wind patterns could have implications for the snow avalanche regime in Svalbard, potentially resulting in shifts between the traditional lee and windward sides.

Similar to Cable car line 1a and 1b, parts of Cable car line 2b were also found to be at high risk to snow avalanches and rockfalls. The beginning part of the Cable car line 2b is situated on west and northwest facing slope, which often tends to be the leeward slope that is sheltered from the wind but accumulates snow deposits. Cornices often develop on the leeward side of ridges, which makes this Cable car line more prone to cornice fall avalanches. This has been observed well by Siewert *et al.* (2012) and Eckerstorfer, Christiansen, Vogel, *et al.* (2013) who studied the cornices in Longyearvalley and found out that cornice fall avalanches were the only observed type of avalanches from the Gruvefjellet edge (Cable car line 2b), whereas no cornice fall avalanches were observed from the Platåfjellet edge (Cable car lines 1a and 1b).

Unlike for the other studied Cable car lines, Cable car lines 1a, 1b and 2b located on a steep slope, exposure to permafrost degradation has not been observed to be as high (according to fieldnotes), which also aligns well with permafrost thickness often being deeper on the high lands (Humlum *et al.*, 2003). For Cable car lines 3, 5, 5-6, and 6, and CH objects in Ny-Ålesund, permafrost degradation was identified as a major hazard. The conditions of these Cable car posts often indicated signs of permafrost degradation in forms of cracking and moving. Moreover, the snow accumulation around Cable car posts in Adventdalen could increase the risk for permafrost degradation as excess water from snow melting could

contribute to thawing. Also, in Ny-Ålesund, some buildings seem to settle into the permafrost and foundations are cracking probably due to developments of the active layer. However, frost heave can be assumed as a contributor to damaged foundations on equal footing, unless ground investigations and measurements of ground temperature are performed.

The analysis focused on assessing the combined risk of natural hazards on CH objects. However, it is also crucial to examine the risk posed by individual hazards, to identify CH objects facing a high risk from specific hazards, even if the overall risk score may not be alarming. Further analysis identified a total of 55 CH objects facing the highest possible risk (both probability and consequence scores being 5/5) from one or, in the case of eight particular CH objects, two natural hazards. The objects that face the highest possible risk by two natural hazards, are located on Cable car lines 1b and 2b, facing the highest risk of both snow avalanches and rockfalls. In general, objects that are exposed to the highest risk of snow avalanches and/or rockfalls are all located on Cable car lines 1a, 1b, 2b, which is not surprising given their position on steep slopes. However, there are also a few CH objects on Cable car line 5 exposed to the highest risk of rockfalls, and on Cable car line 5-6 the highest risk of snow avalanches was identified. These findings highlight that snow avalanches are the most destructive type of natural hazards for the studied CH objects, as 30 of them face the highest risk from this particular hazard. This observation aligns with the fact that snow is the weakest of the earth's surface materials, leading to a higher probability of snow avalanches compared to other hazards like landslides and rockfalls (McClung and Schaerer, 2006).

In addition to snow avalanches and rockfalls, there are some CH objects that are exposed to the highest risk of shallow landslides, permafrost degradation, surface erosion and gullyng, and coastal erosion. Surface erosion and gullyng is mainly an extreme hazard on Cable car line 3, where surface below the objects is eroding and close proximity to steep ravines is very likely to destroy the object within the next 50 years. The highest risk for shallow landslides is found at the beginning of Cable car line 5-6, near posts that are on the northern side of Sukkertoppen. Similarly, Taubanestasjonen in Hiorthhamn is not exposed to most of

the hazards, yet the risk of coastal erosion is very high, and thus the CH object is at high risk of being destroyed within the next 50 years (as the period this study operates), or even much earlier if relying on a detailed analysis of observed erosion rates. Therefore, only looking at the total risk does not give enough information of the CH objects that are in a vulnerable situation. Moreover, analysing the result of and prioritizing CH objects that are posed to the highest risk from specific hazards provides more clarity and manageability.

7.2. Arctic warming and natural hazards

Arctic warming is a significant factor that can impact the risk of natural hazards in the region. The changes in occurrence are mainly driven by rising temperatures, thawing permafrost (e.g thickening of the seasonally thawing active layer), and alterations in precipitation patterns. Of particular concern is the warming permafrost, which may contribute to dangerous feedback loop. As permafrost thaws, it releases soil organic carbon that has been frozen for thousands of years. This carbon can then be decomposed by microbes, which release carbon dioxide and methane, two potent greenhouse gases that contribute to global warming (Biskaborn *et al.*, 2019).

Permafrost degradation poses a threat to all of the Cable car lines and CH objects in Ny-Ålesund, albeit to varying degree. For 50% (4/8) of the Cable car lines, permafrost degradation is the most significant hazard, while being the second biggest risk to one of the Cable car lines. Climate change is expected to intensify permafrost degradation and its impacts on the studied CH objects. The loss of permafrost stability can lead to the destabilization of the ground on which CH sites are built (Esch and Osterkamp, 1990), as observed in field studies conducted in Ny-Ålesund and Longyearbyen. These observations have revealed settling and cracking of the foundations of CH objects due to permafrost thawing. Additionally, frost heave can also contribute to damages of foundations on permafrost. This is supported by Boike *et al.* (2018) who highlight a significant warming of permafrost in the Ny-Ålesund region over the past two decades. Furthermore, research by Westermann *et al.* (2011) demonstrate that rain events can enhance the thermal conductivity of snow and soil, resulting in a reduction in the depth of the permafrost layer. This, in turn,

can impact the stability of the ground and buildings in the region. Therefore, extreme weather events, such as storms and heavy snowfall, can further compromise the integrity of CH objects, adding to the risk associated with permafrost degradation in the future.

Currently, **snow avalanches** pose the highest risk for three out of eight of the Cable car lines and the second highest risk for one Cable car line. However, with snow avalanches, the future direction of occurrences remains complex and uncertain, primarily due to the unpredictable nature of precipitation. Climate change is expected to bring about alterations in precipitation patterns, including a notable shift from solid to liquid forms. The amount of liquid precipitation has already increased and is projected to continue rising (Førland *et al.*, 2011). Generally, a shift from snow to rain would result in less snow avalanches, however, this is not as straightforward on Svalbard. This transition may instead have other effects on the snow avalanches, particularly through the occurrence of rain-on-snow events. Winter events of rain-on-snow can have two different types of impact on snow avalanche occurrences; early in the winter season they may create a thin ice-layer in the snowpack which may reduce snow-pack stability and precondition release of large slab avalanches later in the season (Hansen *et al.*, 2014). If rain-on-snow occurs during the snow-melt season, it may oversaturate the snowpack with water, triggering wet-snow avalanches or slush-avalanches, both of which have large run-out lengths and are relatively erosive and destructive (Hansen *et al.*, 2014). Consequently, the prevalence of both dry and wet snow avalanches may increase in the future, introducing new challenges.

Rockfalls pose the second highest risk for three out of eight Cable car lines, and third highest risk for one of the Cable car lines. There is a potential for changes in the frequency of rockfalls in the future as a result of climate change. One factor that could contribute to increased rockfall occurrences is the more frequent freeze-thaw events resulting from warming climate. As temperatures fluctuate above and below freezing, water within the rocks and soil expands and contracts, leading to destabilization of rock and soil layers (Kuhn *et al.*, 2021). Heavy precipitation and storms associated with climate change (Hanssen-Bauer *et al.*, 2019; Pedersen *et al.*, 2022) can have an impact on the stability of rock formations, further contributing to rockfall formations. However, it is important to note that a warming

climate could also have a positive impact on slope stability by increasing vegetation cover, particularly in regions like Svalbard where vegetation is scarce. Vegetation acts as a protective layer, providing stability to the underlying soil and rock (Matsuoka, 2001) and hence potentially reducing the occurrence of rockfalls.

At present, the risk of **solifluction** primarily affects the Cable car lines in Adventdalen (Line 5-6, Line 5, and Line 6), as well as some CH objects on Cable car line 3. The magnitude and frequency of solifluction events are expected to increase in the future as a combined effect of rising temperatures and reduced slope stability. Similar to other slope processes, induced thawing resulting from climate change, has the potential to temporarily deepen and accelerate soil movement, while the potentially increasing vegetation cover could have a mitigating impact on solifluction (Matsuoka, 2001). Excess water resulting from snow accumulation is likely to exhibit a correlation with various processes, as suggested by Akerman (2005). Therefore, the accumulation of snow around CH objects in Adventdalen (Cable car lines 5-6 and 6) could potentially indicate an increased occurrence of solifluction. Nevertheless, solifluction is a relatively slow process compared to other slope hazards, and as a result, it typically takes longer periods before impacting the landscape and CH objects. This allows for the monitoring of the risk to CH over time.

Debris flows pose a considerable risk for many Cable car lines, including Cable car lines 1b, 2a, 2b, and 5, making them the third biggest hazard for the overall risk of these lines. Additionally, they are the second biggest hazard for Cable car line 1a. However, there are no CH objects with the highest potential risk (both probability and consequence scores being 5) for debris flows. On the other hand, **shallow landslides** pose a comparatively smaller risk to Cable car lines in general. Nonetheless, there are a few CH objects on Cable car line 5-6 where the risk of shallow landslides is very high. Looking into the future, the occurrence of both landslides is expected to increase due to the anticipated active layer melting and heavy rainfall events. As the presence of excess water accumulates in the soil, its stability diminishes, resulting in heightened possibilities of slope failures and the initiation of debris flows and shallow landslides (Hansen *et al.*, 2014; Nicu, Lombardo and Rubensdotter, 2021; Pedersen *et al.*, 2022).

Surface erosion and gullyng are the second biggest contributing hazard to the overall risk for Cable car lines 3 and 6, while **coastal erosion** primarily affects Taubanestasjonen in Hiorthhamn, and some CH objects in Ny-Ålesund near the coastline. Climate change is expected to accelerate erosional processes in Svalbard, with alterations in precipitation patterns playing a role in increasing surface erosion and gullyng. More intense rainfall patterns can lead to greater runoff, which erodes the soil surface and channels it into gullies (Fortier, Allard and Shur, 2007). Thawing permafrost exposes previously frozen soil to increased water infiltration, making it more susceptible to erosion. Coastal erosion processes are also influenced by climate change, as rising temperatures lead to decreased sea ice, exposing the coastline to increased wave action (Guégan, 2015; Jaskólski, Pawłowski and Strzelecki, 2018; Nielsen *et al.*, 2022).

Valley bottoms in Longyearvalley, Endalen and Todalen, which include some of the CH objects on Cable car lines 2b, 5 and 6, face some level of risk for **riverine flooding**. Climate change is expected to have significant impacts on riverine flooding. Altered precipitation patterns can result in higher water levels and intensified flooding events, while the glacial meltwater adds to the river discharge, increasing the volume and intensity of river flows (Hanssen-Bauer *et al.*, 2019; Haverkamp *et al.*, 2022). Also, permafrost thaw alters the hydrological regime, potentially increasing the surface runoff and infiltration.

Finally, **weathering** is only a risk faced by Cable car line 3, where sediments are weathering material and some of the CH objects are located near a cliff. The impact of climate change on weathering hazards is unknown and depends on changes in the freeze-thaw process. Warmer temperatures may reduce the duration and severity of freezing periods, potentially decreasing the rate of rock breakdown. However, if temperatures fluctuate more frequently around the freezing point, the mechanical weathering effects of freeze-thaw processes can intensify (Saemundsson, Morino and Conway, 2021).

7.3. Safeguarding cultural heritage

After conducting a risk assessment on CH objects in Svalbard and identifying those most at risk for natural hazards, the question arises as to what should be done with the results. Traditionally, repairing and restoring buildings and structures have been the common methods employed to preserve CH and extend their lifespan. Yet, there have been rare situations, where relocating a CH object due to a threat of natural hazard like erosion, has become necessary (Barr, 2019). With a large number of CH objects in Svalbard, including 260 objects studied, and the limitations of resources available for their preservation, it is crucial to carefully consider which objects are most significant and worthy of preservation.

When it comes to identifying which CH objects should be prioritized for preservation in Svalbard, it is important to consider the purpose that CH brings to the community, and what is wanted to be achieved by safeguarding it. There are a number of different factors that should be considered. The factors that should be considered may include the historical and cultural significance of the object, its physical condition and vulnerability to damage or decay, its value as a symbol of the cultural identity of the local community, and its potential appeal to tourists and other visitors (Hollesen *et al.*, 2018; Boro and Hermann, 2020; Sesana *et al.*, 2021). Since Svalbard does not have indigenous people, its CH consists of traces from groups who migrated north to take advantage of natural resources (Barr and Chaplin, 2004; Barr, 2019). This heritage tells the story of the people who have lived and worked in Svalbard over the centuries, and their relationship with the unique environment of the archipelago. Thus, its primary purposes could be to educate future generations about the history and culture of the region, but it can also serve as a valuable resource for researchers studying the region's history, culture, and environment. As Barr (2019) notes, history can also be a valuable tool for understanding the impact of climate change on CH objects. For example, through historical records, researchers can gain insights into the original position of a building or structure relative to the shoreline, and how this has changed over time due to coastal erosion.

In the case of the different CH objects studied in Longyearbyen, the fact that majority of them are Cable car posts, presents a unique challenge in terms of identifying which objects are most significant and should be prioritized for preservation. One approach could be to focus on Cable car posts that are in the best physical condition and most vulnerable to damage or decay. By prioritizing the preservation of those objects that are most at risk, it may be possible to prevent their loss and ensure that they are available for future generations to appreciate and learn from. On the other hand, taken for example the Cable car line 1b that is most exposed to natural hazards, its location on a steep slope as well as the high exposure to potentially very destructive hazards such as snow avalanches and rockfalls, it might not make it the best area to focus on. Therefore, it may also be important to consider the safety of the CH objects in terms of their exposure to hazards. For example, Cable car posts that are located in areas that are less prone to destructive hazards such as large avalanches or rock falls may be prioritized for preservation. This approach can be particularly cost-effective, as it allows for the preservation of objects that are less likely to require frequent repairs or replacements due to damage from natural disasters or other hazards.

Finally, an approach could be to prioritize objects that are closest to the town, as they are likely to be more easily accessible for renovation and restoration efforts. This means that it may be easier and more cost-effective to repair and maintain these posts, as they can be reached more easily and without the need for specialized equipment or transportation. Additionally, the proximity of these objects to the town means that they are also more likely to be accessible to locals and tourists, who can appreciate and learn from them more easily.

7.4. Comparison between Version 1 and Version 2

The comparison between Version 1 and Version 2 of the risk assessments reveals similar patterns in the ranking of the most at-risk CH objects (See Appendix 4). In both versions, CH objects on Cable car line 1b consistently appear at the top of the list, indicating their high exposure to natural hazards. In Version 1, 21 of the CH objects on Cable car line 1b are ranked in order as the most at risk, whereas in Version 2, the order is not as consecutive. Additionally, objects on Cable car lines 1a and 2b are also ranked high in both assessments.

However, Version 2 presents a more scattered results compared to Version 1, with CH objects from other Cable car lines also ranking high in terms of risk.

The changes in risk assessment categories, such as dividing one category into two (landslide/debris flow) and adding a feature into another category (surface erosion and gully), contribute to the differences in rankings between the two versions. Out of the top 50 most vulnerable CH objects in Version 2, 17 are not ranked as being at the highest risk in Version 1. These 17 objects are replaced by objects from other Cable car lines, mainly from 5-6. However, most of the objects from Version 1, remain in the top 50 list in Version 2, just their positions have changed.

Examining the total risk values, Version 1 generally has higher scores compared to Version 2, despite Version 2 having one less risk assessment category. This difference can be partly explained by one level adjustments in the PC scores, where some scores were changed from 5 (very likely) to 4 (likely) in Version 2. These adjustments were made when the probability was evaluated as high but not the highest possible, as was done in the previous assessment. This change in PC score, combined with the highest CC score of 5, impacts the average risk of Heritage Loss, reducing it from 30% to 12.5%. Thus, even small changes in the higher scores, have a significant impact on the total risk for each CH.

In Version 2, posts from Cable car lines 5 and 5-6 are more prominently represented on the high-risk list. These objects have rather high PC scores in most hazard categories, but there are no major differs from Version 1 assessment. The detailed and object-specific assessment conducted in Version 2 resulted in distinct differences even between consecutive Cable car posts. In contrast, Version 1 seemed to focus more on evaluating larger areas rather than providing a point-by-point evaluation for each CH object. This was evident as consecutive posts in Version 1 often had received the same PC score, and similar explanations such as “assumption” or “assumption made on study X”. However, in Version 2, the analysis was more object-specific, taking into account each hazard for each object in detail. The assessment incorporated additional material, including maps, literature data, and fieldwork

notes, to provide a quality-improved assessment. These differences in approach further clarify the disparities between the results of Version 1 and 2.

7.5. Limitations and need for future studies

This chapter aims to shed light on the inherent constraints and boundaries encountered during the research process. It critically examines the factors that may have influenced the study's outcomes, potentially affecting the validity and generalizability of the findings. The chapter seeks to enhance the overall credibility of the study and offers valuable insights for future researchers aiming to build upon this work. The chapter also shortly proposes potential future research directions.

7.5.1. Limited data in the Arctic

One of the major limitations in predicting natural hazards in Svalbard is the lack of accurate and up-to-date data. The satellite images used from TopoSvalbard for the study area, for instance, are from 2008-2009 and are of poor quality in some areas. This outdated and limited data makes it difficult to assess the current state of natural hazards and their potential impact on CH objects in the Longyearbyen area and Ny-Ålesund based on the satellite pictures.

More recent remote sensing pictures would provide a more accurate and up-to-date understanding of the risks posed by natural hazards to CH objects in the region. Newer data would help to improve the accuracy of natural hazard predictions and provide a more thorough analysis of the potential hazards faced by CH objects in Svalbard. This would allow for more effective risk assessment and mitigation measures to be put in place to protect CH objects in the region from the effects of natural hazards.

Barr (2019) highlights the potential of technological advances to provide more accurate and up-to-date information on natural hazards and their impacts on CH objects in the Arctic. One such example is the use of drones, monitoring satellites, and scanning technology to improve the understanding of the risks faced by CH objects and guide efforts to protect and preserve them. Drones can be used to monitor heritage sites and measure changes such as erosion increase without the operator having to set foot on the ground. The development of monitoring satellites that cover the Arctic area also opens up new possibilities for remote information gathering. Meanwhile, 3D laser scanning technology can capture extremely complicated heritage sites in a short time by a pair of operators, providing a more detailed and accurate documentation of monuments and sites.

7.5.2. Predictability of natural hazards

Natural hazards have different predictabilities, depending on their underlying causes and the complexity of the system involved. Looking at the hazards in Svalbard, some, such as permafrost degradation, and solifluction, are driven by slow and relatively steady processes that can be monitored over time, making some of them easier to predict than fast-phased debris flows, shallow landslides, rockfalls and snow avalanches that are triggered by sudden events such as heavy rainfall or temperature changes and defined by geocryological conditions that are normally unknown when it comes to detailed soil profile. However, even slow processes can be difficult to predict when the specific impact on individual objects is uncertain.

For fast slope processes, factors such as terrain, geology, and slope angle mainly predict the occurrence of these hazards, and thus the risk for these types of hazards can vary significantly across different parts of Svalbard. Therefore, while the exact timing of these hazards may be impossible to predict, CH objects in areas that have experienced these hazards in the past are likely to be at increased risk of future events. This is especially true in areas where the underlying conditions that contribute to these hazards are particularly pronounced, such as for debris flows and rockfalls on steep slopes with loose sediment or soil, or in areas with frequent heavy rainfall or snowmelt. For rockfalls however, the random element of a single

rock hitting the object make the prediction even more challenging. Similarly, snow avalanches can be difficult to predict, as they depend on complex interactions between snowpack stability, terrain, and weather conditions. Snow avalanches are linear processes and if they will occur within close proximity on a slope above a certain CH object, they will be very likely to have an impact. However, while areas with a history of snow avalanche activity may be at increased risk of future events, the exact timing and severity of these events can still be difficult to predict.

Riverine flooding and gully erosion are also difficult to predict, as they depend on a complex range of factors such as precipitation patterns, snowmelt, and the capacity of rivers and streams to carry water. Gully erosion is a back dripping process which makes the estimation of the future direction almost impossible. It can occur as a result of both natural and human-induced factors, such as changes in land use or the construction of infrastructure, which further makes the estimation challenging. While areas that are prone to gully erosion can be identified, the probability of a gully hitting a certain CH object is very obscure unless the object is already touching the gully. Weathering is a hazard that affects all CH objects in Svalbard to some degree, as it is driven by long-term exposure to the elements. However, the rate at which weathering occurs can vary widely depending on factors such as temperature, precipitation, and the type of rock or soil. As a result, it can be difficult to predict the specific impact of weathering on individual objects or sites.

The challenge of predicting natural hazards in Svalbard is further complicated by the effects of climate change. As temperatures continue to rise, permafrost degradation and solifluction are likely to occur at a faster rate, making their predictability more uncertain. Likewise, changing precipitation patterns and more frequent extreme weather events can lead to an increase in the occurrence and severity of many hazards, including riverine flooding, gully erosion, and snow avalanches. This can make it more difficult to accurately predict the timing and impact of these hazards on CH objects in the region. Furthermore, climate change can also impact the underlying conditions that contribute to the occurrence of natural hazards, making it important to continuously monitor natural hazards in Svalbard.

7.5.3. Scope and subjectivity of the assessment

Despite the efforts to conduct a thorough and rigorous assessment of the natural hazards that pose a risk to CH in Svalbard, there are several limitations to the analysis that should be acknowledged. Firstly, the assessment is based on existing materials and research, which may not capture all potential hazards or risks to CH in the region. While a wide range of sources were collected and evaluated, it is possible that some hazards or risks were overlooked or not given sufficient consideration. However, every effort was made to ensure that all information was gathered and evaluated as comprehensively as possible. The study aimed to cover all relevant natural geo-hazards. However, there are some additional aspects to consider such as the impact of high winds and fungi decay, which can cause damage to CH objects in the region. This recognition underscores the need for ongoing research of CH sites in the region to ensure that all potential threats are identified and addressed.

Secondly, the assessment is also subjective to some extent because it involves the author's judgment in assigning probability scores to different hazards and CH objects. While efforts were made to base these judgments on existing materials and research, the final results of the assessment are ultimately influenced by the author's own interpretations. However, to remain as transparent and consistent as possible, all CH objects were aimed to be assessed using identical logic, and the interpretations made are openly explained in Chapters 5 and 6.

Furthermore, the assessment is limited by the complexity and uncertainty of natural hazards and climate change. These are dynamic and multifaceted entities that are difficult to fully understand or predict, and there may be indirect or cascading effects that are not immediately apparent. As a result, the assessment necessarily includes a significant degree of educated guesswork and uncertainty. This means that the probability scores assigned to different hazards and CH objects may not fully capture the actual risk or impact of these hazards on CH in Svalbard.

Finally, the hazard map created in ArcGIS online is a simplified version with limited features. While efforts were made to create a user-friendly and informative map, additional features and layers could have been added to provide greater detail and nuance. For example, adding a feature that shows the CH objects that have the highest possible risk for any of the natural hazards would provide a more comprehensive picture of the high risks to CH in the region. Nonetheless, the map serves as a useful tool to visualize the overall risk faced by CH in Svalbard.

8. Conclusions

The aim of this study was to assess the risks of natural hazards on technical-industrial CH in Svalbard, with a focus on 260 CH objects in the Longyearbyen area and Ny-Ålesund. To achieve this goal, a multidisciplinary approach was employed that integrated literature analysis, geographical information analysis, data from PCCH-Arctic' Risk Assessment, and fieldwork. The study expanded on the primary assessment conducted by PCCH-Arctic and provided valuable insights into the vulnerabilities and potential risks faced by CH in Svalbard.

Significant variations in natural hazard risks within CH objects were assessed that were influenced for example by local topography, sedimentology, prevailing wind conditions. Cable car line 1b in Longyearbyen was identified as facing the highest total risk, followed by Cable car lines 1a and 2b. Permafrost degradation, snow avalanches and rockfalls were identified as major hazards in the Longyearbyen area, with permafrost degradation being a significant risk especially for objects in low-lying valley bottoms and on rather flat groundings, while snow avalanches and rockfalls pose a major risk for the CH objects on steep slopes. In Longyearbyen, 16% or 37 out of 226 CH objects were classified as being under high total risk. In Ny-Ålesund permafrost degradation is the main hazard, with limited exposure to other hazards for the majority of the CH objects. Luftskipsmasta was identified as the most vulnerable CH object in Ny-Ålesund.

The findings of the study indicate that climate change significantly amplifies the risk of various natural hazards in Svalbard. Thawing permafrost serves as a key factor exacerbating hazards such as solifluction, landslides, erosion and flooding, heightening the vulnerability of CH to natural hazards. Moreover, the projected changes in precipitation patterns and temperature fluctuations further intensify these hazards.

The visualization map created using ArcGIS online was a critical output of this study, offering an accessible and clear representation of the risks posed by different natural hazards

to the CH sites in Svalbard. This tool can serve as a resource for planners and other stakeholders in developing effective management strategies and prioritizing preservation actions. While the study provides insights into the risks posed by natural hazards to CH in Svalbard, it also highlights the need for further research. Future studies could consider the use of remote sensing and geospatial analysis to identify and monitor changes in CH sites and their surroundings. Moreover, long-term monitoring of natural hazards and their interactions with climate change on CH sites in Svalbard could bring valuable insights into the trends and patterns. Finally, the development and evaluation of specific mitigation strategies based on the identified risks could be a fruitful area of future research.

Overall, this thesis enhances our understanding of the vulnerabilities and potential risks faced by the CH objects in Svalbard. By identifying specific objects at risk and the associated natural hazards, it lays the foundation for targeted interventions and resource prioritization to ensure the preservation of these important CH sites for future generations. The study enables proactive measures to be taken to safeguard the most at-risk CH objects in Svalbard.

References

- Aga, J. *et al.* (2023) 'Coastal retreat rates of high-Arctic rock cliffs on Brøgger peninsula, Svalbard, accelerate during the past decade'. Available at: <https://doi.org/10.5194/egusphere-2023-321>.
- Akerman, J. (2005) 'Relations between slow slope processes and active-layer thickness 1972–2002, Kapp Linné, Svalbard', *Norsk Geografisk Tidsskrift-Norwegian Journal of Geography*, 59(2), pp. 116–128. Available at: <https://doi.org/10.1080/00291950510038386>.
- Andre, M.F. (1990) *Frequency of debris flows and slush avalanches in Spitsbergen: a tentative evaluation from lichenometry*.
- André, M.F. (1997) 'Holocene rockwall retreat in svalbard: A triple-rate evolution', *Earth Surface Processes and Landforms*, 22(5), pp. 423–440. Available at: [https://doi.org/10.1002/\(SICI\)1096-9837\(199705\)22:5<423::AID-ESP706>3.0.CO;2-6](https://doi.org/10.1002/(SICI)1096-9837(199705)22:5<423::AID-ESP706>3.0.CO;2-6).
- Barr, S. (2019) 'Cultural Heritage, or How Bad News Can Also Be Good', in N. Sellheim, Y. Zaika, and I. Kelman (eds) *Arctic Triumph Northern Innovation and Persistence*. Springer Polar Sciences, pp. 43–57. Available at: <http://www.springer.com/series/15180>.
- Barr, S. and Chaplin, P. (2004) *Cultural heritage in the arctic and antarctic regions*. ICOMOS.
- Barr, S. and Chaplin, P. (2008) *Historical polar bases : preservation and management*. International Council on Monuments and Sites, International Polar Heritage Committee.
- Barr, S. and Chaplin, P. (2011) *Polar settlements : location, techniques and conservation*. ICOMOS IPHC.
- Bekele, Y. and Sinitzyn, A.O. (2023) 'Risk Analysis of the Impact of Natural Hazards on Cultural Heritage Development of a Risk Assessment Tool'. Available at: <https://dx.doi.org/11250/3085603> (Accessed: 28 September 2023).
- Biskaborn, B.K. *et al.* (2019) 'Permafrost is warming at a global scale', *Nature Communications* 2019 10:1, 10(1), pp. 1–11. Available at: <https://doi.org/10.1038/s41467-018-08240-4>.
- Boike, J. *et al.* (2018) 'A 20-year record (1998-2017) of permafrost, active layer and meteorological conditions at a high Arctic permafrost research site (Bayelva, Spitsbergen)', *Earth Syst. Sci. Data*, 10, pp. 355–390. Available at: <https://doi.org/10.5194/essd-10-355-2018>.
- Boro, M. and Hermann, C. (2020) *Assessing risks and planning adaptation - Guidance on managing the impacts of climate change on northern historic places*. Available at:

<http://nationalarchives.gov.uk/doc/opengovernment-licence/version/3/www.adaptnorthernheritage.org>.

Burke, E.J. *et al.* (2020) ‘Evaluating permafrost physics in the Coupled Model Intercomparison Project 6 (CMIP6) models and their sensitivity to climate change’, *The Cryosphere*, 14, pp. 3155–3174. Available at: <https://doi.org/10.5194/tc-14-3155-2020>.

Christiansen, H.H. *et al.* (2020) ‘Ground ice content, drilling methods and equipment and permafrost dynamics in Svalbard 2016-2019 (PermaSval)’. Available at: <https://doi.org/10.5281/zenodo.4294095>.

Christiansen, H.H., Humlum, O. and Eckerstorfer, M. (2013) ‘Meteorological Dynamics and Periglacial Landscape Response’, *Arctic, Antarctic, Alpine Research*, 45(1), pp. 6–18. Available at: <https://doi.org/10.1657/1938-4246-45.1.6>.

Cisek, M., Makuch, P. and Petelski, T. (2017) ‘Comparison of meteorological conditions in Svalbard fjords: Hornsund and Kongsfjorden’, *Oceanologia*, 59(4), pp. 413–421. Available at: <https://doi.org/10.1016/j.oceano.2017.06.004>.

‘Cultural Heritage Act’ (1978). Available at: <https://www.regjeringen.no/en/dokumenter/cultural-heritage-act/id173106/> (Accessed: 6 August 2023).

Dalheim Ottem, M. (2022) *The Longyearlva River-to-Ocean System*.

Dallmann, W.K. (Winfried K.) (2015) *Geoscience atlas of Svalbard*.

Descamps, S. *et al.* (2017) ‘Climate change impacts on wildlife in a High Arctic archipelago – Svalbard, Norway’, *Global Change Biology*, 23(2), pp. 490–502. Available at: <https://doi.org/10.1111/GCB.13381>.

Eckerstorfer, M. (2012) *Snow avalanches in central Svalbard: A field study of meteorological and topographical triggering factors and geomorphological significance*.

Eckerstorfer, M., Christiansen, H.H., Vogel, S., *et al.* (2013) ‘Snow cornice dynamics as a control on plateau edge erosion in central Svalbard’, *Earth Surface Processes and Landforms*, 38(5), pp. 466–476. Available at: <https://doi.org/10.1002/esp.3292>.

Eckerstorfer, M., Christiansen, H.H., Rubensdotter, L., *et al.* (2013) ‘The geomorphological effect of cornice fall avalanches in the Longyear dalen valley, Svalbard’, *The Cryosphere*, 7, pp. 1361–1374. Available at: <https://doi.org/10.5194/tc-7-1361-2013>.

Eckerstorfer, M. and Christiansen, H.H. (2011a) ‘High Arctic Maritime Snow Climate’, *Arctic, Antarctic, and Alpine Research*, 43(1), pp. 11–21. Available at: <https://doi.org/10.1657/1938-4246-43.1.11>.

Eckerstorfer, M. and Christiansen, H.H. (2011b) ‘Relating meteorological variables to the natural slab avalanche regime in High Arctic Svalbard’. Available at: <https://doi.org/10.1016/j.coldregions.2011.08.008>.

Eckerstorfer, M. and Christiansen, H.H. (2011c) ‘Topographical and meteorological control on snow avalanching in the’. Available at: <https://doi.org/10.1016/j.geomorph.2011.07.001>.

Enevoldsen, K. (2022) *MasterThesis_KristinEnevoldsen (1)*.

Engeset, R. V *et al.* (2020) *Avalanche warning in Svalbard* *Avalanche warning in Svalbard Norwegian Water Resources and Energy Directorate*. Available at: www.nve.no.

Esch, D.C. and Osterkamp, T.E. (1990) *C O L D REGIONS ENGINEERING: CLIMATIC W A R M I N G CONCERNS FOR ALASKA*.

Etzel Müller, B. *et al.* (2011) ‘Modeling the temperature evolution of Svalbard permafrost during the 20th and 21st century’, *The Cryosphere*, 5, pp. 67–79. Available at: <https://doi.org/10.5194/tc-5-67-2011>.

Etzel Müller, B. and Frauenfelder, R. (2009) ‘Factors controlling the distribution of mountain permafrost in the northern hemisphere and their influence on sediment transfer’, *Arctic, Antarctic, and Alpine Research*, 41(1), pp. 48–58. Available at: <https://doi.org/10.1657/1523-0430-41.1.48>.

Van Everdingen, R.O. (1998) ‘MULTI-LANGUAGE GLOSSARY of PERMAFROST and RELATED GROUND-ICE TERMS’.

Flyen, A.-C. and Mattsson, J. (2013) *GRUVEMINNER I LONGYEARBYEN OG HIORTHAMN Fredete taubanebukker: Tilstand og bevaring*. Available at: www.niku.no (Accessed: 4 August 2023).

Førland, E.J. *et al.* (2011) ‘Temperature and Precipitation Development at Svalbard 1900–2100’, *Advances in Meteorology*, 2011, pp. 1–14. Available at: <https://doi.org/10.1155/2011/893790>.

Førland, E.J. *et al.* (2020) ‘Measured and Modeled Historical Precipitation Trends for Svalbard’, *Journal of Hydrometeorology*, 21(6), pp. 1279–1296. Available at: <https://doi.org/10.1175/JHM-D-19-0252.1>.

Fortier, D., Allard, M. and Shur, Y. (2007) ‘Observation of Rapid Drainage System Development by Thermal Erosion of Ice Wedges on Bylot Island, Canadian Arctic Archipelago’. Available at: <https://doi.org/10.1002/ppp.595>.

Frederick, J.M. *et al.* (2016) *SANDIA REPORT The Arctic Coastal Erosion Problem*. Available at: <http://www.ntis.gov/help/ordermethods.asp?loc=7-4-0#online>.

Geldard, J. (2019) *The production of a Quaternary Geological map of Endalen, Svalbard, and assessment of Holocene geomorphic processes*.

Giuliani, F. *et al.* (2021) ‘A simplified methodology for risk analysis of historic centers: the world heritage site of San Gimignano, Italy’, *International Journal of Disaster Resilience in the Built Environment*, 12(3), pp. 336–354. Available at: <https://doi.org/10.1108/IJDRBE-04-2020-0029>.

Gjelten, H.M. *et al.* (2016) *View of Air temperature variations and gradients along the coast and fjords of western Spitsbergen*. Available at: <https://polarresearch.net/index.php/polar/article/view/3265/8687> (Accessed: 26 July 2023).

Glossary – EAWS (2023) *European Avalanche Warning Services*. Available at: <https://www.avalanches.org/glossary/#loose-snow-avalanche-point-release-avalanche> (Accessed: 29 August 2023).

Guégan, E. (2015) *Erosion of permafrost affected coasts: rates, mechanisms and modelling*.

Guégan, E.B.M. and Christiansen, H.H. (2016) ‘Seasonal Arctic Coastal Bluff Dynamics in Adventfjorden, Svalbard’. Available at: <https://doi.org/10.1002/ppp.1891>.

De Haas, T. *et al.* (2015) ‘Surface morphology of fans in the high-Arctic periglacial environment of Svalbard: Controls and processes’. Available at: <https://doi.org/10.1016/j.earscirev.2015.04.004>.

Hall, K. *et al.* (2002) ‘Weathering in cold regions: Some thoughts and perspective’, *Progress in Physical Geography*, 26(4), pp. 577–603. Available at: <https://doi.org/10.1191/0309133302pp353ra>.

Hancock, J.H. (2021) ‘Snow avalanche controls, monitoring strategies, and hazard management in Svalbard’.

Hansen, B.B. *et al.* (2014) ‘Warmer and wetter winters: Characteristics and implications of an extreme weather event in the High Arctic’, *Environmental Research Letters*, 9(11). Available at: <https://doi.org/10.1088/1748-9326/9/11/114021>.

Hanssen-Bauer, I. *et al.* (2019) *Climate in Svalbard 2100 Editors-a knowledge base for climate adaptation Title: Date*. Available at: <http://www.miljodirektoratet.no/M1242> (Accessed: 25 July 2023).

Harris, C. *et al.* (2007) ‘Field instrumentation for real-time monitoring of periglacial solifluction’, *Permafrost and Periglacial Processes*, 18(1), pp. 105–114. Available at: <https://doi.org/10.1002/ppp.573>.

Harris, C. *et al.* (2011) ‘The Role of Interannual Climate Variability in Controlling Solifluction Processes, Endalen, Svalbard’, *Permafrost and Periglacial Processes*, 22(3), pp. 239–253. Available at: <https://doi.org/10.1002/ppp.727>.

Harvey, S. *et al.* (2018) *Caution - Avalanches*. Available at: www.wildruhe.ch (Accessed: 28 August 2023).

Haverkamp, P.J.; *et al.* (2022) ‘Increasing Arctic Tundra Flooding Threatens Wildlife Habitat and Survival: Impacts on the Critically Endangered Siberian Crane (*Grus leucogeranus*) Increasing Arctic Tundra Flooding Threatens Wildlife Habitat and Survival: Impacts on the Critically’. Available at: <https://doi.org/10.3389/fcsc.2022.799998>.

Highland, L.M. and Bobrowsky, P. (2008) *The Landslide Handbook-A Guide to Understanding Landslides*.

Hjem - Kulturminnesøk (no date). Available at: <https://www.kulturminnesok.no/> (Accessed: 26 July 2023).

Hollesen, J. *et al.* (2018) 'Climate change and the deteriorating archaeological and environmental archives of the Arctic', *Antiquity*, 92(363), pp. 573–586. Available at: <https://doi.org/10.15184/aqy.2018.8>.

Holmgaard, S.B. *et al.* (2019) 'Monitoring and Managing Human Stressors to Coastal Cultural Heritage in Svalbard', *Humanities 2019, Vol. 8, Page 21*, 8(1), p. 21. Available at: <https://doi.org/10.3390/H8010021>.

Home - Riksantikvaren (no date). Available at: <https://www.riksantikvaren.no/en/> (Accessed: 26 July 2023).

Humlum, Ole *et al.* (2003) *Permafrost in Svalbard: a review of research history, climatic background and engineering challenges*, *Polar Research*.

Hungr, O., Leroueil, S. and Picarelli, L. (2014) 'The Varnes classification of landslide types, an update', 11, pp. 167–194. Available at: <https://doi.org/10.1007/s10346-013-0436-y>.

Instanes, A. (2016) 'Incorporating climate warming scenarios in coastal permafrost engineering design-Case studies from Svalbard and northwest Russia'. Available at: <https://doi.org/10.1016/j.coldregions.2016.09.004>.

Instanes, A. (2017) *Coastal permafrost-foundation design Incorporating climate warming scenarios*.

IPCC (2021) *Climate Change 2021: The Physical Science Basis. Contribution of Working Group I to the Sixth Assessment Report of the Intergovernmental Panel on Climate Change*.

Isaksen, K. *et al.* (2016) 'Recent warming on Spitsbergen—Influence of atmospheric circulation and sea ice cover', *Journal of Geophysical Research: Atmospheres*, 121(20), pp. 11,913–11,931. Available at: <https://doi.org/10.1002/2016JD025606>.

Isaksen, K. *et al.* (2022) 'Exceptional warming over the Barents area', *Scientific Reports*, 12(1). Available at: <https://doi.org/10.1038/s41598-022-13568-5>.

Jaskólski, M.W., Pawłowski, Ł. and Strzelecki, M.C. (2018) 'High Arctic coasts at risk—the case study of coastal zone development and degradation associated with climate changes and multidirectional human impacts in Longyearbyen (Adventfjorden, Svalbard)', *Land Degradation and Development*, 29(8), pp. 2514–2524. Available at: <https://doi.org/10.1002/ldr.2974>.

Knudsen, E. and Tokle Yri, H. (2010) *Teknisk industrielle kulturminner i Longyearbyen med omegn*. Available at: www.sysselmannen.no (Accessed: 6 August 2023).

Kuhn, D. *et al.* (2021) 'Back analysis of a coastal cliff failure along the Forkastningsfjellet coastline, Svalbard: Implications for controlling and triggering factors'. Available at: <https://doi.org/10.1016/j.geomorph.2021.107850>.

Lantuit, H. *et al.* (2011) 'Coastal erosion dynamics on the permafrost-dominated Bykovsky Peninsula, north Siberia, 1951-2006', *Polar Research*, 30(SUPPL.1). Available at: <https://doi.org/10.3402/polar.v30i0.7341>.

Lofthus, J.B. (2020) *Snow Avalanches on Svalbard: Investigating changes in depositional patterns and their palaeoclimatic significance*.

Lombardo, L., Tanyas, H. and Nicu, I.C. (2020) 'Spatial modeling of multi-hazard threat to cultural heritage sites', *Engineering Geology*, 277, p. 105776. Available at: <https://doi.org/10.1016/J.ENGGEOL.2020.105776>.

Martin, Yvonne *et al.* (2002) 'Sediment transfer by shallow landsliding in the Queen Charlotte Islands, British Columbia', *Can. J. Earth Sci*, 39, pp. 189–205. Available at: <https://doi.org/10.1139/E01-068>.

Matsuoka, N. (2001) 'Solifluction rates, processes and landforms: a global review', *Earth-Science Reviews*, 55, pp. 107–134. Available at: www.elsevier.com/locate/earscirev (Accessed: 26 July 2023).

Matsuoka, N. and Murton, J. (2008) 'Frost Weathering: Recent Advances and Future Directions'. Available at: <https://doi.org/10.1002/ppp.620>.

Matveev, A. (2019) 'Variable effects of climate change on carbon balance in northern ecosystems', *IOP Conf. Ser.: Earth Environ. Sci*, 226, p. 12023. Available at: <https://doi.org/10.1088/1755-1315/226/1/012023>.

McClung, D. and Schaerer, P. (2006) *The Avalanche Handbook*. 3rd edn. The Mountaineers Books. Available at: https://books.google.fi/books?id=njsUCgAAQBAJ&pg=PT43&hl=fi&source=gbs_toc_r&cad=2#v=onepage&q&f=false (Accessed: 29 August 2023).

Melvær, Y. (2014a) *Kartdata Svalbard 1:100 000 (S100 Kartdata) / Map Data [Data set]*, Norwegian Polar Institute. Available at: <https://doi.org/https://doi.org/10.21334/npolar.2014.645336c7>.

Melvær, Y. (2014b) *Terrengmodell Svalbard (S0 Terrengmodell) [Data set]*, Norwegian Polar Institute. Available at: <https://doi.org/https://doi.org/10.21334/npolar.2014.dce53a47>.

MET Norway (2023) *Observations and weather statistics - Seklima, The Norwegian Meteorological Institute*. Available at: <https://seklime.met.no/observations/> (Accessed: 31 August 2023).

Meyer, A. (2022) 'Physical and feasible: Climate change adaptation in Longyearbyen, Svalbard'. Available at: <https://doi.org/10.1017/S0032247422000079>.

Miccadei, E., Piacentini, T. and Berti, C. (2016) 'Geomorphological features of the Kongsfjorden area: Ny-Ålesund, Blomstrandøya (NW Svalbard, Norway)', *Rendiconti Lincei*, 27, pp. 217–228. Available at: <https://doi.org/10.1007/s12210-016-0537-3>.

Multiconsult (2016) 'Skredfarekartlegging i utvalgte områder på Svalbard'. Available at: www.nve.no (Accessed: 26 July 2023).

Nicu, I.C. *et al.* (2020) 'Coastal Erosion Affecting Cultural Heritage in Svalbard. A Case Study in Hiorthhamn (Adventfjorden)—An Abandoned Mining Settlement', *Sustainability* 2020, Vol. 12, Page 2306, 12(6), p. 2306. Available at: <https://doi.org/10.3390/SU12062306>.

Nicu, I.C. *et al.* (2021a) 'Coastal Erosion of Arctic Cultural Heritage in Danger: A Case Study from Svalbard, Norway', *Water* 2021, Vol. 13, Page 784, 13(6), p. 784. Available at: <https://doi.org/10.3390/W13060784>.

Nicu, I.C. *et al.* (2021b) 'Coastal Erosion of Arctic Cultural Heritage in Danger: A Case Study from Svalbard, Norway', *Water* 2021, Vol. 13, Page 784, 13(6), p. 784. Available at: <https://doi.org/10.3390/W13060784>.

Nicu, I.C. *et al.* (2022) 'A glimpse into the northernmost thermo-erosion gullies in Svalbard archipelago and their implications for Arctic cultural heritage', *CATENA*, 212, p. 106105. Available at: <https://doi.org/10.1016/J.CATENA.2022.106105>.

Nicu, I.C. *et al.* (2023) 'Multi-hazard susceptibility mapping of cryospheric hazards in a high-Arctic environment: Svalbard Archipelago', *Earth Syst. Sci. Data*, 15, pp. 447–464. Available at: <https://doi.org/10.5194/essd-15-447-2023>.

Nicu, I.C., Lombardo, L. and Rubensdotter, L. (2021) 'Preliminary assessment of thaw slump hazard to Arctic cultural heritage in Nordenskiöld Land, Svalbard', *Landslides*, 18(8), pp. 2935–2947. Available at: <https://doi.org/10.1007/s10346-021-01684-8>.

Nielsen, D.M. *et al.* (2022) 'Increase in Arctic coastal erosion and its sensitivity to warming in the twenty-first century', *Nature Climate Change*, 12(3), pp. 263–270. Available at: <https://doi.org/10.1038/s41558-022-01281-0>.

Nordli, Ø. *et al.* (2014) 'Long-term temperature trends and variability on spitsbergen: The extended svalbard airport temperature series, 1898-2012', *Polar Research*, 33(1 SUPPL), pp. 1898–2012. Available at: https://doi.org/10.3402/POLAR.V33.21349/SUPPL_FILE/ZPOR_A_11818879_SM0001.PDF.

Nordli, Ø. *et al.* (2020) 'Revisiting the extended svalbard airport monthly temperature series, and the compiled corresponding daily series 1898–2018', *Polar Research*, 39, pp. 1–15. Available at: <https://doi.org/10.33265/polar.v39.3614>.

Pallesen, L.M. (2022) *Sediment source-to-sink in a warming Arctic Thawing moraines, slope processes and river erosion in Longyeardalen, Svalbard.*

Paolini, A. *et al.* (2012) *Risk management at heritage sites: a case study of the Petra world heritage site*. Available at: https://unesdoc.unesco.org/in/documentViewer.xhtml?v=2.1.196&id=p::usmarcdef_0000217107&file=/in/rest/annotationSVC/DownloadWatermarkedAttachment/attach_import_252f61c6-fe54-40f3-b5e6-792b661a9a85%3F_%3D217107mul.pdf&locale=en&multi=true&ark=/ark:/48223/pf0000217107/PDF/217107mul.pdf#%5B%7B%22num%22%3A45%2C%22gen%22%3A0%7D%2C%7B%22name%22%3A%22XYZ%22%7D%2C0%2C842%2Cnull%5D (Accessed: 7 December 2023).

Pedersen, Å.Ø. *et al.* (2022) ‘Five decades of terrestrial and freshwater research at Ny-Ålesund, Svalbard’, *Polar Research*. Norwegian Polar Institute. Available at: <https://doi.org/10.33265/polar.v41.6310>.

Pilgøj, N. *et al.* (2019) ‘Temporal changes in wind conditions at Svalbard for the years 1986–2015’, *Geografiska Annaler, Series A: Physical Geography*, 101(2), pp. 136–156. Available at: <https://doi.org/10.1080/04353676.2019.1572973>.

Population of Svalbard (2023). Available at: <https://www.ssb.no/en/befolkning/folketall/statistikk/befolkningen-pa-svalbard> (Accessed: 6 August 2023).

Prestvold, K. (2015) *Svalbard's history - The Cruise Handbook for Svalbard*. Available at: <https://cruise-handbook.npolar.no/en/svalbard/history.html> (Accessed: 6 August 2023).

Prick, A. (2003) *Frost weathering and rock fall in an arctic environment, Longyearbyen, Svalbard*. A.A. Balkema.

Rantanen, M. *et al.* (2022) ‘The Arctic has warmed nearly four times faster than the globe since 1979’, *Communications Earth & Environment* 2022 3:1, 3(1), pp. 1–10. Available at: <https://doi.org/10.1038/s43247-022-00498-3>.

Reymert, P.K. (2016) *Ny-Ålesund Verdens nordligste gruveby*.

Riverine Flooding / National Risk Index (no date). Available at: <https://hazards.fema.gov/nri/riverine-flooding> (Accessed: 6 August 2023).

Rubensdotter, L. *et al.* (2015) ‘Quaternary geological map, 1:25,000. Landforms and sediments in Todalen and upper Gangdalen and Bødalen.’, *Geological Survey of Norway* [Preprint].

Rubensdotter, L. (no date) ‘Data set on landslide susceptibility in Adventdalen’, *Unpublished* [Preprint].

Rubensdotter, L. (unpublished) (2022) ‘Preliminary map of Longyeardalen valley, Svalbard: Geomorphology and Quaternary geology. Quaternary geological map, 1:10,000’, *unpublished* [Preprint].

Saemundsson, Þ., Morino, C. and Conway, S.J. (2021) 'Mass-Movements in Cold and Polar Climates'. Available at: <https://doi.org/10.1016/B978-0-12-818234-5.00117-6>.

Sesana, E. *et al.* (2021) 'Climate change impacts on cultural heritage: A literature review', *Wiley Interdisciplinary Reviews: Climate Change*. John Wiley and Sons Inc. Available at: <https://doi.org/10.1002/wcc.710>.

Siewert, M.B. *et al.* (2012) 'Arctic rockwall retreat rates estimated using laboratory-calibrated ERT measurements of talus cones in Longyeardalen, Svalbard', *EARTH SURFACE PROCESSES AND LANDFORMS* [Preprint]. Available at: <https://doi.org/10.1002/esp.3297>.

Sinitsyn, A. *et al.* (2022) 'Case study objects in PCCH-Arctic. Selection criteria, list of the structures, and desktop data collection'. Available at: <https://sintef.brage.unit.no/sintef-xmlui/handle/11250/3035580> (Accessed: 26 July 2023).

Sinitsyn, A.O. *et al.* (2020) *Development of coastal infrastructure in cold climate Summary Guideline SFI SAMCoT REPORT*. Available at: www.sintef.no/community.

Skauen Sandodden, I. (2013) *KATALOG PRIORITERTE KULTURMINNER OG KULTURMILJØER PA SVALBARD [Catalogue of the cultural heritage sites with high priority in Svalbard]*. Available at: https://www.sysselmesteren.no/contentassets/a8a4f6d45992499f96f4b2f2ea69ea32/katalog_prioriterte_kulturminner_paa_svalbard_versjon_1_1_2013_komprimert-1.pdf (Accessed: 13 September 2023).

Skauen Sandodden, I., Tokle Yri, H. and Solli, H. (2013) *Kulturminneplan for Svalbard 2013-2023*. Available at: www.sysselmannen.no (Accessed: 6 August 2023).

Skred AS (2022) 'Faresoneutredning skred i bratt terreng – Svalbard'. Available at: www.nve.no (Accessed: 25 July 2023).

Søreide, J.E. *et al.* (2020) 'Environmental status of Svalbard coastal waters: coastscapes and focal ecosystem components (SvalCoast)'. Available at: <https://doi.org/10.5281/zenodo.4293849>.

Svalbard Archipelago - UNESCO World Heritage Centre (no date). Available at: <https://whc.unesco.org/en/tentativelists/5161> (Accessed: 6 August 2023).

'Svalbard Environmental Protection Act' (2001). Available at: <https://www.regjeringen.no/en/dokumenter/svalbard-environmental-protection-act/id173945/> (Accessed: 6 August 2023).

Svalcoast (no date) *Maps, data and research results related to coastal processes, sediments and landforms on Svalbard*. Available at: <https://svalcoast.com> (Accessed: 25 October 2023).

The Svalbard Treaty (1920). Available at: http://library.arcticportal.org/1909/1/The_Svalbard_Treaty_9ssFy.pdf (Accessed: 6 August 2023).

TopoSvalbard - Norsk Polarinstitutt (no date). Available at: <https://toposvalbard.npolar.no/> (Accessed: 25 July 2023).

UNESCO (2021) *Operational Guidelines for the Implementation of the World Heritage Convention UNITED NATIONS EDUCATIONAL, SCIENTIFIC AND CULTURAL ORGANIZATION INTERGOVERNMENTAL COMMITTEE FOR THE PROTECTION OF THE WORLD CULTURAL AND NATURAL HERITAGE WORLD HERITAGE CENTRE R I M O N I O M U N D I A L*. Available at: <https://whc.unesco.org/fr/orientations>.

UNESCO World Heritage Centre - World Heritage List (no date). Available at: <https://whc.unesco.org/en/list/> (Accessed: 24 August 2023).

Uwera, S. (2019) *Geocryology*. Ashland: Delve Publishing.

Valagussa, A. *et al.* (2021) ‘Multi-risk analysis on European cultural and natural UNESCO heritage sites’, *Natural Hazards*, 105(3), pp. 2659–2676. Available at: <https://doi.org/10.1007/s11069-020-04417-7>.

Veillette, A., Fortier, D. and Godin, E. (2015) *Contrasting patterns of thermo-erosion gullies formed in syngenetic ice wedge polygonal terrains on Bylot Island, eastern Canadian Arctic: case studies from three different sedimentary environments*. Available at: <https://www.researchgate.net/publication/282156374>.

Vogel, S., Eckerstorfer, M. and Christiansen, H.H. (2012) ‘Cornice dynamics and meteorological control at Gruvefjellet, Central Svalbard’, *The Cryosphere*, 6, pp. 157–171. Available at: <https://doi.org/10.5194/tc-6-157-2012>.

Weathering (no date) *National Geographic*. Available at: <https://education.nationalgeographic.org/resource/weathering/> (Accessed: 6 August 2023).

Westermann, S. *et al.* (2011) ‘Modeling the impact of wintertime rain events on the thermal regime of permafrost’, *Cryosphere*, 5(4), pp. 945–959. Available at: <https://doi.org/10.5194/tc-5-945-2011>.

Wickström, S. *et al.* (2020) ‘Present Temperature, Precipitation, and Rain-on-Snow Climate in Svalbard’, *Journal of Geophysical Research: Atmospheres*, 125(14), p. e2019JD032155. Available at: <https://doi.org/10.1029/2019JD032155>.

Wu, Y. *et al.* (2018) ‘Snowmelt water drives higher soil erosion than rainfall water in a mid-high latitude upland watershed’, *Journal of Hydrology*, 556, pp. 438–448. Available at: <https://doi.org/10.1016/j.jhydrol.2017.11.037>.

Zachar, D. (1982) *Soil Erosion*. Elsevier. Available at: <https://books.google.fi/books?id=o8ny2dUkpM8C&printsec=frontcover&hl=fi#v=onepage&q&f=false> (Accessed: 26 September 2023).

Zheng, L. *et al.* (2019) 'Changing Arctic River Dynamics Cause Localized Permafrost Thaw', *Journal of Geophysical Research: Earth Surface*, 124(9), pp. 2324–2344. Available at: <https://doi.org/10.1029/2019JF005060>.

Appendix

Appendix 1. Case study object GPS coordinates and locations on a map in the Longyearbyen area.

	Object	ID number in Askeladden -database	GPS coordinates
1.	Bukk nr 32 - Taubane 3	158619-32	33X E512630 N8684553
2.	Taubanesentralen (in Longyearbyen)	87889-6	33X E514041 N8683404
3.	Bukk nr 5 - Taubanelinje 2b	158986-5	33X E513997 N8681535
4.	Bukk nr 6 - Taubanelinje 1b	158657-6	33X E513275 N8681726
5.	Bukk nr 6 - Taubane delstrekning gruve 5 og 6	87889-14	33X E514779 N8682885
6.	Bukk nr 34 - Taubane delstrekning gruve 5 og 6	87889-43	33X E517047 N8681233
7.	Bukk nr 16 - Taubane delstrekning gruve 5	87889-63	33X E517778 N8679886
8.	Bukk 7 - Taubane delstrekning gruve 6	87889-112	33X E520513 N8678451
9.	Bukk 8 - Taubane delstrekning gruve 6	87889-111	33X E520456 N8678498
10.	Taubanesentralen, Bygning I (Hiorthamn)	93040-6	33X E515929 N8686184
11.	Boligbrakke - Bygning G (Hiorthamn)	146668-7	33X E515973 N8686605

Appendix 2. Fieldwork

Snow depth measurements in the Longyearbyen area 25.-26.4.2023 and 3.5.2023. Anni Vehola, Juditha Aga, Clarissa Willmes, and Peter Hamrock. Weather conditions: Week before the measurements 17.-23.4., warm, +3 °C on some days, snow melting; 25.-26.4. Sunny, -10 to -5 °C, no wind; 3.5. cloudy, snowy, -5 °C, no wind. Structures and Buildings [measurements in cm]:

Points	Titankrana 3.5.2023	Taubanesentralen 3.5.2023	Taubanestasjon in Hiorthhamn 25.4.2023	Boligbrakke G 25.4.2023
1	0	0	22	3 of ice
2	15	63 piled snow	19 ice starts at 15	snow free
3	3	17	36	16
4	44	6 rocks	16	8 ice, 8 snow
5	0	47	1	51
6	2+ice	8	0	86
7	1	10	35	45
8	21	17	16	29
9	20	1-2+ ice	0	
10	1+thin layer of ice	0 ice and pooling water, drip roof		
11	0	47		
12	5	5		
13	31	16		
14	9	54		
15	30	0		
16	4	water drip causing ice+20		
17		40		
18		13		
19		6 +ice		
20		0		
21		0		
22		0		
23		0		
24		0		
Comments	Lot of ice and coal deposits	Lot of ice		

Cable car posts [Case study objects in bold]:

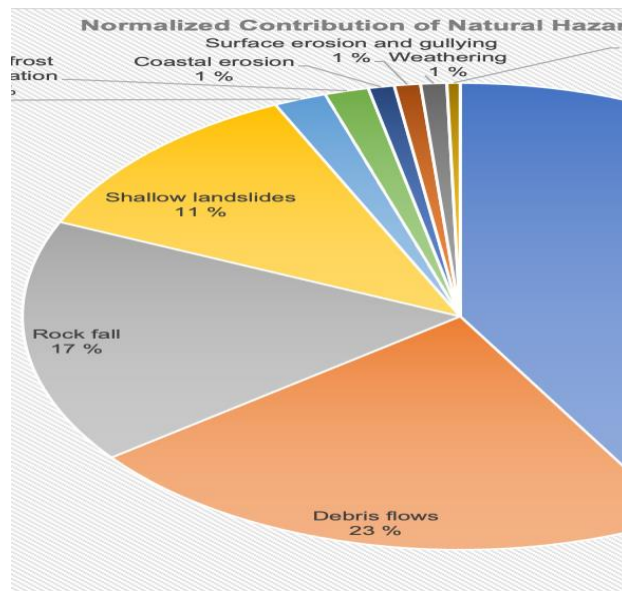
Cableway post	Date of measurement	A [cm]	B-North [cm]	C-North [cm]	B-East [cm]	C-East [cm]	B-South [cm]	C-South [cm]	B-West [cm]	C-West [cm]	Notes
Nr 32 – Line 3	3.5.2023	0-1 +ice coal	9	0 + ice and snow edge	1+ice	16	7	13	15	12	pooling at corners, coal
Nr 6 – Line 1b	26.4.2023	31	57	84, in snowslide	25	27	43	on rock deposition, 30 but next to it free rocks and little snow/ice	81	42, slope of 50 deg towards highest gradient	about 45 degree slope, 0-1-10cm refrozen snow and thin ice layers on rock deposit
Nr 23 – Line 1b	26.4.2023	0, coal pile	0-1	64 scooter tracks	0	1-2, scooter track	0	56	0	31	sitting on lot of coal, 10 in the direction of platoberget, flattens out and after 10m to north steeper again
Nr 5 – Line 2b	26.4.2023	0	0	18	25	7	15	46	18	0	coal around the object, mainly on the north side; east side 40 degree slope(rock deposit), generally 34 degree
Nr 6 – Line 2b	26.4.2023	12	15	40	33	0-3, on rock depo, seems windblown, little ice	44	87, higher deposition of snow behind little ridge, see pics	43	27	about 36 degrees slope; east side has rock deposition and 44 degree angle slope
Nr 7 – Line 2b	26.4.2023	5, 0-4cm of ice	34, 15 next to it	50	0-2, ice	42	39 +ice	31	16 + ice	29	slope around 20 degrees, always measuring towards the highest gradient
Nr 8 – Line 2b	26.4.2023	66	83	65, next to artificial snow deposition of approx 2.7m higher	32	36	69	62, on scooter track	61	38	relatively flat, east side about 8 degrees
Nr 3 – Line 5-6	3.5.2023	19	17	0	28	road 0	15	55 snow pile beside in natural snow 14	0	14	downhill
Nr 4 – Line 5-6	3.5.2023	41	60	66	55	next to river bed 84	58	rocks and ice 0-1	55	8	rocks ice
Nr 5 – Line 5-6	3.5.2023	76	41	road	40	road	44	114	11	49	
Nr 6 – Line 5-6	3.5.2023	34	34	10	33 with ice layer	16	43	32	67	45	pooling at corners
Nr 7 – Line 5-6	3.5.2023	28	59	scooter track 102	72	90	91	40	104	146	
Nr 8 – Line 5-6	3.5.2023	90	86	scooter track 167	69	94	100	96	100	107	
Nr 34 – Line 5-6	3.5.2023	30	10	39	46	22	64	37	38	33	
Nr 16 – Line 5	25.4.2023	60	20	86	3	73	1	78	42	108	feels like frozen ground beneath
Nr 7 – Line 6	25.4.2023	31	34	39	32	52	45	16	27	66	
Nr 8 – Line 6	25.4.2023	38	39	27	46	42	67	52	53	61	
Nr 5 – Line 6	25.4.2023	0	13	1	46	132	40	16	44	42	
Nr 10 – Line 6	25.4.2023	63	55	45	40	67	81	43	69	111	
Nr 15 – Line 6	25.4.2023	13	4	19	9	22	31	20	33	47	
Nr 20 – Line 6	25.4.2023	0	3	19	7	45	28	22	19	39	
Nr 25 – Line 6	25.4.2023	0	0	11	13	81	13	24	10	27	
Nr 30 – Line 6	25.4.2023	37	42	43	49	40	63	39	46	66	
Nr 35 – Line 6	25.4.2023	56	65	38	55	56	85	51	58	57	
Nr 40 – Line 6	25.4.2023	60	40	29	63	5	61	5	58	80	

Appendix 3. Results for each Cable car line from the PCCH-Arctic Excel Tool Risk Assessment.

Cable car line 1a

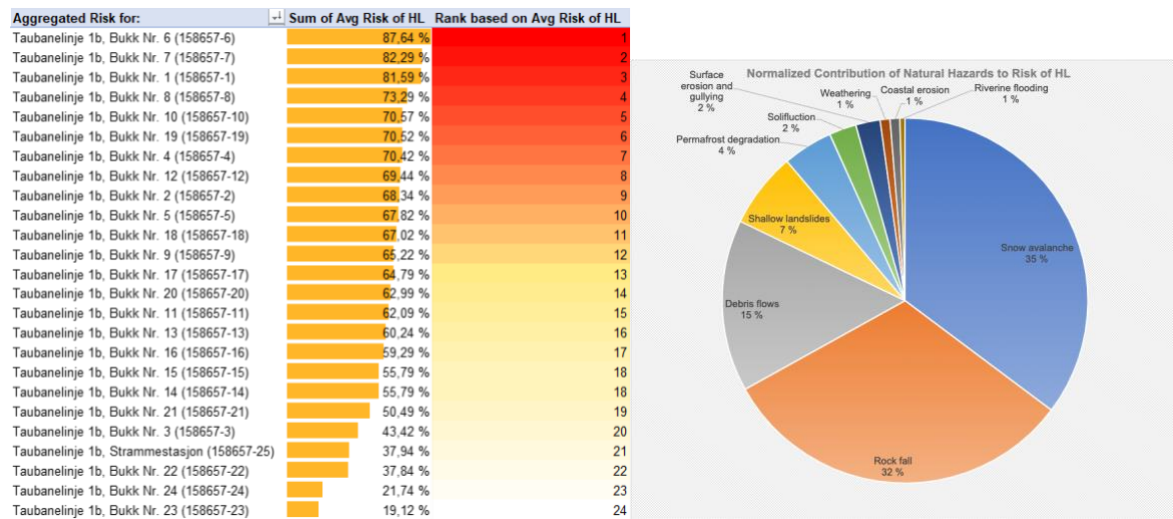
Aggregated Risk for:	Sum of Avg Risk of HL	Rank based on Avg Risk of HL
Taubanelinje 1a, Foundation 7 (159054-7)	67.69 %	1
Taubanelinje 1a, Foundation 9 (159054-9)	67.69 %	1
Taubanelinje 1a, Foundation 8 (159054-8)	67.69 %	1
Taubanelinje 1a, Foundation 5 (159054-5)	67.69 %	1
Taubanelinje 1a, Foundation 6 (159054-6)	67.69 %	1
Taubanelinje 1a, Foundation 4 (159054-4)	61.44 %	2
Taubanelinje 1a, Foundation 10 (159054-10)	50.19 %	3
Taubanelinje 1a, Foundation 11 (159054-11)	50.19 %	3
Taubanelinje 1a, Foundation 3 (159054-3)	49.89 %	4
Taubanelinje 1a, Foundation 2 (159054-2)	32.39 %	5
Taubanelinje 1a, Foundation 1 (159054-1)	18.49 %	6

Risk ranking of posts within Cable car line 1a.



Pie chart presenting aggregated risk of Heritage Loss from different natural hazards for Cable car line 1a.

Cable car line 1b

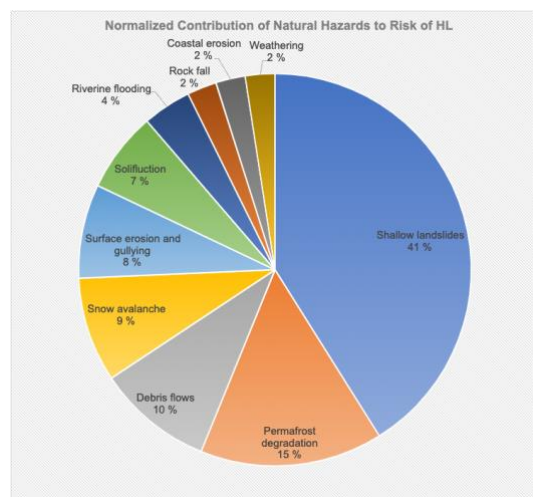


Risk ranking of posts within Cable car line 1b. Pie chart presenting aggregated risk of Heritage Loss from different natural hazards for Cable car line 1b.

Cable car line 2a

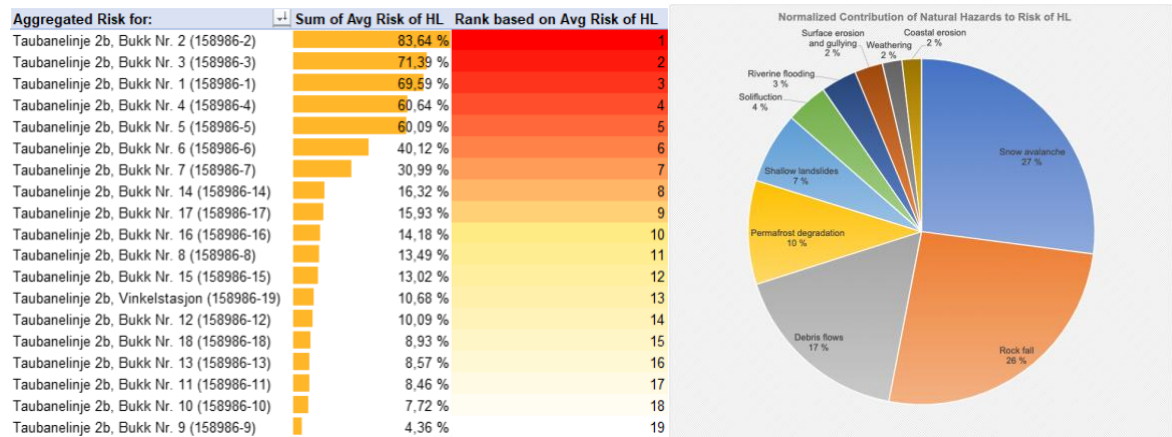
Aggregated Risk for:	Sum of Avg Risk of HL	Rank based on Avg Risk of HL
Taubanelinje 2a, Fundament Nr.3, NS (158987-3)	25,87 %	1
Taubanelinje 2a, Fundament maskinhus, NS (136714-3)	25,87 %	1
Taubanelinje 2a, Fundament Nr.4, NS (158987-4)	25,87 %	1
Taubanelinje 2a, Fundament Nr.1, NS (158987-1)	20,13 %	2
Taubanelinje 2a, Fundament Nr.2, NS (158987-2)	10,07 %	3

Risk ranking of posts within Cable car line 2a.



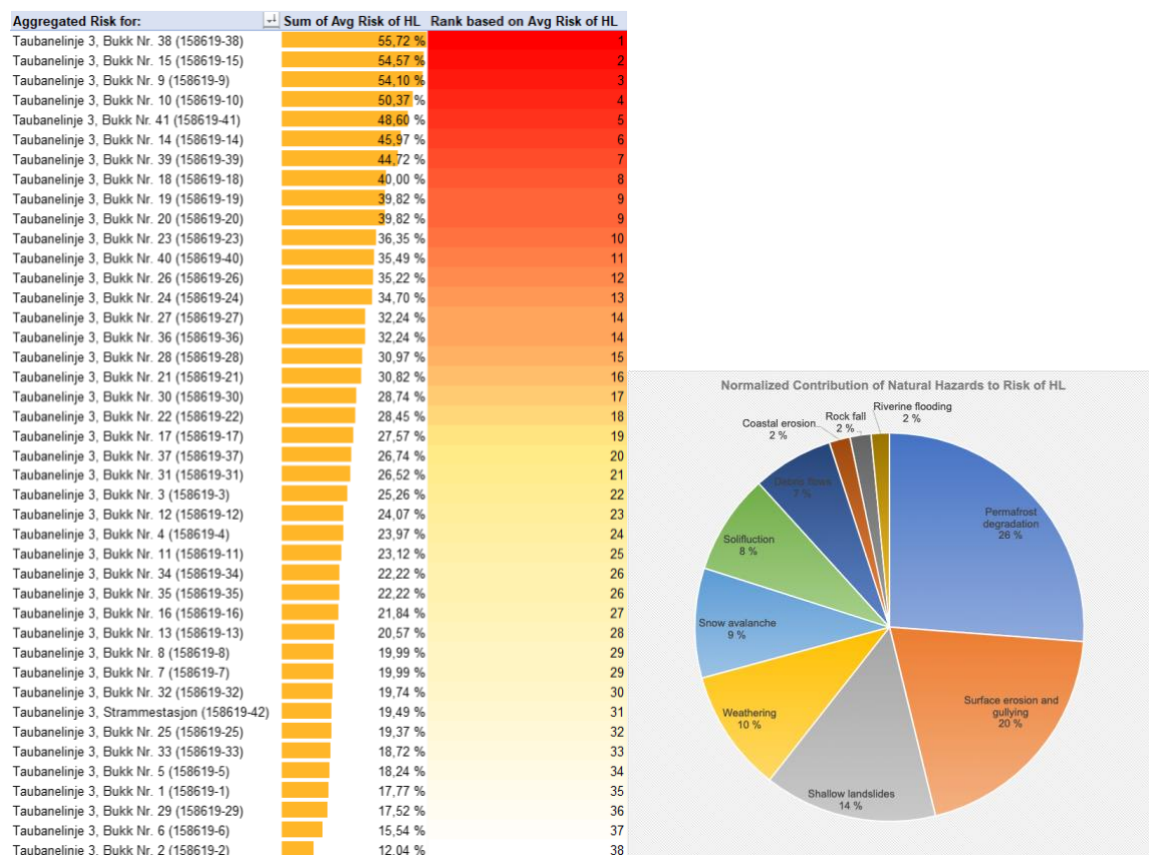
Pie chart presenting aggregated risk of Heritage Loss from different natural hazards for Cable car line 2a.

Cable car line 2b



Risk ranking of posts within Cable car line 2b. Pie chart presenting aggregated risk of Heritage Loss from different natural hazards for Cable car line 2b.

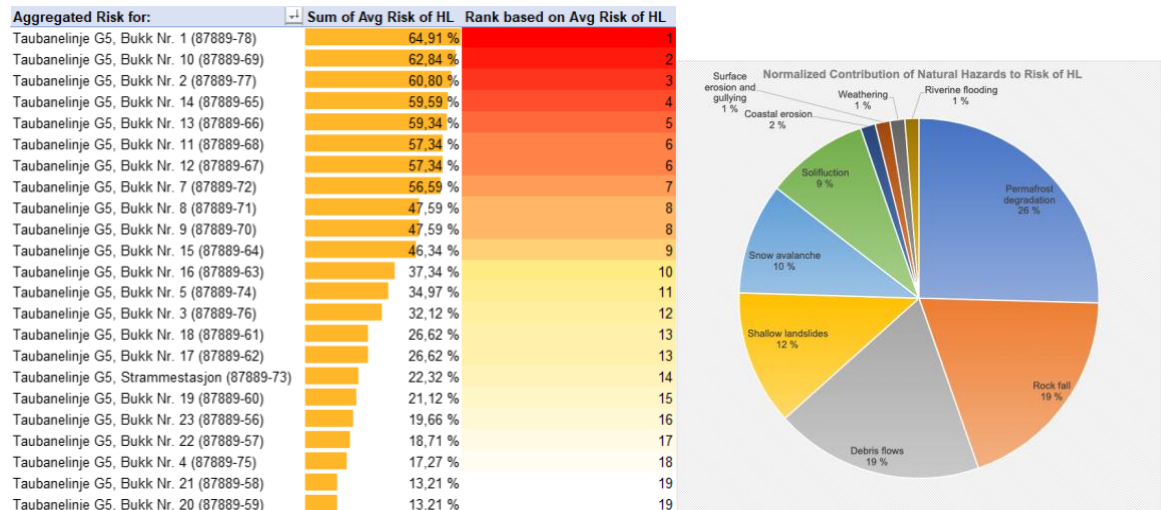
Cable car line 3



Risk ranking of posts within Cable car line 3.

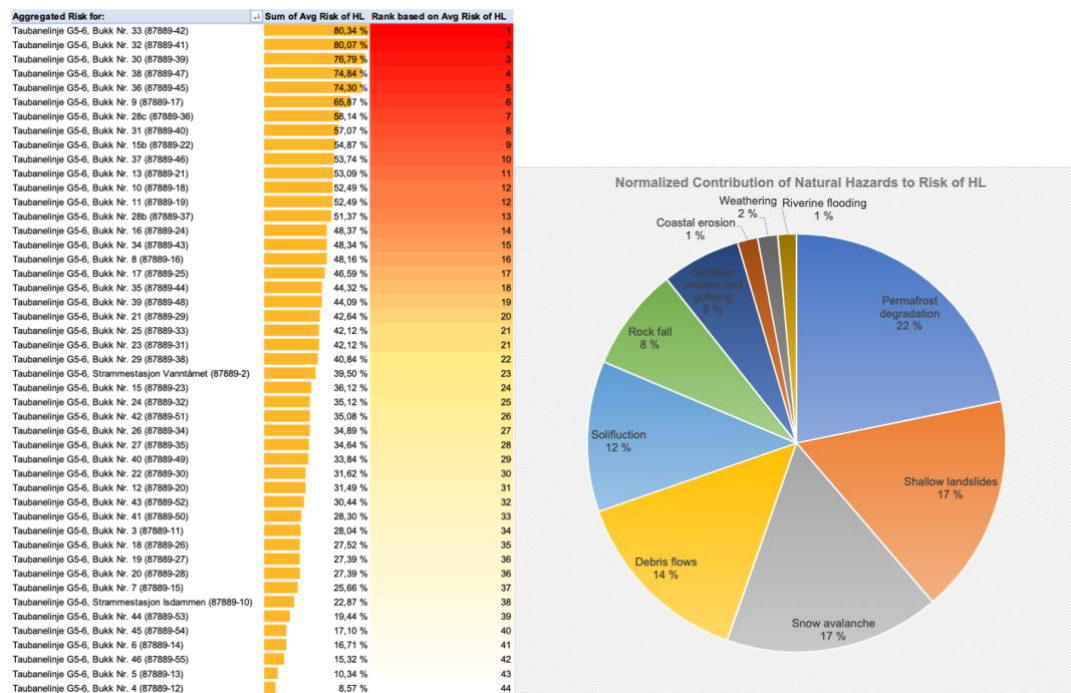
Pie chart presenting aggregated risk of Heritage Loss from different natural hazards for Cable car line 3.

Cable car line 5



Risk ranking of posts within Cable car line 5. Pie chart presenting aggregated risk of Heritage Loss from different natural hazards for Cable car line 5.

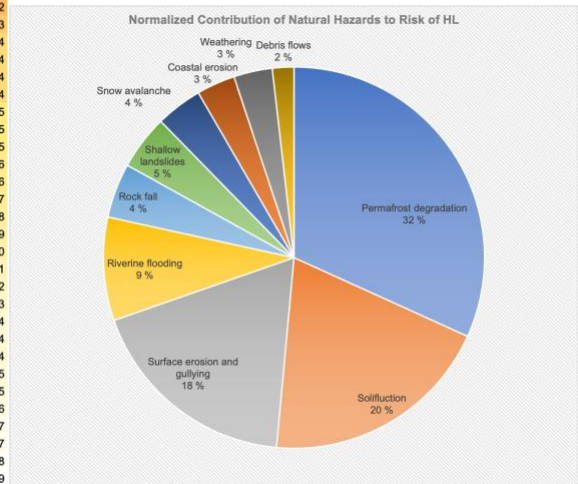
Cable car line 5-6



Risk ranking of posts within Cable car line 5-6. Pie chart presenting aggregated risk of Heritage Loss from different natural hazards for Cable car line 5-6.

Cable car line 6

Aggregated Risk for:	Sum of Avg Risk of HL	Rank based on Avg Risk of HL
Taubanelinje G6, Bukk Nr. 2 (87889-117)	31,86 %	1
Taubanelinje G6, Bukk Nr. 3 (87889-116)	28,13 %	2
Taubanelinje G6, Bukk Nr. 4 (87889-115)	28,13 %	2
Taubanelinje G6, Bukk Nr. 32 (87889-87)	27,30 %	3
Taubanelinje G6, Strammestasjon Totalen (87889-11)	24,68 %	4
Taubanelinje G6, Bukk Nr. 1 (87889-118)	23,49 %	5
Taubanelinje G6, Bukk Nr. 35 (87889-84)	23,27 %	6
Taubanelinje G6, Bukk Nr. 16 (87889-102)	22,91 %	7
Taubanelinje G6, Bukk Nr. 14 (87889-104)	21,67 %	8
Taubanelinje G6, Bukk Nr. 34 (87889-85)	21,05 %	9
Taubanelinje G6, Bukk Nr. 36 (87889-83)	21,05 %	9
Taubanelinje G6, Bukk Nr. 24 (87889-95)	18,06 %	10
Taubanelinje G6, Bukk Nr. 20 (87889-99)	17,41 %	11
Taubanelinje G6, Bukk Nr. 5 (87889-114)	16,16 %	12
Taubanelinje G6, Bukk Nr. 40 (87889-79)	16,06 %	13
Taubanelinje G6, Bukk Nr. 17 (87889-101)	15,68 %	14
Taubanelinje G6, Bukk Nr. 19 (87889-100)	15,68 %	14
Taubanelinje G6, Bukk Nr. 21 (87889-98)	15,68 %	14
Taubanelinje G6, Bukk Nr. 22 (87889-97)	15,68 %	14
Taubanelinje G6, Bukk Nr. 11 (87889-108)	15,55 %	15
Taubanelinje G6, Bukk Nr. 33 (87889-86)	15,55 %	15
Taubanelinje G6, Bukk Nr. 12 (87889-107)	15,55 %	15
Taubanelinje G6, Bukk Nr. 37 (87889-82)	15,32 %	16
Taubanelinje G6, Bukk Nr. 13 (87889-105)	15,32 %	16
Taubanelinje G6, Bukk Nr. 15 (87889-103)	15,18 %	17
Taubanelinje G6, Bukk Nr. 29 (87889-90)	15,07 %	18
Taubanelinje G6, Bukk Nr. 23 (87889-96)	14,56 %	19
Taubanelinje G6, Bukk Nr. 28 (87889-91)	13,93 %	20
Taubanelinje G6, Bukk Nr. 8 (87889-111)	13,47 %	21
Taubanelinje G6, Bukk Nr. 26 (87889-93)	12,81 %	22
Taubanelinje G6, Bukk Nr. 25 (87889-94)	12,34 %	23
Taubanelinje G6, Bukk Nr. 12b (87889-106)	9,82 %	24
Taubanelinje G6, Bukk Nr. 9 (87889-110)	9,82 %	24
Taubanelinje G6, Bukk Nr. 10 (87889-109)	9,82 %	24
Taubanelinje G6, Bukk Nr. 38 (87889-81)	8,47 %	25
Taubanelinje G6, Bukk Nr. 31 (87889-88)	8,47 %	25
Taubanelinje G6, Bukk Nr. 27 (87889-92)	8,43 %	26
Taubanelinje G6, Bukk Nr. 30 (87889-89)	6,72 %	27
Taubanelinje G6, Bukk Nr. 7 (87889-112)	6,72 %	27
Taubanelinje G6, Bukk Nr. 6 (87889-113)	6,22 %	28
Taubanelinje G6, Bukk Nr. 39 (87889-80)	4,64 %	29



Risk ranking of posts within Cable car line 6. Heritage Loss from different natural hazards for Cable car line 6.

Appendix 4.

The top 50 most exposed CH objects to total risk, with color-coding in Figure B, showing which objects in Version 2 are also listed in Version 1 (Figure A) (top 50 highest risk list).

Aggregated Risk for:	Sum of Avg Risk of HL	Rank based on Avg Risk of HL	Aggregated Risk for:	Sum of Avg Risk of HL	Rank based on Avg Risk of HL
Taubanelinje 1b, Bukk Nr. 10 (158657-10)	133.07 %	1	Taubanelinje 1b, Bukk Nr. 6 (158657-6)	87.64 %	1
Taubanelinje 1b, Bukk Nr. 9 (158657-9)	122.87 %	2	Taubanelinje 2b, Bukk Nr. 2 (158986-2)	83.64 %	2
Taubanelinje 1b, Bukk Nr. 1 (158657-1)	115.84 %	3	Taubanelinje 1b, Bukk Nr. 7 (158657-7)	82.29 %	3
Taubanelinje 1b, Bukk Nr. 2 (158657-2)	108.84 %	4	Taubanelinje 1b, Bukk Nr. 1 (158657-1)	81.59 %	4
Taubanelinje 1b, Bukk Nr. 21 (158657-21)	99.12 %	5	Taubanelinje G5-6, Bukk Nr. 33 (87889-42)	80.34 %	5
Taubanelinje 1b, Bukk Nr. 19 (158657-19)	99.12 %	5	Taubanelinje G5-6, Bukk Nr. 38 (87889-47)	74.84 %	6
Taubanelinje 1b, Bukk Nr. 22 (158657-22)	98.25 %	6	Taubanelinje G5-6, Bukk Nr. 32 (87889-41)	74.34 %	7
Taubanelinje 1b, Bukk Nr. 11 (158657-11)	95.25 %	7	Taubanelinje 1b, Bukk Nr. 8 (158657-8)	73.29 %	8
Taubanelinje 1b, Bukk Nr. 15 (158657-15)	94.99 %	8	Taubanelinje 2b, Bukk Nr. 3 (158986-3)	71.39 %	9
Taubanelinje 1b, Bukk Nr. 17 (158657-17)	93.40 %	9	Taubanelinje 1b, Bukk Nr. 4 (158657-4)	70.42 %	10
Taubanelinje 1b, Bukk Nr. 5 (158657-5)	93.40 %	9	Taubanelinje 2b, Bukk Nr. 1 (158986-1)	69.59 %	11
Taubanelinje 1b, Bukk Nr. 8 (158657-8)	93.40 %	9	Taubanelinje 1b, Bukk Nr. 12 (158657-12)	69.44 %	12
Taubanelinje 1b, Bukk Nr. 16 (158657-16)	93.40 %	9	Taubanelinje 1b, Bukk Nr. 2 (158657-2)	68.34 %	13
Taubanelinje 1b, Bukk Nr. 7 (158657-7)	93.40 %	9	Taubanelinje 1b, Bukk Nr. 5 (158657-5)	67.82 %	14
Taubanelinje 1b, Bukk Nr. 14 (158657-14)	93.40 %	9	Taubanelinje 1a, Foundation 9 (159054-9)	67.69 %	15
Taubanelinje 1b, Bukk Nr. 13 (158657-13)	93.40 %	9	Taubanelinje 1a, Foundation 8 (159054-8)	67.69 %	15
Taubanelinje 1b, Bukk Nr. 4 (158657-4)	93.40 %	9	Taubanelinje 1a, Foundation 6 (159054-6)	67.69 %	15
Taubanelinje 1b, Bukk Nr. 6 (158657-6)	93.40 %	9	Taubanelinje 1a, Foundation 5 (159054-5)	67.69 %	15
Taubanelinje 1b, Bukk Nr. 18 (158657-18)	93.40 %	9	Taubanelinje 1a, Foundation 7 (159054-7)	67.69 %	15
Taubanelinje 1b, Bukk Nr. 20 (158657-20)	93.40 %	9	Taubanelinje 1b, Bukk Nr. 18 (158657-18)	67.02 %	16
Taubanelinje 1b, Bukk Nr. 3 (158657-3)	93.40 %	9	Gruve2b (136716)	66.62 %	17
Taubanelinje 1a, Foundation 5 (159054-5)	92.80 %	10	Taubanelinje G5-6, Bukk Nr. 9 (87889-17)	65.87 %	18
Taubanelinje 1a, Foundation 11 (159054-11)	92.80 %	10	Taubanelinje G5-6, Bukk Nr. 30 (87889-39)	65.34 %	19
Taubanelinje 1a, Foundation 3 (159054-3)	92.80 %	10	Taubanelinje G5, Bukk Nr. 1 (87889-78)	64.91 %	20
Taubanelinje 1b, Strammestasjon (158657-25)	92.80 %	10	Taubanelinje 1b, Bukk Nr. 10 (158657-10)	64.84 %	21
Taubanelinje 1a, Foundation 6 (159054-6)	92.80 %	10	Taubanelinje 1b, Bukk Nr. 19 (158657-19)	64.79 %	22
Taubanelinje 1b, Bukk Nr. 12 (158657-12)	92.80 %	10	Taubanelinje 1b, Bukk Nr. 17 (158657-17)	64.79 %	22
Taubanelinje 1a, Foundation 4 (159054-4)	92.80 %	10	Taubanelinje 1b, Bukk Nr. 20 (158657-20)	62.99 %	23
Taubanelinje 1a, Foundation 1 (159054-1)	92.80 %	10	Taubanelinje G5, Bukk Nr. 10 (87889-69)	62.84 %	24
Taubanelinje 1a, Foundation 2 (159054-2)	92.80 %	10	Taubanelinje 1b, Bukk Nr. 11 (158657-11)	62.09 %	25
Taubanelinje 1a, Foundation 8 (159054-8)	92.80 %	10	Taubanelinje 1a, Foundation 4 (159054-4)	61.44 %	26
Taubanelinje 1a, Foundation 10 (159054-10)	92.80 %	10	Taubanelinje G5, Bukk Nr. 2 (87889-77)	60.80 %	27
Taubanelinje 1a, Foundation 7 (159054-7)	92.80 %	10	Taubanelinje 2b, Bukk Nr. 4 (158986-4)	60.64 %	28
Taubanelinje 1a, Foundation 9 (159054-9)	92.80 %	10	Taubanelinje 1b, Bukk Nr. 13 (158657-13)	60.24 %	29
Taubanelinje 2b, Bukk Nr. 4 (158986-4)	74.50 %	11	Taubanelinje 2b, Bukk Nr. 5 (158986-5)	60.09 %	30
Taubanelinje 2b, Bukk Nr. 6 (158986-6)	73.82 %	12	Taubanelinje G5, Bukk Nr. 14 (87889-65)	59.59 %	31
Taubanelinje G5-6, Bukk Nr. 28b (87889-37)	71.59 %	13	Taubanelinje 1b, Bukk Nr. 9 (158657-9)	59.49 %	32
Taubanelinje 2b, Bukk Nr. 5 (158986-5)	71.59 %	13	Taubanelinje G5, Bukk Nr. 13 (87889-66)	59.34 %	33
Taubanelinje G5-6, Bukk Nr. 28c (87889-36)	71.59 %	13	Taubanelinje 1b, Bukk Nr. 16 (158657-16)	59.29 %	34
Taubanelinje 2b, Bukk Nr. 2 (158986-2)	71.00 %	14	Taubanelinje G5-6, Bukk Nr. 28c (87889-36)	58.14 %	35
Taubanelinje 2b, Bukk Nr. 3 (158986-3)	71.00 %	14	Taubanelinje G5, Bukk Nr. 12 (87889-67)	57.34 %	36
Taubanelinje 2b, Bukk Nr. 1 (158986-1)	69.05 %	15	Taubanelinje G5, Bukk Nr. 11 (87889-68)	57.34 %	36
Gruve 6, Daganlegget Bygning Nord (87889-3)	67.82 %	16	Taubanelinje G5, Bukk Nr. 7 (87889-72)	56.59 %	37
Gruve 6, Daganlegget Bygning Sør (87889-9)	67.82 %	16	Taubanelinje 1b, Bukk Nr. 15 (158657-15)	55.79 %	38
Gruve 6, Daganlegget Bygning Aust (87889-8)	67.82 %	16	Taubanelinje 1b, Bukk Nr. 14 (158657-14)	55.79 %	38
Gruve2b (136716)	65.68 %	17	Taubanelinje 3, Bukk Nr. 38 (158619-38)	55.72 %	39
Gruve 5 (87889-4)	65.68 %	17	Taubanelinje G5-6, Bukk Nr. 15b (87889-22)	54.87 %	40
Gruve 1a (136713)	65.57 %	18	Taubanelinje G5-6, Bukk Nr. 37 (87889-46)	53.74 %	41
Taubanelinje G5-6, Bukk Nr. 33 (87889-42)	63.89 %	19	Taubanelinje G5-6, Bukk Nr. 13 (87889-21)	53.09 %	42
Taubanelinje G5-6, Strammestasjon Vanntårnet (87889-2)	59.12 %	20	Taubanelinje G5-6, Bukk Nr. 10 (87889-18)	52.49 %	43

A. The 50 most exposed CH objects in Version 1.

B. The 50 most exposed CH objects in Version 2.

The objects that are also listed in Version 1 as the top 50 most exposed objects are squared. Colours of the squares indicate different Cable car lines.

Figures are taken from PCCH-Arctic Risk Assessment Excel Tool.